A GISCIENCE FRAMEWORK FOR SUSTAINABLE DEVELOPMENT, TOURISM AND MANAGEMENT OF COASTAL BARRIER ISLANDS IN GEORGIA

by

Byungyun Yang

(Under the Direction of Marguerite Madden)

ABSTRACT

This research considered a variety of scientific approaches in Geographic Information Science (GIScience) that can be used to provide geospatial input to reliable decision making systems for sustainable development and preservation planning. Theoretical aspects of GIScience including conceptualizations, modeling, spatio-temporal representations, and spatial analysis were combined with emerging geospatial technologies such as Light Detection and Ranging (LiDAR), very high resolution (VHR) imagery, and image fusion in Remote Sensing and Web-based geographic information systems (GIS) services. These methods were used to provide criteria and scientific findings that can be used to create master plans for coastal development and conservation. Questions considered in this dissertation are: (1) How should coastal barrier islands be demarcated and assessed for polices limiting the percentage of development?; (2) Can the availability of sandy beaches be estimated and predicted for tourism recreational purposes while regarding criteria of cultural and natural resource preservation?; (3) How effective are revetment rocks as a protector of the mainland from physical processes of erosion, accretion and wave action and what geospatial tools can be used to monitor coastal shorelines?; and (4) What image processing techniques produce optimal VHR satellite images identifying land use land cover (LULC) in coastal environments?

With respect to these considerations, this dissertation aimed to geospatially demarcate the land and ocean boundary of Jekyll Island State Park off the coast of Georgia, USA based on different tide level assumptions used by state and federal agencies. Results quantified differences in island size up to 7.2 % depending on jurisdictional sea levels and different back-barrier marshland and ocean-front shoreline elevations in Chapter 2. Beach availability was geospatially assessed for recreational tourism management and vulnerability of shoreline integrity in revetment rock areas in Chapter 3. Finally optimum pansharpening techniques were evaluated using VHR satellite imagery for best geospatial data to identify features in dynamic coastal zones in Chapter 4. These findings will allow coastal managers, residents, and tourists to make appropriate decisions for sustainable development and preservation of coastal barrier islands.

INDEX WORDS: GIScience, remote sensing, LiDAR, coastal barrier island, sustainable development and preservation, Jekyll Island, shoreline change, coastal tourism.

A GISCIENCE FRAMEWORK FOR SUSTAINABLE DEVELOPMENT, TOURISM AND MANAGEMENT OF COASTAL BARRIER ISLANDS IN GEORGIA

by

BYUNGYUN YANG

B.S., Kyung Hee University, Republic of Korea, 2002

M.S., Kyung Hee University, Republic of Korea, 2004

A Dissertation Submitted to the Graduate Faculty of The University of Georgia in Partial Fulfillment of the Requirements for the Degree

DOCTOR OF PHILOSOPHY

ATHENS, GEORGIA

2011

A GISCIENCE FRAMEWORK FOR SUSTAINABLE DEVELOPMENT, TOURISM AND MANAGEMENT OF COASTAL BARRIER ISLANDS IN GEORGIA

by

Byungyun Yang

Major Professor:	Marguerite Madden
Committee:	Thomas R. Jordan
	J. Marshall Shepherd
	Xiaobai Yao
	Lan Mu

Electronic Version Approved:

Maureen Grasso
Dean of the Graduate School
The University of Georgia
December 2011

DEDICATION

This dissertation is dedicated to my family and the people I have met in the Department of Geography at the University of Georgia (UGA). In particular, I want to express my great appreciation for my wife, two daughters, and our expected new baby. Since I began my Ph.D. program in 2007, I have not been able to fully give all of my time to my family, and I am sorry for that. If not for their support, I would not have completed this program. Above all, my beautiful daughters, Yunseo and Yoonsol, with their smiles, laughter and unconditional love, continually remind me of what is important in life. They came into the world and made mine complete. So, I would like to attribute my successes and honors to my wife and growing family. Also, I am deeply appreciative of the support and prayers of my parents. All I have done has been possible because of their unconditional love and belief in me.

Lastly, I dedicate this dissertation to God, my Load, and my beloved wife, my two daughters and a new baby. All I have done to this point has come from all of the support from their heart.

ACKNOWLEDGEMENTS

I extend my gratitude to those I have met at UGA for their assistance in helping me complete my dissertation. In particular, I am grateful to Dr. Marguerite Madden, who is the Director of the Center for Remote Sensing and Mapping Science (CRMS) at UGA and who served as my major advisor. She has always given me expert guidance as a scholar and a mentor and she has always shown me kindness even during difficulties. It is my desire to be a scientist or a professor like her.

I would also like to thank all of my committee members, Drs. Thomas R. Jordan, J. Marshall Shepherd, Xiaobai Yao and Lan Mu who provided valuable advice to me for my doctoral research. Drs. George Brook and Ken Cordell also motivated and encouraged me to carry out my research. Additionally, the faculty of the Department of Geography gave me the opportunity to remain at UGA. Had they not provided me with support for four years, I would have not completed my goal of obtaining a Ph.D. In addition, I would like to express my appreciation to all the staff members of the Geography Department and CRMS.

My work on this dissertation was supported by many. Chapter 2 was supported by the CRMS, the Initiative to Protect Jekyll Island State Park (IPJI) and the Glynn County GIS office. I gratefully acknowledge their financial assistance and shared data in defraying the cost of this research. Chapter 3 was supported by a Dean's Award from the Graduate School of the University of Georgia in spring 2009. I gratefully acknowledge the assistance this award provided me to conduct field work in support of this research. Chapter 4 was supported by three different organizations. I would like to thank the GeoEye Foundation and the Korean Aerospace

Research Institute (KARI) for allowing the use of IKONOS and KOMPSAT II satellite images, respectively. QuickBird satellite imagery was provided by CRMS. Finally, the Korean-American Association for Geospatial Environmental Sciences (KAGES), the America Society for Photogrammetry and Remote Sensing (ASPRS), Environmental and Systems Research Institute (ESRI), the UGA Research Foundation, and the Tourism Sciences Society of Korea (TOSOK), all provided support for conference travel and participation, which was invaluable in my academic and professional development and led to receiving critical feedback used to further develop manuscripts for publication. I acknowledge that the findings and conclusions in this report are those of myself and co-authors.

TABLE OF CONTENTS

Page

LIST OF TABLES

Page

LIST OF FIGURES

Page

CHAPTER 1

INTRODUCTION AND LITERATURE REVIEW

1. 1 Introduction and Study Area

Sustainability has been traditionally used synonymously with words such as long term, durable, sound or systematic (Filho, 2000). In its broadest sense sustainability has economic, social and cultural, political, geographical, and ecological aspects (Aronsson, 2000). When considering the economic aspect, sustainability primarily requires satisfying human material needs and goals; whereas the ecological aspects concern protecting the natural biodiversity and preserving natural cycles (Coccossis and Nijkamp, 1995). According to Travis (1992), the use of the term "sustainability" has become widespread and used in so many different ways that there is no longer a consensus in its meaning. Nevertheless, there has been growing interest in sustainable development towards the goal of reducing human impact so that global ecosystems can continue to indefinitely sustain human life and societies (Sofield, 2003).

The World Conservation Strategy (WCS) defines sustainable development as development "that meets the needs of the present without compromising the ability of future generations to meet their own needs." (WCED, 1987). The WCS also emphasizes the relationship between economic development and the preservation of natural resources (Hall and Lew, 1998). However, economic development and preservation are sometimes perceived to be incompatible because the weight of public opinion may be on one side or the other. In other words, conflicts may arise when individuals have different ideas about development and

preservation depending on their affiliation and perspectives. Therefore, efforts are needed to maintain an appropriate balance to ensure economic and environmental health for future generations.

Coastal areas are particularly prone to conflicts of interest between development and preservation because they embody multiple values as places for residence, commerce, outdoor recreation, wildlife habitat, nurseries of commercial fisheries and ecosystem services (Klein, Osleeb, and Viola, 2004). There is growing concern, however, that increasing human activity and urban sprawl threatens the coastal environment and measures need to be taken to protect coastlines from development pressure. This is especially true for coastlines of barrier islands which are naturally dynamic areas and easily changed over time. That is, barrier islands are rapidly reshaped by: 1) high energy events such as hurricanes, typhoons, tsunamis, earthquakes, and severe storms; 2) constant impacts from wind and tides, and 3) more gradual processes of soil accretion, erosion and sea level rise (Beatley, Brower, and Schwab, 2002). Along the coast of the southeastern United States, for example, the barrier islands of Georgia are subjected to accretion and erosion because of extreme tide ranges and along shore currents. Four of these islands, Tybee Island, St. Simons Island, Jekyll Island, Sea Island (Figure 1.1) have been highly developed to satisfy residential, recreational and commercial needs, and have traditionally favored the consideration of economic development. These islands also act as physical buffers to protect the mainland from damage by storms while serving as recreational destinations for tourists, thus having major environmental and economic impact on coastal communities (Zhang and Leatherman, 2011).

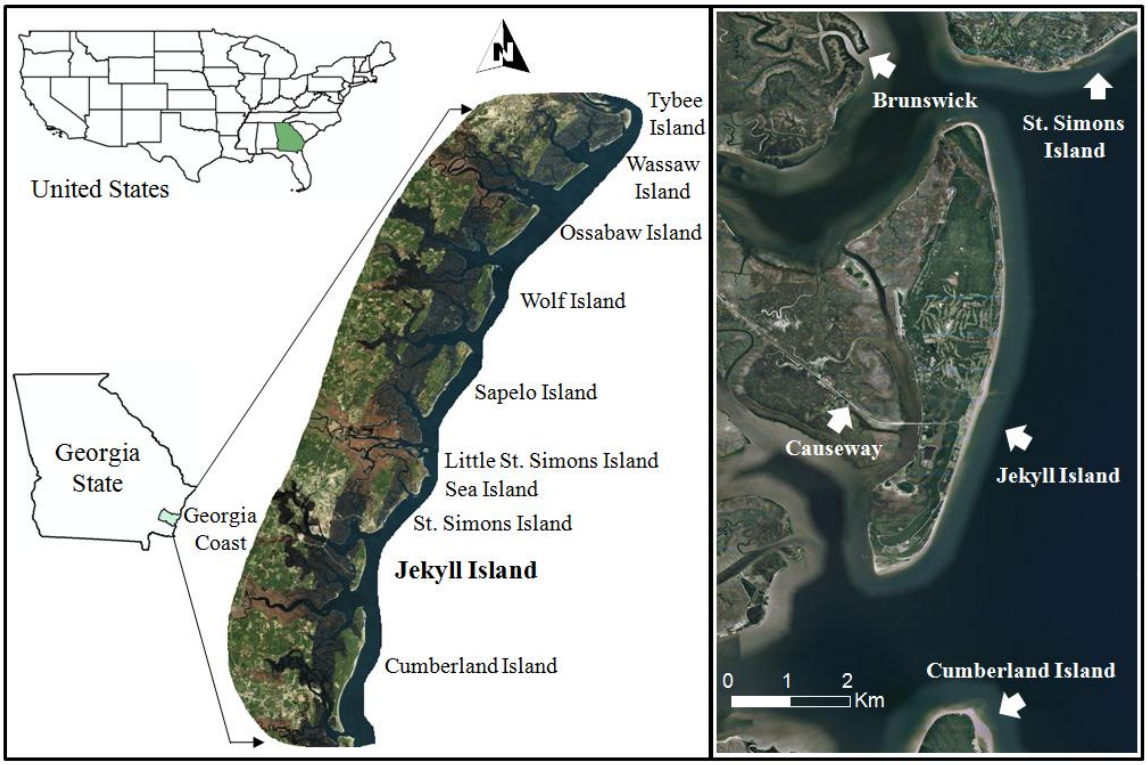

Figure 1.1. Study area (Jekyll Island, GA, USA).

Among the Georgia barrier islands, Jekyll Island was selected for this research because it is a state owned and managed island with growing interest by coastal managers, conservationists and residents to consider both development and preservation concerns (Figure 1.1). Located in Glynn County, Georgia, USA and popularly known as one of Georgia's Golden Isles, Jekyll Island and its neighboring barrier islands have been occupied for thousands of years. Evidence exists that human inhabitation began with Native American occupation dating back to around 2,500 B.C. European occupation began when British General James Edward Oglethorpe established Georgia as a colony in 1732 and named Jekyll Island in honor of his friend, Sir Joseph Jekyll (Bagwell, 2001). In 1794, Christophe Du Bignon, who was a decorated French naval captain, purchased the entire island from the British. Afterward, the Island was used for plantations supported by the labor of slaves. Following the American Civil War (1861-1865),

Christophe Du Bignon and his son, Henri Charles, divided the Island among his four children. From the time of John Eugene Du Bignon's purchase of parts of Jekyll Island from his family in the late 1870s, Jekyll Island had been a winter retreat for some of the wealthiest families in the United States until World War II. The partnership among Du Bignon, his brother-in-law, and the millionaire capitalists such as J.P. Morgan, Joseph Pulitzer, William K. Vanderbilt, Marshall Field, and the Rockefeller family formed the Jekyll Island Club and they had exclusive use of the Island for five generations (Figure 1.2b). The Great Depression and World Wide War II, however, forced the closing of the Jekyll Island Club. Governor Melvin Thompson purchased Jekyll Island from the remaining members for the price of $675,000 in 1947. Since transportation to the Island was only available by boat from St. Simons Island, a causeway and draw bridge were built in 1954 and Jekyll Island was officially opened to the public (Bagwell, 2001). Since 1960, motels, homes, a convention center, shopping centers, and a golf course have been constructed. Now, many retirees reside in Jekyll Island, and annual visitation is estimated at just below 1.5 million (BAG, 2008). It is also a coastal destination for tourists, who enjoy over 16km of unspoiled beaches, historical buildings and natural areas of marsh, dunes and maritime forests (Figure 1.2).

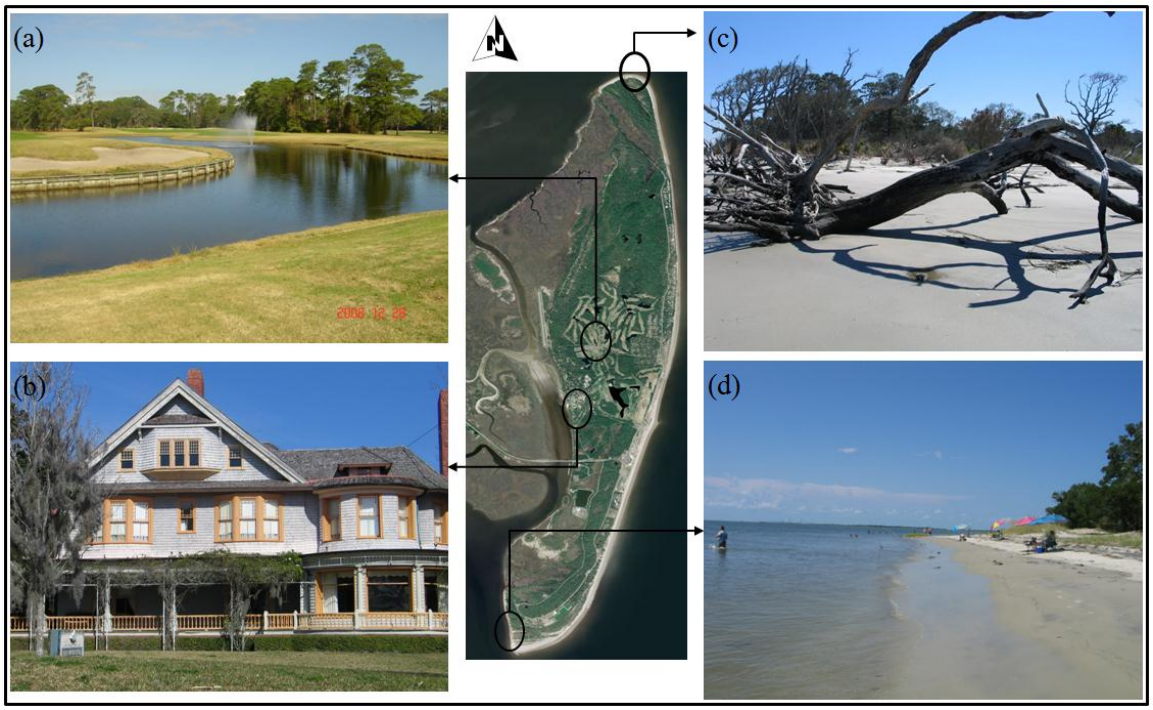

Figure 1.2. Cultural and natural resources: (a) golf course, (b) historical cottage, (c) driftwood, and (d) beach.

The Jekyll Island Authority (JIA) was created in February 1950 under the direction of Governor Herman Talmadge to oversee the Island's management decisions and balance development and use of the Island with the conservation of ecologically valuable resources. Development of the Island and concern for the protection of natural resources led to the State of Georgia 1971 Act, limiting development of Jekyll Island to 35 percent of the total island area. Once this 65/35 undeveloped to developed ratio is reached, artificial structures and impervious surfaces such as tourist resorts, parking lots, or paved roads cannot be built. At the time of the publication of a JIA 1996 Master Plan, the JIA determined about 109 acres of the Island are still available for development (JIA, 1996). In response to subsequent development plans in the early 2000s, a volunteer, non-profit organization named the Initiative to Protect Jekyll Island (IPJI)

was created in 2006 to support preservation of natural areas and unique characteristics of the Island (IPJI, 2009). Jekyll Island is now faced with management issues of balancing tourism and development with resource conservation. The controversy of the future development of Jekyll Island entirely depends on methods to accurately determine the area of developed land relative to the total size of the Island (McDonald, 2010). Additionally, there is a need to develop methods and means to inform policy makers, developers, managers, and conservationists with current status and trends in the use of island cultural and natural resources.

In response to the need for accurate and current monitoring of Jekyll Island, as well as the needs of coastal managers worldwide, the following questions are asked in this research.

1) How can Geography help the private and public sectors in coastal areas?

2) How can we find scientific grounds for better decision-making?

3) How can geographic information science (GIScience) support sustainable development and relieve the conflicts created by differencing points of view?

This research attempts to develop and investigate geographic methods for the balanced promotion of sustainable development, preservation, coastal management, planning and tourism through a case study of one of Georgia's barrier islands. The three manuscripts of this dissertation demonstrate methods in GIScience that provide coastal managers, conservationists, law-makers, and representatives of private and public sectors with geospatial approaches and tools that can be incorporated into a decision making system to perform modeling, representation, and analysis of island processes and human projects.

1.2 Research Objectives

Coastal management issues of sustainable development are global in scope and growing in importance. Approximately 40 % of the world's population currently lives within 50 kilometers of the coast (Small and Nicholls, 2003) and 37 % of the total U.S. population resides in coastal counties considering both ocean and Great Lake Shores (Crowell *et al*., 2007). The global coastal population is vulnerable to the increasing severity and frequency of storm events such as typhoons, hurricanes and tsunamis along with human impacts such as the devastating British Petroleum oil spill affecting the U.S. Gulf Coast during the summer of 2010 (Alvania, 2011). In addition, the global sea level has risen 18 to 59 cm, with one area showing a 4-6 m difference over the past 100 years or more (IPCC, 2007). This trend is predicted to continue at an estimated rate of 32 cm by 2050 and rise of 4-6 m or more after 2100 (IPCC, 2007). Methods, therefore, are desperately needed to assist managers and policy makers in developing of tools for accurately assessing shoreline change, vulnerability to sea level rise and changes in cultural/natural resources. These tools will support a decision making process that will foster economic growth and tourism in coastal zones while simultaneously protecting natural and cultural resources, recreational opportunities and ecosystem services provided by barrier islands, beaches, maritime and mangrove forests, marshes, and fragile dune areas.

In the case of Jekyll Island, Georgia, State legislation limits current development to be less than 35 % of the total size of the Island. Although this is a seemingly simple and straightforward law, it causes many questions to arise for managers. What definitions of developed and undeveloped Land Use Land Cover (LULC) can be used to consistently and fairly to identify the percentage of developed land? What is the methodology for most accurately measuring the total size of dynamic environments such as coastal barrier islands? Has the

percentage of developed land on Jekyll Island changed since the JIA 1996 Master Plan? How can we monitor coastal areas and manage the construction of retaining structures and revetment rocks, especially pertaining to beach availability and the quality of sandy beaches that are highly prized by tourists and fundamental to the survival of the endangered loggerhead sea turtle? Can we utilize GIScience in general and geospatial data and analyses in particular, to detect, monitor and spatially assess coastal areas towards best practices of coastal development and disaster response?

In response to these challenges, this dissertation calls for advanced GIScience methodologies that address the following considerations: (1) How can coastal barrier islands be accurately demarcated to measure their size and assess suitability for development and preservation?; (2) Is it possible to assess the spatio-temporal quality, quantity and availability of sandy beaches for tourism and recreational purposes?; (3) Do revetment rocks act as a protector to the mainland and can they be monitored for long-term effectiveness for coastal preservation?; and (4) Will very high resolution satellite images provide managers with insights to optimum conditions for development, document trends in LULC and provide image backdrops for communication of management plans to the general public? Based on these considerations, this dissertation aims to address GIScience methods and theory that can be applied to coastal management based on the following objectives.

1. Assess emerging geospatial technologies such as Light Detection and Ranging (LiDAR) and very high resolution satellite image data to determine the best methods to accurately estimate the total area of a coastal barrier island considering sea level datums, remote sensing data availability and differences between the back-barrier and ocean- front shoreline delineation.

2. Use LiDAR and photogrammetry-based shoreline change analysis of the dry beach and spatial statistics for shoreline change trends to support the creation of a geospatial tool for tourism purposes and for urban planners who manage coastal zones for flood and storm event protection.

3. Estimate soil accretion and erosion of coastal barrier islands based on historical shoreline datasets and current LiDAR-derived shorelines to identify areas vulnerable to sea level rise.

4. Simulate shoreline movements referenced to historical tidal records using LiDAR multiple return points to identify stretches of barrier island beaches and revetment rocks that are vulnerable to storm surges and sea level rise.

5. Analyze image fusion operators and image data from different satellite programs to assist in applications of LULC for coastal mapping and monitoring.

In sum, methods developed in this research are aimed to allow coastal managers, law-makers, and public sectors to make better decisions with reliable findings. The methods are intended to be used for future master plans for sustainable development and preservation of Jekyll Island, but they also may be applied to coastal concerns worldwide.

1.3 Literature Review

1.3.1 Previous Management of Jekyll Island

Since Jekyll Island opened to the public after 1960, many development projects have been undertaken, such as the construction a of hotels, houses, golf course, a draw bridge, marina facilities, a 4-H center, and a convention center. Guiding this development, these have been three

master plans, prepared in 1973, 1981, and1983 by the Jekyll Island Authority (JIA) that have guided the Island's development (McDonald, 2010). The 1981 study observed that "there has been considerable debate on how much of Jekyll Island can be developed and leased." At the time, State Law 1971 was interpreted to mean that the JIA could not sell or lease more than 35% of the Island's area (McDonald, 2010), but currently, the Law is seen as imposing a ban on development if the current development level exceeds 35% of the Island's area. In 1997, the JIA produced a Fact Sheet which called for the Governor and Legislature to increase tourism on Jekyll Island. Another study projected by Hammer, Siler, George Associates which included market analysis aimed at increasing visitation to the Island (Hammer, 1981). In 1983, The University of Georgia's Institute for Community and Area Development (ICAD) produced a Comprehensive Land Use Plan for the JIA. This project stated that "a linear belt of land lying along the beach shall be classified as a 'zone of no encroachment'." However, according to McDonald (2010), these recommendations had been ignored in the development planning in the first decade of the 21st century.

In March 1995, a new master plan for the management, preservation, protection, and development of Jekyll Island was required, and the 1996 Master Plan was completed to delineate the Island based upon an aerial survey and a land survey (JIA, 1996). Additionally, the master plan investigated the present and future uses of the Jekyll land area, which lies above water at mean high tide. The project was supervised by the JIA and was completed by the project team of Robert Charles Lesser & Co. and Tunnell-Spangler & Associates. Based on the 1996 Master Plan, the issue of developable lands in Jekyll Island State Park was addressed, and a draft revised Master Plan was released in 2004 (JIA, 1996 and 2004). Delineation of the Island was based on 1:6,000-scale, 1980 aerial photographs, field surveys and a shoreline of 1.31-m (4.3 ft) above

mean high water (MHW) referenced to the National Geodetic Vertical Datum of 1929 (NGVD 29). At the time of the 1996 Master Plan, there were about 0.44 km² (109 acres) (2.6% out of 35%) of the Island that were still available for development. State plans to renovate some existing structures and expand development in the mid-2000s met with opposition by groups with environmental concerns and led to the 2006 formation of the volunteer, non-profit organization named the Initiative to Protect Jekyll Island State Park (IPJI) (IPJI, 2009). The objective of the IPJI is to collect public opinion on Jekyll redevelopment and to engage in a wide range of educational and outreach activities, research, and information dissemination (McDonald, 2010). In 2009, they requested a recalculation of the amount of developed area from the University of Georgia Center for Remote Sensing and Mapping Science (CRMS), and CRMS calculated a value of 33.2% using LiDAR data and airborne digital camera imagery taken in 2007 and 2006, respectively. Details of this work are provided in Chapter 2. Afterward, the JIA also recalculated the total of developed area, and reached a result similar to that of CRMS. Thus, the 0.44 km² (109 acres) amount was readjusted in 2010 to 0.40 km² (99 acres).

In contrast with development planning, the JIA also made a conservation plan in 2006 conducted by the Cabin Bluff Land Management Inc. This project summarized Jekyll Island's natural history and important natural values, and then outlined the management activities that are needed to maintain and enhance the ecologic and economic values associated with the Island's natural resources (Cabin Bluff Management, 2007). A subsequent conservation plan was produced in July 2011 by the Architecture, Engineering, Consulting, Operations and Management (AECOM) which is a professional technical and management support services firm (AECOM, 2011). The 2011 Conservation Plan created a framework for protecting and managing the natural resources of Jekyll Island in cooperation with the Georgia Department of Natural

Resources (GDNR) which conducted extensive work on Jekyll Island from 2007 through 2010. This Conservation Plan is differentiated from the previous conservation plan, when it comes to specific classifications for both natural resources (undeveloped items) and urban areas (developed areas) which have been defined by the JIA. However, the 2011 Conservation Plan does not provide details on the methods or scientific grounds used to determine the total area of the Island, nor their definitions for the classification of developed and undeveloped areas.

In response to the development and conservation plans described above, several questions may be raised. What are the reasonable and scientific methods for the demarcation of State boundaries of coastal public lands? What is the best monitoring system to maintain a sustainable conservation plan? Furthermore, what geospatial methods can be used for assessing natural resources while simultaneously satisfying development aspects? With respect to these considerations, this research draws on geographic information science (GIScience) principles and techniques such as the use of very high resolution satellite imagery, airborne digital camera imagery, and Light Detection and Ranging (LiDAR) to derive geospatial information in support of sustainable development and conservation of coastal barrier islands.

1.3.2 Geospatial Approaches for Barrier Island Management

Shoreline Delineation

Today, GIScience is commonly used in many fields as the scientific use and study of methods and tools for the capture, storage, distribution, analysis, display, and exploitation of geocoded information (Longley, 2010). The theoretical principles of GIScience are used for conceptualizations, models, representations, and spatial analysis for geographic phenomena (Burrough, 2002; Goodchild, 2003). More specifically, GIScience contributes to the creation of

a spatial decision supporting system (SDSS) that enables planners and scientists to make sound management decisions based on accurate geographic information (Longley, 2010; Madden,2004 and Madden *et al*,. 2009). Especially in cases of coastal studies, we can recognize the benefit of using tools and methods including LiDAR, spatial analysis, spatial statistics, remote sensing techniques, geodatabase construction and distribution via Web-based GIS servers for maintain current data in dynamic environments.

This research attempted to assess geospatial methods for coastal studies in terms of measuring shoreline change, coastal processes of erosion and accretion and coastal feature delineation. Studies related to shoreline changes have been conducted (Dolan *et al*., 1980; Crowell *et al.,* 1991; Martin, 1997; Morton and Speed, 1998; Moore, 2000; Overton *et al*., 1999; Langley *et al*., 2003; Overton and Fisher, 2003; Crowell *et al*., 2007). Recent studies of the historical changes in the MHW shoreline of Georgia indicate that there are several basic causes of shoreline change including accretion and erosion. First is the worldwide rise in sea level (an average of 1.0to 0.61-m per century). Second is seasonal storms and hurricanes. Although the Georgia coast has not had a major hurricane (defined as at least a category 3 hurricane) since the late 1890s, hurricanes forced in the Atlantic Ocean each year have the potential of directly or indirectly impacting the Georgia Coast (Henry, 2005). Third is human impact by activities, including channel dredging with offshore disposal of dredged material, jetty construction, shoreline structures, and damming of rivers. Therefore, shoreline change is a complex process and regular monitoring and analysis should be conducted using the most advanced geospatial methods.

Regarding the above information, the methodological approach to coastal mapping and shoreline delineation was traditionally organized into three major categories: ground surveying,

photogrammetric measurement of remotely sensed images and modern LiDAR technology (Chen and Rau, 1998). Ground surveying using traditional Total Station (TS) surveying equipment and Global Positioning System (GPS) survey techniques are the most accurate methods, but also are the most time consuming and labor intensive (Bossler, 2010). Remote sensing and photogrammetry are useful means of making accurate shoreline measurements over large areas from above ground images such as airborne aerial photographs (including digital camera images) and spaceborne satellite images (Dolan *et al*., 1980; Crowell, Leatherman, and Buckley, 1991; Martin, 1997; Morton and Speed, 1998; Overton *et al*., 1999; Moore, 2000; and Overton and Fisher, 2003). However, users of the spaceborne imagery have limited control over the timing of satellite data acquisitions. Air photo acquisition, on the other hand, is more flexible and can be custom planned to coincide with a particular tidal stage.

The manual interpretation of aerial photographs as a technique for detecting shoreline change began in the late 1950's (McCurdy, 1950; Dolan *et al.,* 1978 and 1980; Anders *et al.,* 1991). From an image, the wet/dry shoreline is interpreted from aerial photography and this line has traditionally been used to represent the shoreline and calculate shoreline change rate (Dolan *et al*., 1980; Crowell, Leatherman, and Buckley, 1991; Martin, 1997; Morton and Speed, 1998; Overton *et al*., 1999; Moore, 2000; and Overton and Fisher, 2003). The wet/dry line position, however, is real-time wave and tide dependent (Martin, 1997). In some instances, the wet/dry line can be considered equivalent to or an approximation of the often-used high water line, which has received thorough scientific attention (Moore *et al*., 2010). Although wet/dry line position can define a real shoreline at a specific time, the exact MHW level cannot be recognized on aerial photographs. The MHW level has been used officially in Georgia State legislation as the

shoreline that defines the boundary between land and sea (NOAA, 2011). Therefore, a geospatial method of mapping this tidal stage is important to barrier island managers.

LiDAR

In recent years, a new altimetry technology has been used to extract MHW shorelines from topographic LiDAR data. Although expensive to acquire, airborne topographic LiDAR can generate high-resolution elevation data over large areas relatively quickly and is particularly useful for coastal applications because vertical measurements are accurate to approximately ±15 cm for bare earth points (Pe'eri and Long, 2011). LiDAR surveys have been used to investigate, for instance, large-scale beach morphology (Stockdon *et al*., 2002), human impacts in the coastal zone (Thornton *et al*., 2006), and sea cliff failure and hurricane-induced beach change (Robertson e*t al.*, 2007). If empirical data exist for tide levels over an extended period of time, then a MHW sea level can be computed. This sea level can then be extracted from the LiDAR DEM to create a shoreline dataset.

Image Fusion of VHR Satellite Images

In another approach for the application of remote sensing for coastal studies, image fusion methods are introduced in this section as a technique for automated coastal mapping. Image processing algorithms for image fusion, also known as pansharpening, provide methods for combining high spatial resolution panchromatic images with lower spatial resolution multispectral images to produce fused images at the finest spatial resolution and containing color information from the multiple spectral bands (Cliche´ *et al*., 1985; Welch and Ehlers 1987; Ehlers, 1991). More specifically, the fused image generated by fusion methods using VHR

satellite images permit better interpretation to identify small ground features by LULC classification. Image fusion techniques that were developed in the mid 1980s were subsequently assessed to evaluate the quality of the resulting fused images (Welch and Ehlers 1987; Ehlers, 1991; Ling *et al*., 2007; Ling *et al*., 2008). The fused images were found to enhance the information content provided by remotely-sensed images for interpretation and analysis for many applications including mapping urban surface features, vegetation and rural land use (Couloigner *et al*., 1998; Dai and Khorram, 1999; Kurz, 2000; Lau, 2000; Tu *et al*., 2001; Chen *et al*., 2003; Sun *et al*., 2003).

Following Pohl and Genderen (1988) and Gangkofner (2008), image pansharpening techniques can be categorized into three types: spectral (or component) substitution, arithmetic transform, and spatial-domain merge. Spectral (or component) substitution techniques involve resampling the two images to a common spatial resolution, usually the finest pixel size, converting a multispectral image (e.g., Red, Green, Blue or RGB) into its color components (e.g., Intensity, Hue, Saturation or IHS), and replacing intensity values with digital values of a high spatial resolution panchromatic image in image fusion. Arithmetic merging methods conduct pixel-level arithmetic operations with panchromatic and multispectral images during an image fusion procedure. Multiplicative (MP) and Brovey transform (BT) belong to the arithmetic pansharpening technique. Spatial-domain fusion techniques derive spatial information from a panchromatic image that is injected into a multispectral image in a fusion procedure (Aiazzi *et al*., 2002; Klonus and Ehlers, 2007; and Ranchin *et al*., 1997). High pass filter (HPF), subtractive resolution merge (SRM), and wavelet-based transform are classified as spatial-domain methods. Details about the algorithms and procedures for implementing these image fusion techniques are provided in Appendix I.

Although fused images combine the favorable aspects of high spatial and high spectral resolution images, they also may maintain spatial distortions and/or sub-optimal spectral characteristics caused by the resampling and fusion process. The results, therefore, need to be assessed using both qualitative and quantitative approaches to determine the spectral similarity of the pansharpened image with the original input multispectral scene. Generally, visual assessment is a qualitative approach that is typically used and enables us to see overall color similarity between fused and original multispectral images. This technique, however, can be controversial because of human subjectivity (Li *et al*., 2000). On the contrary, quantitative approaches such as correlation coefficients (CC), relative difference to mean and standard deviation (See Appendix I for details), provides numeric indices to overcome the subjectivity of visual comparisons (Karathanassi *et al*., 2007; Kim *et al*., 2011). The use of proper image fusion techniques may be critical for coastal resources managers who require optimal VHR satellite imagery for determining fine details on the current status of coastal development in compliance of development policy and laws.

1.4 Dissertation Structure

This dissertation presents a variety of scientific approaches in GIScience that may be used to support a reliable decision making system for sustainable development and preservation plans of Jekyll Island State Park. First, in Chapter 2, this study attempts to analyze the demarcation of Jekyll Island State Park considering a number of environmental policies, regulations, and laws Geospatial data such as aerial photography and LiDAR were used to create geographic information system (GIS) shapefiles that define sea levels and outline the shoreline of Jekyll Island State Park. In Chapter 3, geospatial analysis of beach availability was conducted

for recreational tourism management on Jekyll Island. Aerial digital imagery, in combination with LiDAR data and GIS mapping and analysis, were employed to delineate accurate shorelines with regard to accessible and available beach area. In addition, a Web-based GIS application was developed to provide tourists, residents and coastal manager with GIS and field-based data in a user-friendly map interface. Additionally, a LiDAR-derived simulation was created to visualize and monitor shoreline changes related to revetment rocks placed on sandy beaches to prevent erosion. Chapter 4 presents an assessment of image fusion approaches to quantify best pansharpening results compared to original panchromatic and multispectral images to be utilized for barrier island research. The results were assessed by spectral and spatial quality assessments. A summary and conclusions are finally presented in Chapter 5.

References

AECOM, 2011. *Jekyll Island Conservation Plan*, Orlando, Florida: AECOM, 79p.

Aiazzi, B., Alparone, L., Baronti, S., and Garzelli, A., 2002. Context-driven fusion of high spatial and spectral resolution images based on oversampled multiresolution analysis. *IEEE Transactions on Geoscience and Remote Sensing* 40(10), 2300-2312.

Alvania, R., 2011. Silk Science: Will new BP funds keep Gulf genomics afloat?. *Cell* 146 (3), 343-345.

Anders, F.J. and Byrnes, M.R., 1991, Accuracy of shoreline change rates as determined from maps and aerial photographs, *Shore and Beach* 59(1), 17-26

Aronsson, L., 2000. *The Development of Sustainable Tourism*. London, New York: Continuum, 193p.

Bagwell, T. E., 2001. *Images of America: Jekyll Island State Park A State Park*, Charleston, SC: Arcadia Publishing, 272p.

Beatley, T. Brower, D.J., and Schwab, A.K., 2002. *An Introduction to Coastal Zone Management* (2nd ed.), Washington, D.C.: Island Press, 329p.BAG (Bleakly Advisory Group)., 2008. Analysis of Long Term Impacts of Development on Jekyll Island: Preliminary Revitalization & Fiscal Forecasts. *Jekyll Island State Park Authority*, http://www.savejekyllisland.org/Visitation_Analysis_Business_Plan_09_15_Board_Presentation.pdf (Accessed 01.27.2011).

Bossler, J.D., Campbell, J.B., McMaster, R.B., Rizos, C., 2010. *Manual of Geospatial Science and Technology* (2nd ed.), Boca Raton, FL: CRC Press/Taylor & Francis, 648p.

Burrough, P.A., 2002. Geographic information systems and science. *International Journal of Geographical Information Science* 16(5), 505-507.

Cabin Bluff Management, 2007. *Jekyll Island State Park Conservation Plan*.

Chen, L. C., and Rau, J. Y., 1998. Detection of shoreline changes for tideland areas using multi-temporal satellite images. *International Journal of Remote Sensing* 19(17), 3383-3397.

Cliché, G., Bonn, F., and Teillet, P., 1985. Integration of the SPOT Pan channel into its multispectral mode for image sharpness enhancement. *Photogrammetric Engineering and Remote Sensing* 51(3), 311–316.

Coccossis, H. and Nijkamp, P., 1995. *Sustainable Tourism Development*. Avebury, Aldershot, USA; Brookfield, 198p.

Couloigner, I., Ranchin, T., Valtonen, V.P., and Wald, L., 1998. Benefit of the future SPOT-5 and of data fusion to urban roads mapping. *International Journal of Remote Sensing* 19(8), 1519-1532.

Crowell, M., Leatherman, S.P., and Buckley, M.K., 1991. Historical shoreline change - error analysis and mapping accuracy. *Journal of Coastal Research* 7(3), 839-852.

Crowell, M., Edelman, S., Coulton, K., and McAfee, S., 2007. How many people live in coastal areas? *Journal of Coastal Research* 23(5), Iii-Vi.

Dai, X. and Khorram, S., 1999. Data fusion using artificial neural networks: a case study on multitemporal change analysis. *Computers Environment and Urban Systems* 23(1), 19-32.

Dolan, R.; Hayden, B.P., and Heywood, J., 1978. A new photogrammetric method for determining shoreline erosion. *Coastal Engineering* 2(1), 21–39

Dolan, R., Hayden, B.P., May, P., and May, S.K., 1980. The reliability of shoreline change measurements from aerial photographs. *Shore and Beach* 48(4), 22-29.

Ehlers, M., 1991. Multisensor image fusion techniques in remote sensing. *ISPRS Journal of Photogrammetry and Remote Sensing* 46(1), 19–30.

Filho, W.L., 2000. Dealing with misconceptions on the concept of sustainability, *International Journal of Sustainability in Higher Education* 1(1), 9 – 19.

Gangkofner, U.G., Pradhan, P.S., and Holcomb, D.W., 2008. Optimizing the high-pass filter addition technique for image fusion. *Photogrammetric Engineering and Remote Sensing* 74(9), 1107-1118.

Goodchild, M.E., 2003. Geographic information science and systems for environmental management. *Annual Review of Environment and Resources* 28, 493-519.

Hall, C.M., and Lew, A.A., 1998. *Sustainable Tourism: A Geographical Perspective*. Harlow, Essex, Eng.: Longman, 236p.

Hammer and Company Associates, Wallace Roberts & Todd., 1981. *Plan and Development Recommendations. Jekyll Island, Georgia*. Hammer, Siler, George Associates, Atlanta, GA.

Henry, V. J. (2005). *Jekyll Island Erosion*. The new Georgia encyclopedia, http://www.georgiaencyclopedia.org/nge/Article.jsp?id=h-2777 (Accessed 10.09. 2009).

IPJI, 2009. The Initiative to Protect Jekyll Island State Park (IPJI): Who We Are and What We Stand For. http://www.savejekyllIsland.org/who.html (Accessed 04.04.2009).

IPCC (Intergovermental Panel on Climate Change), 2007. *Summary for Policymakers, in Parry, M.L., Climate Change 2007: Impacts, Adaptation and Vulnerability*. Contribution of Working Group II to the Fourth Assessment Report of the Intergovermental Panel on Climate Change, Cambridge university Press, Cambridge, United Kingdon and New York.

JIA, 1996. *The Jekyll Island State Park State Park Authority (JIA): Final Master Plan for The Management Preservation, Protection, and Development of Jekyll Island State Park*. http://www.jekyllislandauthority.org (Accessed 08.02. 2008).

JIA, 2004. *Jekyll Island State Park Island-wide Master Plan Update*. http://www.jekyllislandauthority.org (Accessed 04.05.2011).

Karathanassi, V., Kolokousis, P., and Ioannidou, S., 2007. A comparison study on fusion methods using evaluation indicators. *Internaional Journal of Remote Sensing* 28(10), 2309-2341.

Kim, M., Holt, J.B., and Madden, M., 2011. Comparison of Global-and Local-scale Pansharpening for Rapid Assessment of Humanitarian Emergencies. *Photogrammetric Engineering and Remote Sensing* 77(1), 51-63.

Klein, Y. L., Osleeb, J. P., and Viola, M. R., 2004. Tourism-generated earnings in the coastal zone: A regional analysis. *Journal of Coastal Research* 20(4), 1080-1088.

Klonus, S., and Ehlers, M., 2007. Image fusion using the Ehlers spectral characteristics preservation algorithm. *GIScience and Remote Sensing* 44(2), 93-116.

Kurz, F., 2000. Empirical estimation of vegetation parameters using multisensor data fusion. *International Archives of Photogrammetry and Remote Sensing* 33, 733-737.

Lau, W., 2000. The influences of image classification by fusion of spatially oriented images. *International Archives of Photogrammetry and Remote Sensing* 33, 752-759.

Langley, S.K. Alexander, C.R. Bush, D.M., and Jackson, C.W., 2003. Modernizing shoreline change analysis in georgia using topographic survey sheets in a GISEnvironment. In: Byrnes, Mark R., Crowell, Mark, and Fowler, Cindy, (eds.), *Shoreline Mapping and Change Analysis: Technical Considerations and Management Implications*, Journal of Coastal Research Special Issue No. 38, pp. 168-177.

Li, Y.Y., Venkatesh, Y.V., and Ko, C.C., 2000. Multisensor image fusion using influence factor modification and the ANOVA methods. *IEEE Transactions on Geoscience and Remote Sensing* 38(4), 1976-1988.

Ling, Y.R., Ehlers, M., Usery, E.L., and Madden, M., 2007. FFT-enhanced IHS transform method for fusing high-resolution satellite images. *ISPRS Journal of Photogrammetry and Remote Sensing* 61(6), 381-392.

Ling, Y.R., Ehlers, M., Usery, E.L., and Madden, M., 2008. Effects of spatial resolution ratio in image fusion. *International Journal of Remote Sensing* 29(7), 2157-2167.

Longley, P., 2010. *Geographic Information Systems and Science* (3rd ed.), Chichester, Englandk: John Wiley and Sons, 560p.

Martin, J., 1997. *Analysis of the Wet/Dry line as an Indicator of Shoreline Position on a Sand Beach*. Master Thesis, North Carolina State University, 71p.

Madden, M., 2004. Remote sensing and GIS methodologies for vegetation mapping of invasive exotics, *Weed Technology* 18, 1457-1463.

Madden, M., Jordan T., Kim, M.N., Allen, H., and Xu, B., 2009. Integrating remote sensing and GIS: From overlays to GEOBIA and geo-visualization. In: Madden M, (ed.) *Manual of Geographic Information Systems*, Chapter 36, Bethesda, MD: American Society for Photogrammetry and Remote Sensing (ASPRS), 701-720p.

McDonald, B., 2010. *Remember Jekyll Island State Park*. Minneapolis, MN: Langdon Street Press, 290p.

McCurdy, P.G., 1950. Coastal delineation from aerial photographs. *Photogrammetric Engineering* 16(4), 550–555.

Moore, L.J., 2000. Shoreline mapping techniques, *Journal of Coastal Research* 16(1), 111-124.

Morton, R.A., and Speed, F.M., 1998. Evaluation of shorelines and legal boundaries controlled by water levels on sandy beaches*, Journal of Coastal Research* 14(4), 1373-1384.

NOAA, 2011. *Shoreline Website: a Guide to National Shoreline Data and Terms* (Boundary Determination). http://www.ngs.noaa.gov/RSD/coastal/importance.html (Accessed 09.27.2011).

Overton, M.F., Grenter, R.R., Judge, E.K., and Fisher, J.S., 1999. Identification and analysis of coastal erosion hazard areas: Dare and Brunswick Counties, North Carolina., In: Crowell, Mark; and Leatherman, S.P. (eds.), Coastal Erosion Mapping and Management*, Journal of Coastal Research* Special Issue. No. 28, pp. 69-84.

Overton, M.F., and Fisher, J.S., 2003. *The 1998 Long-term Erosion Rate Update for the North Carolina Shoreline*. NC Department of Environment and Natural Resources, Division of Coastal Management, Raleigh, NC, 17p.

Pe'eri, S., and Long, B., 2011. LIDAR technology applied in coastal studies and management. In: Pe'eri, S. and Long, B. (eds.), Applied LIDAR Techniques, *Journal of Coastal Research*, Special Issue, No. 62, pp. 1–5.

Pohl, C., and Van Genderen, J.L., 1998. Multisensor image fusion in remote sensing: concepts, methods and applications. *International Journal of Remote Sensing* 19(5), 823-854.

Ranchin, T., Mangolini, M., and Wald, L., 1997. Fusion of satellite images of different spatial resolutions: assessing the quality of resulting images. *Photogrammetric Engineering and Remote Sensing* 63(6), 691-699.

Robertson, W., Zhang, K.Q., and Whitman D., 2007. Hurricane-induced beach change derived from airborne laser measurements near Panama City, Florida, *Marine Geology* 237 (3/4), 191-205.

Small, C. and Nicholls, R.J., 2003. A global analysis of human settlement in coastal zones. *Journal of Coastal Research* 19(3), 584-599.

Sofield, T.H.B., 2003. *Empowerment for Sustainable Tourism Development* (1st ed.), Pergamon, Amsterdam; Boston, 401p.

Sun, W.X., Heidt, V., Gong, P., and Xu, G., 2003. Information fusion for rural land-use classification with high-resolution satellite imagery. *IEEE Transactions on Geoscience and Remote Sensing* 41(4), 883-890.

Stockdon, H. F., Sallenger, A. H., List, J. H., and Holman, R. A., 2002. Estimation of shoreline position and change using airborne topographic lidar data. *Journal of Coastal Research* 18(3), 502-513.

Thornton, E.B., Sallenger, A., Sesto, J.C., Egley, L., McGee, T., and Parsons, R., 2006. Sand mining impacts on long-term dune erosion in southern Monterey Bay. *Marine Geology*, 229, 45-58.

Travis, A.S., 1992. *Sustainable Tourism Planning and Development: A Paper for Norway and Sweden*. In: Aronsson, Lars. 2000. The Development of Sustainable Tourism. Continuum, Wellington House.

Tu, T.M., Su, S.C., Shyu, H.C., and Huang, P.S., 2001. A new look at IHS-like image fusion methods. *Information Fusion* 2(3), 177-186.

Welch, R., and Ehlers, M., 1987. Merging multiresolution Spot HRV and Landsat TM data. *Photogrammetric Engineering and Remote Sensing* 53(3), 301-303.

WCED, 1987. *Our Common Future. - The World Commission on Environment and Development (WCSD)*. Chair: Gro Harlem Brundtland. Oxford, UK: Oxford University Press, p400.

Zhang, K., and Leatherman, S., 2011. Barrier island population along the U.S. Atlantic and Gulf Coasts. *Journal of Coastal Research* 27(2), 356-63.

CHAPTER 2

GEOSPATIAL APPROACH FOR DEMARCATING JEKYLL ISLAND STATE PARK: GEORGIA BARRIER ISLAND[1]

[1] Yang, B. Y., Madden, M., Jordan, T. R. and Cordell, K.H., 2012. *Ocean & Coastal Management* 55(1), 42-51. Reprinted here with permission of ELSEVIER.

Abstract

Demarcation of the upland and water/marsh boundary is a critical issue for management and protection of barrier island ecosystems. Most accurate, precise and confident approaches are required to resolve conflicts related to developable lands and conservation areas. Barrier islands are especially prone to these conflicts because they are highly dynamic systems that are formed and reformed by the rise and fall of tides and seal levels. In response, this research analyzes the demarcation of Jekyll Island State Park, Georgia, USA that is faced with management issues of balancing tourism and development with resource conservation. Questions addressed by this research include: (1) What are the standard sea levels used to demarcate barrier islands? (2) What are the best methods for most accurately estimating the total area of coastal barrier islands? (3) Do differences in tide elevations between back-barrier and ocean-front shorelines of barrier islands exist? Specifically, this research considers a number of environmental policies, regulations, and laws along with geospatial data such as aerial photography, Light Detection and Ranging (LiDAR) and GIS shapefiles. These data are used to define sea levels and outline the Jekyll Island State Park based on Mean High Water (MHW) levels with respect to 0.79-m, 0.85-m, 0.94-m, 1.00-m, and 1.49-m sea levels for the entire Jekyll Island State Park. The demarcations of different back-barrier marshland and ocean-front side shorelines of the Island were also considered. Results indicate that the total area of Jekyll Island State Park may vary by as much as 3.31-km² or 7.2 % depending on the jurisdictional sea level that is used to demarcate the Island boundary.

Key words: Sustainable development and conservation; Aerial photograph; LiDAR; Geospatial data; Barrier islands; Barrier island tide elevations; Coastal island area; Coastal tourism.

2.1 Introduction

Delineating coastal boundaries, and thereby demarcating the outline of barrier islands, is critical to resource managers, government administrators, developers and scientists specializing in coastal processes and impacts of climate change. Barrier islands are constantly changing, perpetually reformed by the conflicting processes of soil erosion and accretion and are forever affected by the ocean's rise and fall (Hoyt, 1967). Despite a 400-year history of coastal mapping along the eastern shoreline of the United States, there is still no clear delineation of the coast and boundaries of barrier islands.

This study is about the demarcation of Jekyll Island State Park off the Georgia coast (United States) which is essential to the legal management, development and conservation of an ecologically valuable national heritage (Figure 2.1). The State-owned and managed island is rich in both cultural and natural resources. From around 2,500 B.C, Native Americans inhabited Jekyll Island and Colonists (first European occupation by the Spanish) arrived there in the late sixteenth century. In 1733, James Oglethorpe established the English colony of Georgia at the location of the present-day city of Savannah. Jekyll had been named by General Oglethorpe to honor his friend, Sir Joseph Jekyll (McCash, 2005). Over the next many years, Jekyll Island was privately owned by wealthy residents and after 1950, the Island became a part of the State Parks system of Georgia.

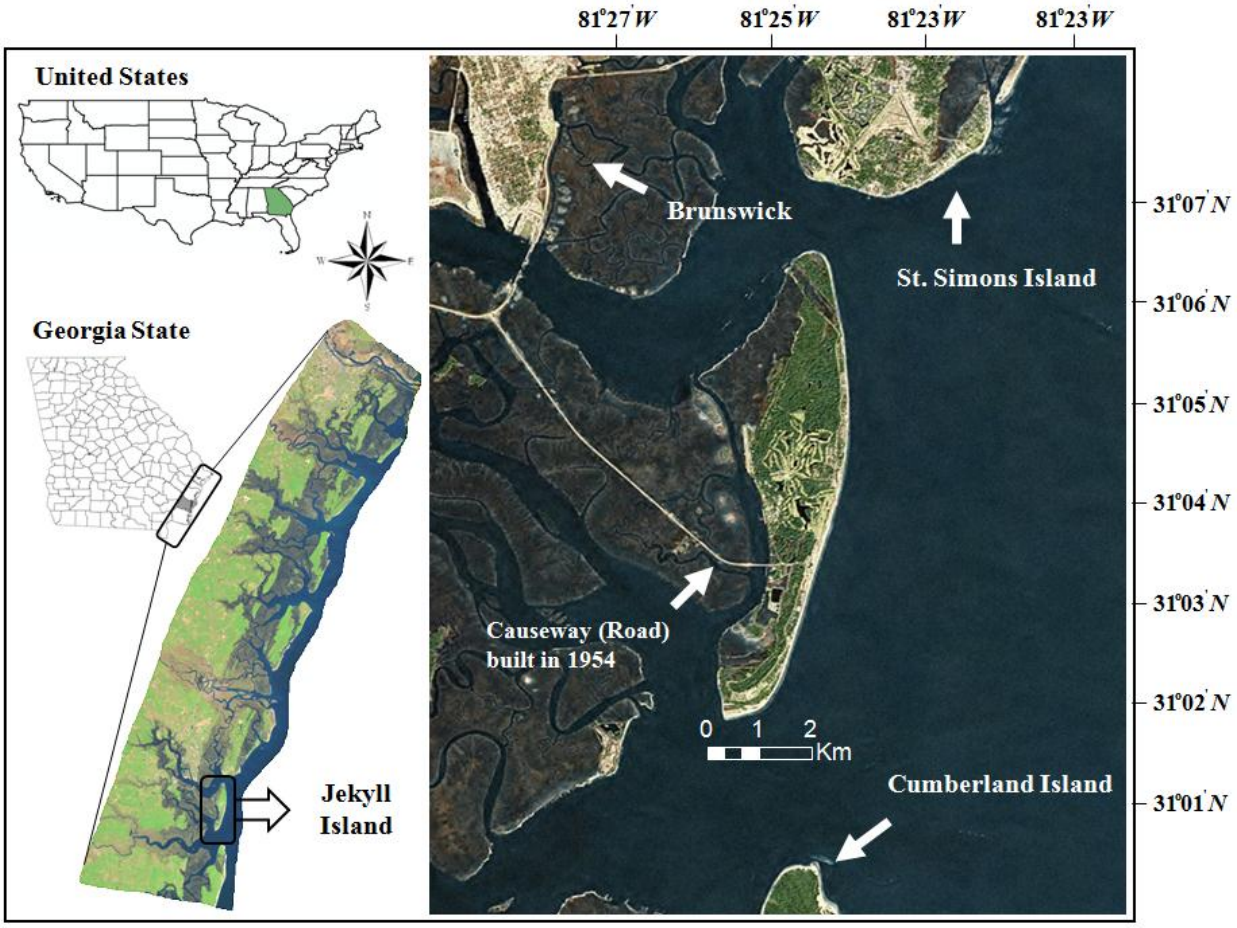

Figure 2.1. Jekyll Island State Park (Aerial digital imagery with 0.15-m spatial resolution, *source*: Glynn County, GA).

Today, the Island is operated by the Jekyll Island State Park Authority (JIA) which oversees both development and preservation of natural and cultural resources (Hunter, 2008). It offers a diversity of habitats including marine, beach, dune, saltwater marsh, upland, and freshwater that support an estimated 845 plant species, 219 invertebrates, 215 fish, 41 amphibians, 66 reptiles, 346 birds, and 50 mammal species, as well as over 16-km of unspoiled beaches (Cabin Bluff Management, 2007). At present, Jekyll Island State Park is protected by the State of Georgia 1971 Act No. 427, and development is limited to 35 % of the total island area.

Once this 65/35 ratio for undeveloped-to-developed area is reached, artificial structures and impervious surfaces such as tourist resorts, parking lots, or paved roads cannot be built. In response, the law has evoked controversy among conservation advocates, coastal planners and developers. State Park managers also need to improve visitor amenities while protecting island resources. The issue of percentage of developed land is directly related to demarcation of the Island boundary. Consequently, Georgians require methods for accurately delineating the boundary of Jekyll Island State Park, defining upland from ocean and marshland and defining developed and undeveloped areas.

Regardless of the point of view, there is a need for methods that are most accurate and reasonable to demarcate the area of the Island. According to Georgia State legislation, when defining a boundary between privately owned upland and public submerged land, a tidal datum is used to establish the shoreline at the Mean High Water (MHW) level (NOAA, 2011a). However, barrier islands are separated from the mainland and marsh zones exist between barrier islands and the mainland (Hayes, 2005). These marsh zones have a direct influence on the location of the shoreline that defines the end of marsh influenced by ocean tides/currents and the beginning of upland dominated by inland factors. Furthermore, there is evidence that the ocean-side shoreline of barrier islands should not be treated the same way as the inland or back-barrier shoreline. According to Jackson (2007), back-barrier shoreline changes of Cumberland Island, (Georgia), were significantly different from ocean-side shoreline changes based on historical aerial photographs and topographic maps provided by the National Oceanic and Atmospheric Administration (NOAA) shoreline data dating back to 1857 (Jackson, 2007).

In response, this research investigates methods used to demarcate ocean-side and back-side shorelines of coastal barrier islands and assesses the impact of variable legal criteria in

defining tidal datums for shoreline delineation. Our main question is what are the reasonable scientific methods for the demarcation of coastal State boundaries of public lands? Delineating barrier islands calls for the following considerations: (1) scientifically defensible standards to demarcate barrier islands; (2) methods for accurately estimating the total area of coastal barrier islands, once defensible shorelines are delineated; and (3) estimation of differences between back-barrier and ocean-front shorelines. With respect to these considerations, this research aims to demarcate the land and ocean boundary of Jekyll Island State Park based on different tide level assumptions used by state and federal agencies. This will provide a geographic framework in which decisions about sustainable development can be made with conservation of cultural and natural resources of public coastal lands.

2.2 Study Area

Coastal barrier islands preserve not only diverse aquatic habitats, but also act as a protector of the mainland against the impacts of severe coastal storms and erosion (Zhang and Leatherman, 2011). These islands, however, consist primarily of unconsolidated sediments such as sand, gravel, and wetland substrate. Therefore, the entire shape of barrier islands is constantly being reformed by waves, wind, and especially, tidal forces. The State of Georgia has 11 barrier islands managed by various government agencies, private organizations and private landowners (GADNR, 2011). All have interests in preserving ocean-side beaches, reducing erosion and maintaining healthy marshlands.

Along a state coastline of approximately 310-km, Jekyll Island State Park has 15.5-km of ocean-front. The study area of Jekyll Island State Park, known as Georgia's Jewel, encompasses the entire upland and marshlands of the 23.88-km² island. It is located in Glynn County

approximately 11-km east of the city of Brunswick with St. Simons Island directly to the north and Cumberland Island to the south (Figure 2.1). The Island has a wealth of both historic and natural attractions, and provides many recreational activities such as fishing, boating, dolphin/whale tours, golf, and heritage tourism (Lenz, 1999; Schoettle, 1996). Today, Jekyll Island State Park is faced with management issues of balancing tourism and development with cultural and natural resource conservation. The Jekyll Island State Park Authority (JIA) was created in February 1950 under the direction of Governor Herman Talmadge to oversee the Island's management decisions and balance development and use of the Island with the conservation of ecologically valuable resources (Bagwell, 2001). According to the State of Georgia 1971 Act No. 427, development is limited to 35 percent of the total island area. Once this 65/35 ratio for undeveloped-to-developed land is reached, artificial structures and impervious surfaces such as tourist resorts, parking lots, or paved roads cannot be built.

The issue of developable lands on Jekyll Island State Park has been addressed by the JIA through the publication of the 1996 Master Plan and the recent release of a draft revised Master Plan in 2004 (JIA, 1996 and 2004). Based on 1:6,000-scale,1980 aerial photographs, field surveys and a shoreline of 1.31-m (4.3 ft) above MHW, at the time of the 1996 Master Plan there were about 0.44-km² (2.6% out of 35%) of the Island that were still available for development. In 2008, a private engineering firm, Thomas and Hutton of Brunswick, Georgia was contracted by the JIA to update the total developed area (JIA, 2008), and it was readjusted in 2010 to 0.40-km².

State plans to renovate some existing structures and expand development in the mid-2000s met opposition by groups with environmental concerns and led to the 2006 formation of the volunteer, non-profit organization named the Initiative to Protect Jekyll Island State Park (IPJI) (IPJI, 2009). The objective of the IPJI is to collect public opinion on Jekyll redevelopment

and to engage a wide range of educational and outreach activities, research, and information dissemination (McDonald, 2010).

Premised by the critical need to establish a current area of developed land relative to the total size of Jekyll Island State Park, advanced geospatial techniques and the newly acquired elevation data using Light Detection and Ranging (LiDAR) technology were used to investigate accurate methods for demarcating the shoreline of Jekyll Island State Park. The following sections will discuss background on federal and state use of tide gauge station data and tidal datums to define jurisdictional shorelines, methods for estimating total area of barrier island upland/marshland and considerations of differences between back-barrier side and ocean-front shorelines of Georgia barrier islands.

2.3 Background on Critical Issues of Barrier island Demarcation

2 .3.1 What is the Standard to Demarcate Barrier Islands?

Tidal datums at tide gauge stations are sea level elevation values that are determined from a time series of recorded observations (Gill and Schultz, 2001). Because the sea level rises and falls with diurnal, seasonal and storm related tides, tidal datums range from Mean Higher High Water (MHHW), Mean High Water (MHW), and Mean Tide Level (MTL), to Mean Low Water (MLW), and Mean Lower Low Water (MLLW) (Hicks, 2006). A shoreline at MHW level is a widely recognized standard to separate the extent of upland and marine areas. It commonly determines jurisdictional coastal boundaries in legal descriptions, and is the boundary between public and private ownership (NOAA, 2011a). As shown in Table 2.1, the State of Georgia uses MHW to delineate jurisdictional shorelines. Other states, however, use different tidal datums to delineate shorelines, which serve many legal, technical, and general uses (NOAA, 2011a).

Reasons for this include variations in tidal ranges and timing of tides for different regions of the county, different shoreline configurations and materials, unique coastal terrains and historical uses of coastlines.

Table 2.1.Various Tidal Datums to delineate shorelines for oceanic coastal states (*Source:* Remote Sensing Division Coastal Mapping Program; NOAA, 2011a).

Tidal Datums	States
Mean Higher High Water or Highest High Water (MHHW)	Hawaii, Louisiana, and Texas.
Mean High Water (MHW)	Alabama, Alaska, California, Connecticut, Florida, Georgia, Maryland, Mississippi, New Jersey, New York, North Carolina, Oregon, Rhode Island, South Carolina, and Washington.
Mean Lower Low Water (MLLW)	Delaware, Massachusetts, Maine, New Hampshire, and Virginia.

Given Georgia's definition of the coastal shoreline at the MHW level, one may question how the sea level is measured and what historical record of sea levels is used to calculate MHW level. According to NOAA, sea level is calculated at tide stations by connecting tidal bench mark networks to the National Spatial Reference System (NSRS) maintained by the National Geodetic Survey (NGS) of NOAA. The bench marks are fixed physical objects or markers used as references for measuring the sea level relative to a vertical datum. Generally, the locations of tide stations are hierarchically organized into a hierarchy as primary, secondary, and tertiary stations (Maune, 2007). A select number of primary level stations have monitored sea levels for more than 19 years and provide sea level data as references to a larger number of secondary stations which, in turn, provide sea level information to numerous tertiary stations.

A determination of the principal tidal datums is based on the average of observations over a 19-year period, established by the Coast and Geodetic Survey, a predecessor of NOAA. The 19-year period is used when determining the MHW line. Nineteen is also the length of the Metonic cycle of recurrence of the lunar phases. The National Tidal Datum Epoch (NTDE) is based on a 19-year cycle and previous tidal datum epochs for the United States were determined for the periods 1924-42, 1941-59, and 1960-78. The present NTDE is 1983-2001 (Szabados, 2008). Recently, however, NOAA has considered revising NTDE policy to every 20-25 year to take into account relative sea level changes caused by global sea level rise (Church and White, 2006). According to some research, global sea-level rise under accelerated conditions such as the melting of Greenland or Antarctic ice and terrestrial water storage variations could lead to a total sea level rise of as much as 0.8 meter by 2100 (Pfeffer, Harper and O'Neel, 2008). Based on records of monthly mean sea level data from 1935 to 2006 from a bench mark at Fort Pulaski on the Georgia coast, the mean sea level trend is 2.98 mm/yr with a 95% confidence interval of +/- 0.33 mm/yr, which is equivalent to a change of 0.29-m in 100 years (NOAA, 2011d). Mean sea level means the arithmetic mean of hourly heights observed over the NTDE (NOAA, 2011c).

Projected sea level rise for specific portions of the U.S. coastline must be tied to sea levels in order to accurately assess changes in barrier island size. At this time, only predicted and not actual sea levels are available for Jekyll Island State Park from the NOAA Tides and Currents website (NOAA, 2011b). Fortunately for this research, verified tidal datum data (i.e., actual sea level measurements rather than predicted sea levels are provided by the tidal station of nearby St. Simons Island located about 1.8-km north of Jekyll Island State Park. The MHW sea level of 0.79-m based on an average of 10 years of MHW measurements on St. Simons Island was thus used to demarcate one scenario of the Jekyll Island State Park boundary.

2.3.2 What is the Methodology for Most Accurately Estimating the Area of Coastal Barrier Islands?

Once the MHW level dividing ocean from marsh upland is established (for example 0.79-m in this case), the second consideration for demarcating the extent of a barrier island and calculating its size is obtaining accurate terrain or elevation data. In the JIA 1996 Master Plan, the JIA planning team was assisted by Robert Charles Lesser & Co. and Tunnell-Spangler & Associates, using 1:6000-scale 1980 aerial photographs and field surveys to delineate elevation contours and the shoreline for the purpose of calculating the total area of Jekyll Island State Park. The shoreline for this JIA effort was defined as 1.31-m (4.3 ft) above MHW referenced to the National Geodetic Vertical Datum of 1929 (NGVD 29) as used by the Georgia Department of Transportation (DOT) and certified by the U.S. Army Corps of Engineers for construction permitting of the new Jekyll Creek Bridge (JIA, 1996; Figure 2.2).

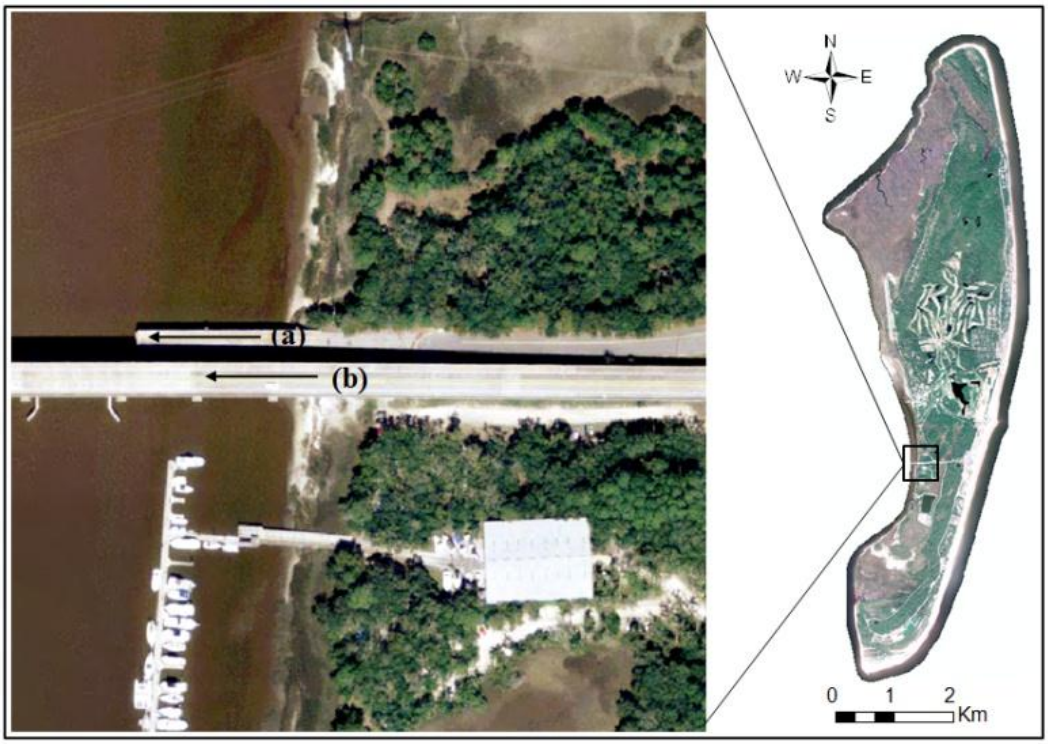

Figure 2.2. The old Jekyll Creek drawbridge (a) was constructed in 1954. Construction of the M.E. Thompson Memorial Bridge (b) was based on a shoreline of 1.31m referenced to the NGVD 29 datum.

Generally, heights on the earth are measured relative to a geodetic vertical datum such as NGVD 29. This datum was recently updated to the North American Vertical Datum of 1988 (NAVD 88), which increased the accuracy of the mathematical calculation of the shape of the earth geoid for several reasons. First, the NGVD 29 was independently adjusted between United States and Canada. Second, NGVD 29 assumed MSL was the same at all locations and did not consider actual conditions of differences in MSL at each tidal station (i.e., tide gauge observation with associated survey bench marks). Finally, some existing bench marks may have been moved due to crustal motion activity, postglacial rebound (uplift), and subsidence resulting from the withdrawal of underground liquids (Zilkoski, Balazs and Bengston, 1991). Although NGVD 29

was historically readjusted to address these errors, NAVD 88 is now commonly used because of better accuracy. Overall differences for the conterminous United States between vertical heights referenced to NGVD 29 and NAVD 88 range from – 40 cm to +150 cm. The Georgia coast has differences of - 32 cm between NGVD 29 and NAVD 88 (Zilkoski, Richards and Young, 1992).

In sum, sea levels referenced to NGVD 29 must be readjusted and converted to the most accurate NAVD 88 datum for comparison and consistency of measurements. To do so, NOAA's NGS, Office of Coast Survey (OCS), and Center for Operational Oceanographic Products and Services (CO-OPS) provide a Vertical Datum Transformation Tool (VDatum), which allows users to convert data from different horizontal and vertical references in desired reference levels (NOAA, 2010). Another conversion tool, the North American VERTical Datum CONversion (VERTCON), is provided by NGS for mapping purposes. The VERTCON computes the modeled difference in vertical height between NAVD 88 and NGVD 29 for a given location specified by latitude and longitude (Mulcare, 2004). Based on the VERTCON tool, the Jekyll Island State Park 1.31 m shoreline referenced to NGVD 29 was transformed to 1.00 m referenced to NAVD 88 for use in this research.

2.3.3 Do Differences between Back-Barrier and Ocean-Front Shorelines Exist?

Barrier islands are physically separated from the mainland and are therefore subjected to different ocean currents, tidal channel flows, inland freshwater flows and beach-dune complexes vs. wetlands on the back-barrier and ocean-front sides (Hayes, 2005). In addition to differences in sea levels between back-barrier and ocean-front sides, the shorelines of barrier islands along the U.S. Atlantic coast are influenced by constant processes of soil erosion from the north ends of the Islands and soil accretion at the south ends due to north to south ocean currents and

sediment transport. Thus, barrier island shorelines are constantly changing especially on the ocean-front side that is subjected to currents. The fact that islands cannot be demarcated by a single elevation contour must be considered when establishing administrative boundaries and for studies of sea level rise. Many researchers have studied sea level rise on ocean-front shorelines, but only a few studies have compared differences in sea levels and sea level rise on back-barrier shorelines. For example, Gibeaut *et al*., (2003) produced beach profiles to analyze shoreline changes of the West Bay. These beach profiles represented different sea levels and different rates of sea level change on the back- and ocean-front sides of barrier islands (Gibeaut *et al*., 2003). Jackson (2010) revealed shoreline changes on the back-side of Georgia barrier islands. He calculated an erosion rate of 77% for the back-barrier side of Jekyll Island State Park, which is much larger than the 69% erosion rate on the ocean-front. In addition, the northern inlet-facing side has a much higher erosion rate than the southern inlet-facing side, 97% compared to only 5%, respectively (Jackson, 2010).

Since Jekyll Island State Park's only tidal station no longer exists, the difference between back-barrier and ocean-front sea levels and shorelines are not measured directly. We can, however, assume sea levels measured on St. Simons Island directly north of Jekyll Island State Park will be similar. As shown in Figure 2.3, St. Simons Island has 3 tidal stations on the back-barrier side (Figure 2.3a, b, and c) and 1 tidal station (Figure 2.3d) on the ocean-side of the Island. All station sea levels are referenced to the local MLLW datum. The tidal station at the south end reports a sea level of 2.26-m, and the tidal station on the back side north and west of the south end station reports 2.35-m. When converting these MLLW sea levels relative to NAVD 88, 2.35-m equals 1.07-m and 2.26-m, is 0.98-m. Thus, the difference between the back-barrier

and ocean-front side of St. Simons Island is 0.09-m which will be considered in this research to represent the difference in back-barrier and ocean-front shorelines of Jekyll Island State Park.

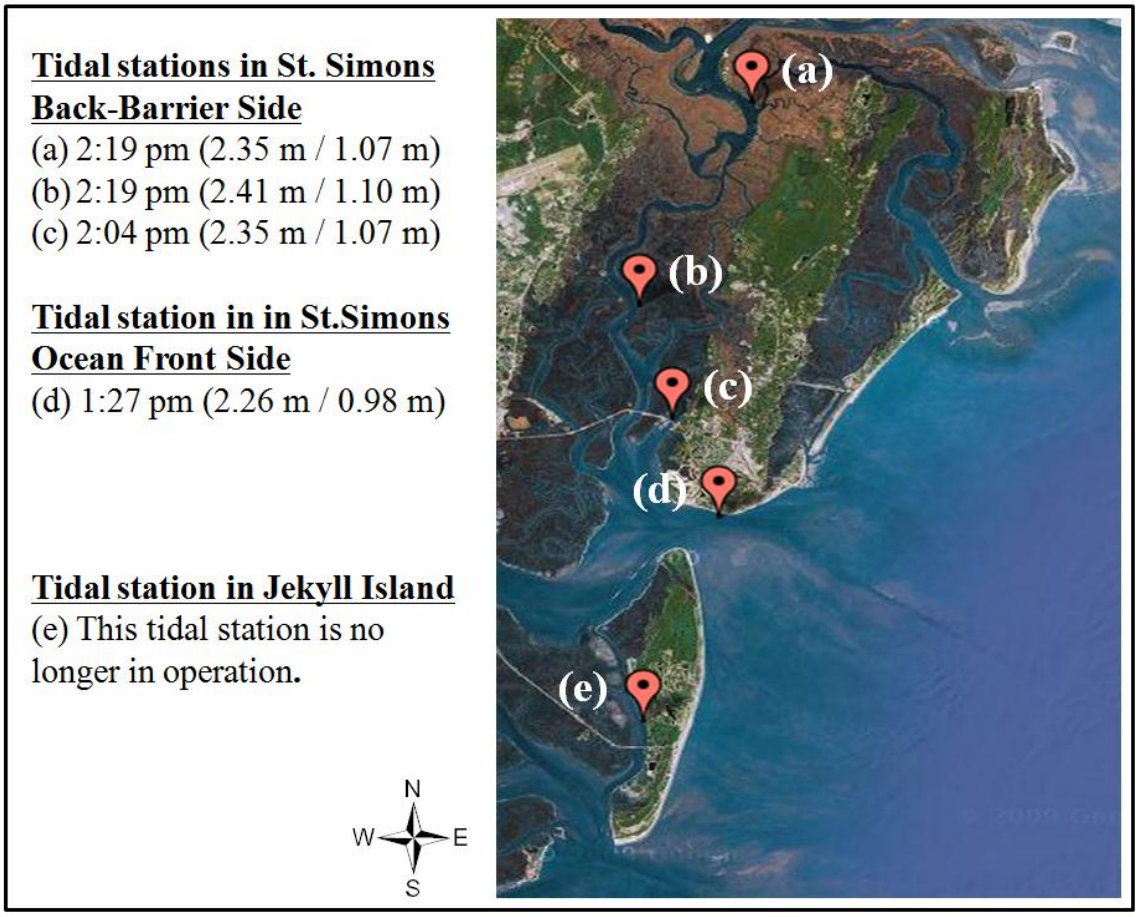

Figure 2.3. Tidal stations and sea levels relative to local MLLW datum /NAVD 88 on the ocean-front and back-barrier side of St. Simons Island (NOAA's Center for Operational Oceanographic Products & Services).

2.4 Methods and Data Construction

2.4.1 Shoreline Demarcation Methods

Demarcating boundaries, especially those that have administrative power, have typically made for conflict (Harvey, 2006). Generally following roads, property lines, natural features, degrees of latitude and longitude and drainage ditches, administrative boundaries may be

demarcated using ground surveying, remote sensing measurement and modern altimetry technology such as LiDAR. Shoreline boundaries, in particular, are often demarcated using manual digitization (Chen and Rau, 1988) and satellite images (Braud and Feng, 1998; Frazier and Page, 2000; Ryu, Won and Min, 2002; Smith, 1997). Although ground surveying is the most accurate, it is also most time consuming and labor intensive. Detection using satellite images or aerial photographs can cover large areas and delineate actual shorelines, but also may have less accuracy than ground surveying, depending on the scale and resolution of the remotely sensing images (Yang *et al*., in press). Although expensive to acquire, airborne topographic LiDAR technology can be used to generate high-resolution and accurate elevation data over large areas relatively quickly (Gibeaut *et al*., 2000). Thus, this research uses LiDAR data to demarcate the most accurate boundaries of Jekyll Island State Park under a variety of sea levels established by different management agencies. Differences in shorelines, in turn, will greatly affect developable land areas and total marshlands protected by federal laws.

2.4.2 Sea Levels used in this Research

Sea levels analyzed in this research include 0.79-m, which comes from verified data provided by NOAA, and is the average of MHW levels from 1999 to 2008 as measured at the south tidal station of St Simons Island.

Second is the MHW sea level of 0.85-m that was recently proposed by Coastal Hazards Specialist, Douglas C. Marcy from the NOAA Coastal Services Center (personal communication). The 0.85-m MHW was estimated by the VDatum modeled tidal surface based on an off-shore average from three locations on Jekyll Island State Park: the south end, the front shore at the convention center and the north end fishing pier. These three points are considered in

this research to mark the extent of the ocean-front side of Jekyll Island State Park. Specifically, the North Fishing Pier MHW 0.85-m, Central Beach MHW is 0.84-m, and South end MHW is 0.85-m with all three points referenced to NAVD 88, and averaging 0.85-m. This "modeled tidal surface" was created by NOAA using a hydrodynamic model of tide surface elevations (heights) over a long period and averaging sea levels for each grid cell to produce the various Tidal Datums (MHW, MLW, etc...) (Parker *et al*., 2003).

The third sea level used in this research is 1.31-m NGVD 29 as defined by the JIA in the 1996 Management Plan and converted to 1.00-m NAVD 88.

A fourth sea level investigated in this research focuses on the boundary that defines marshland from upland and controls what lands are available for development. According to the Georgia Department of Natural Resource (GADNR), Coastal Marshlands Protection Act of 1970 (CMPA), coastal marshland below 1.71-m referenced to the local datum of MTL, should be protected. 'Mean Tide Level' is a tidal datum measured as the arithmetic average of the MHW and MLW. In order to compare the coastal marshland jurisdiction areas to the three other state and federal sea levels, the 1.71-m should be converted to a sea level which is referenced to the NAVD 88 datum or 1.49-m.

Finally, a 0.09-m difference in MHW levels between the back-side and ocean-side of Jekyll Island State Park was applied to more accurately account for the differences in back to front island sea levels applied to each of the four federal/state sea levels discussed above.

2.4.3 Geodatabase Construction

LiDAR data used in this research have multiple return points known as a point cloud recorded as X, Y and Z coordinates in LAS v1.2 format, which is a standard format of LiDAR

data. These data, provided by Glynn County, GA, were acquired from March 1 to April 1, 2007 and were processed in this research to produce a bare earth surface. Essentially all non-ground points were stripped out of the data set to leave only those points reflected from the bare earth surface. The accuracy of these data is reported by U.S. National Standard for Spatial Accuracy (NSSDA) standards to be accurate to about 0.18-m. The lowest elevation in the Jekyll Island LiDAR bare earth surface is -0.64-m and the highest height is 13.99-m on the upland portion of Jekyll Island State Park. The aerial digital camera imagery also provided by the Glynn County GIS project team was derived from 1:12,000-scale large format digital imagery acquired using a VEXCEL UltraCamD aerial camera at 6-inch resolution from March 8 to 13, 2007.

LiDAR bare earth points in LAS format were next converted to an ArcGIS shapefile of points for editing and ultimate creation of shoreline contours (Figure 2.4). Once imported to ArcGIS, the LiDAR point features were converted to a Triangular Irregular Network (TIN) model in order to represent the terrain surface in more detail. In the next step, contours at 0.03-m Contour Interval, were created. Next, four versions of the Jekyll Island State Park shorelines were extracted using the values of 0.79-m, 0.85-m, 0.94-m, 1.00-m and 1.49-m sea levels. These island demarcation boundary lines were refined by standard ArcGIS editing methods such as Split, Dissolve, Merge, Erase, and Converting Polygons to Polylines. Finally, all island demarcation boundaries were saved in a geodatabase, which efficiently manages geospatial data such as shapefiles, satellite imagery, and all GIS data in vector and raster formats. All images and GIS data were saved to a common horizontal datum (North American Datum of 1983, NAD 83), ellipsoid (Global Reference System of 1980, GRS 80) and projection (Universal Traverse Mercator, UTM) for X and Y coordinates. For Z (i.e., elevation) values, data were referenced to NAVD 88.

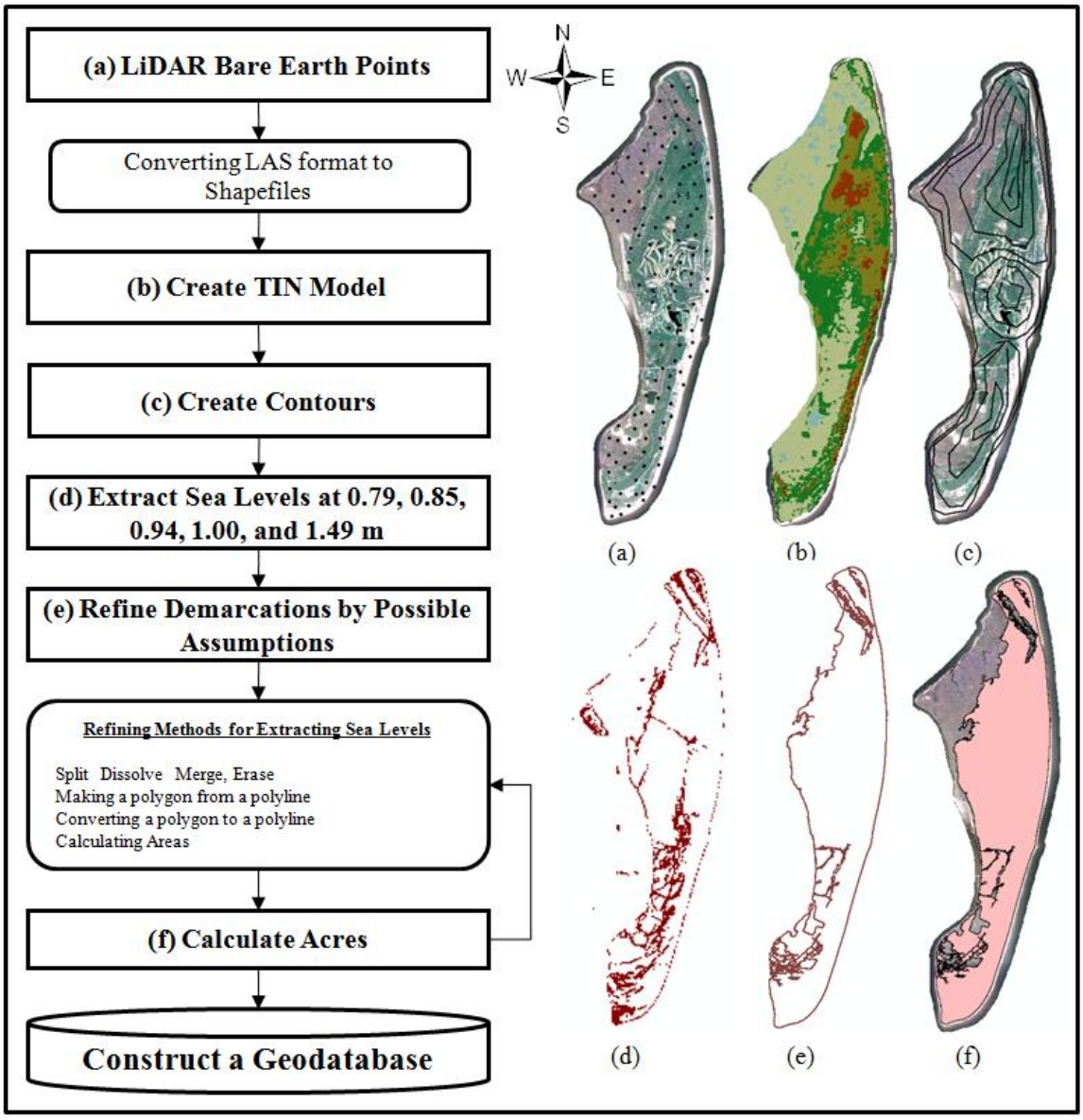

Figure 2.4. Work-flow for creating different Jekyll Island State Park shoreline boundaries demarcating upland from ocean using LiDAR multiple point data.

2.5 Results

2.5.1 One Shoreline for the Entire Jekyll Island State Park

Jekyll Island State Park shoreline boundaries for the entire island (i.e., the case of no difference in back-barrier island and ocean-front sea levels at 0.79-m, 0.85-m, 1.00-m, and 1.49-

m sea levels were extracted from the LiDAR-derived bare-earth digital surface model (Figure 2.5). Demarcations of the shoreline at the four different sea levels are highlighted in enlarged views of the north and south portions of the Island. The greatest differences are visible on the back-barrier side, while there is little change along the ocean side.

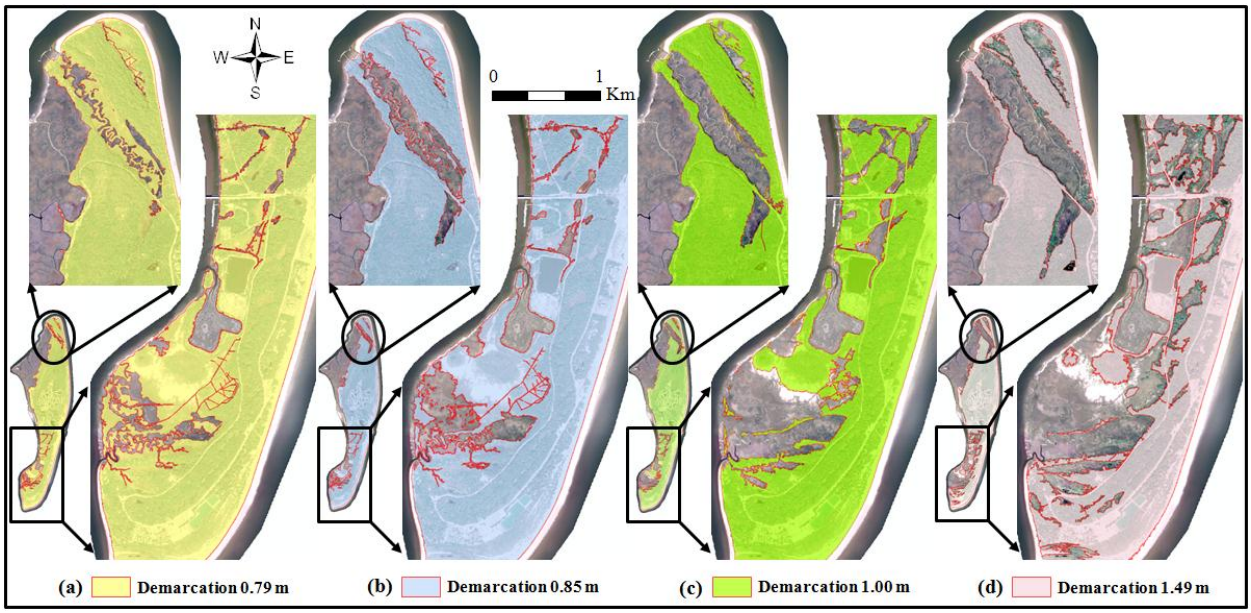

Figure 2.5. Demarcations of the Jekyll Island shoreline at four different sea levels and enlarged sections of the north and south areas of the Island show greatest differences on the back-barrier side of the Island and little change along the ocean-front side.

2.5.2 Differences in the Back-Barrier and Ocean-front Shorelines

A difference of 0.09-m was considered for the higher sea level of the back-barrier side compared to the ocean-front side of Jekyll Island State Park. Of particular interest was demarcating the Island shoreline and upland area using the 0.85-m ocean-front sea level established by NOAA by interpolating sea levels at the three locations on Jekyll Island State Park. In this research there were two cases for back-barrier sea levels: 1) 0.94-m which is 0.09-m

added to the NOAA sea level of 0.85-m; and 2) the back-barrier sea level of 1.49-m established by the CMPA to protect coastal marshlands (Figure 2.6).

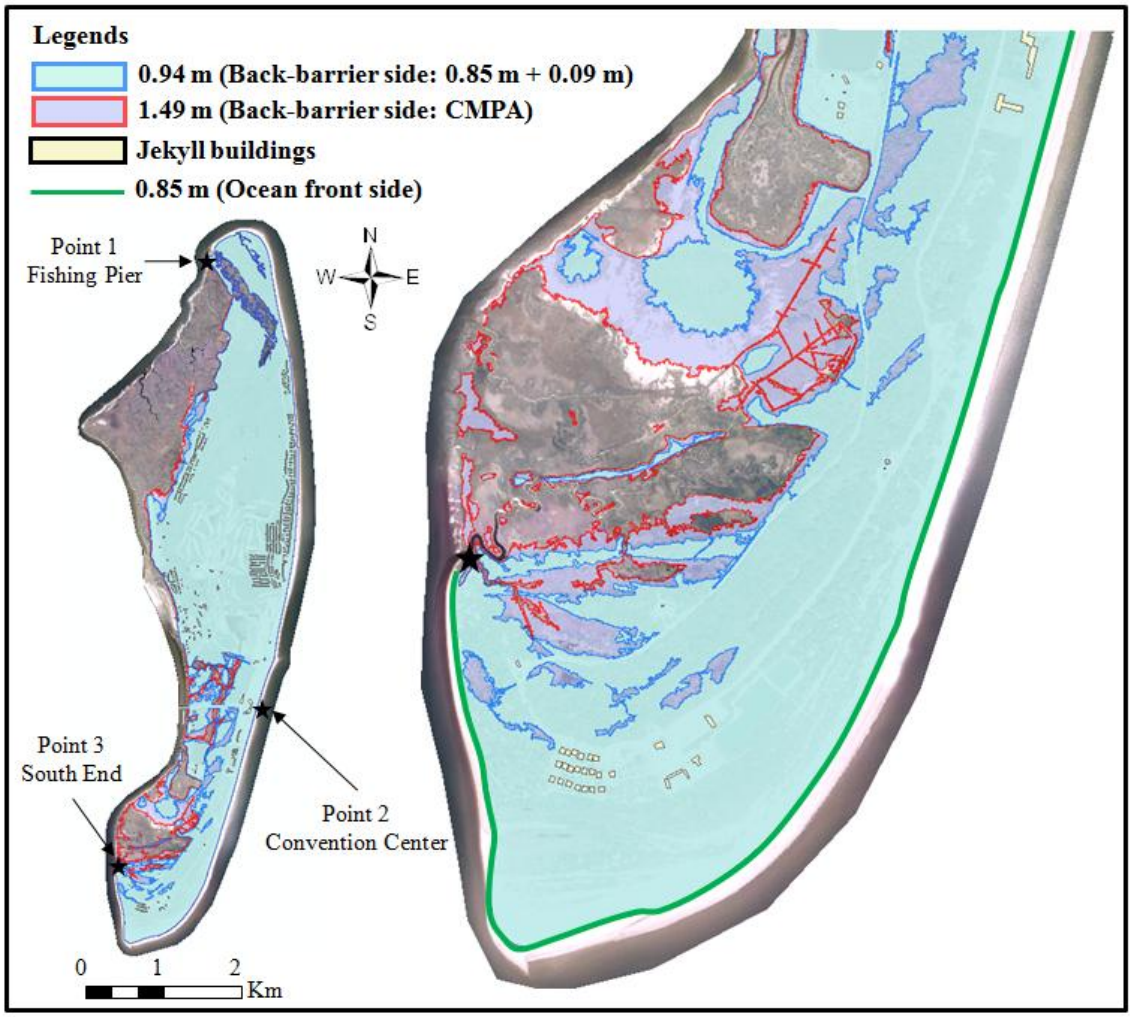

Figure 2.6. Separate demarcation of back-barrier and ocean-front sides of the Jekyll Island State Park shoreline results in more accurate calculation of island area.

As shown in Figure 2.6, demarcation of the ocean-front (beach side) shoreline at 0.85-m extends from the South End (Point 3) NOAA interpolation point, along the east-side ocean beach (Point 2) and north to the Fishing Pier (Point 1) interpolation point on Jekyll Island State Park.

The back-barrier (marsh side) shoreline demarcated shows the interior marshlands using the two sea levels, 0.94-m and 1.49-m.

Figure 2.7 illustrates the shorelines and island upland areas for the two cases of back-barrier sea levels, 0.94-m which is 0.09-m higher than the front ocean sea level of 0.85-m (Figure 2.7a) and back-barrier sea level of 1.49-m (Figure 2.7b) which is based on the Georgia Coastal Marshlands Protection Act. Of note are the minimal differences in marshland-upland demarcation in the northern part compared to the dramatic differences in southern marshlands. The marsh along the northern Clam Creek, for example, is approximately the same width and length in both cases, while the marsh extent at the south end is less expansive and more fragmented at 0.94-m than at 1.49-m back-barrier sea levels. Island area calculations using the four different shorelines defined by state and federal agencies, as well as the Island areas using different back-barrier and ocean-front sea levels are presented in Table 2. Also presented are the percent of developed land and developable areas for these variable shorelines holding developed lands constant.

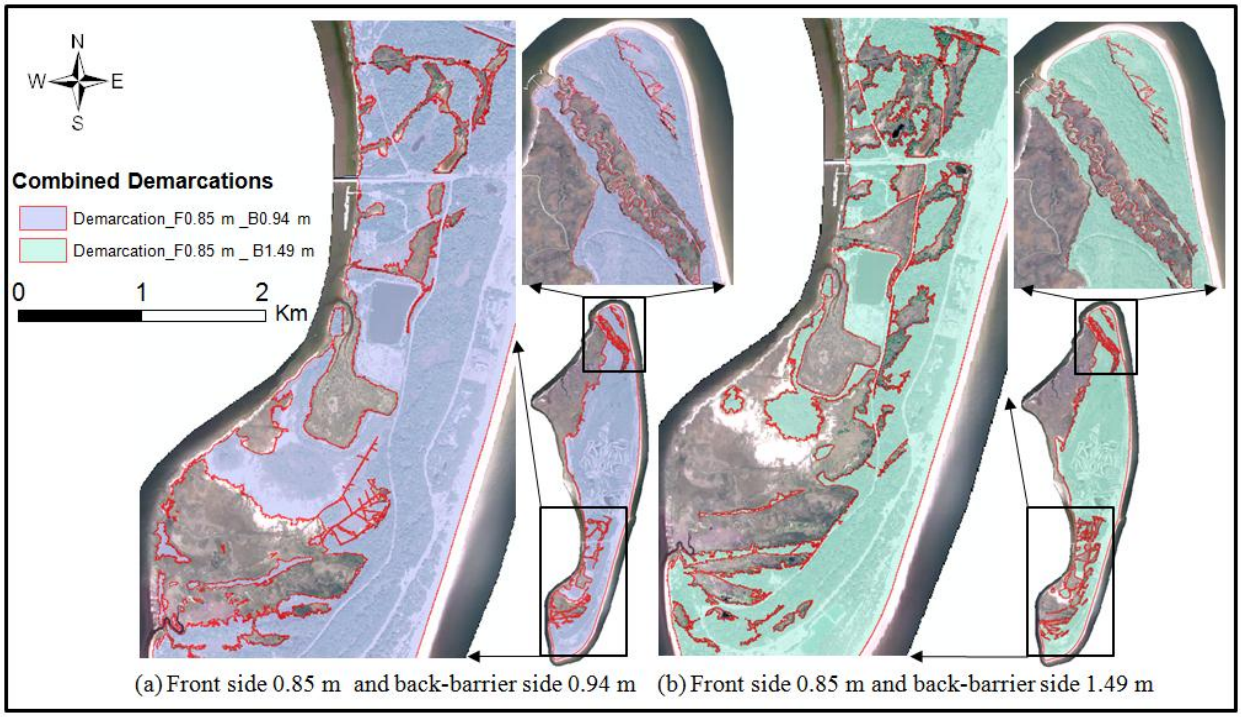

Figure 2.7. Differences in back-barrier island marsh areas are evident when considering two cases: (a) the back-barrier sea level being 0.94m or 0.09m higher than the ocean side sea level of 0.85m; and (b) the back-barrier 1.49m sea level established by the Georgia Coastal Marshlands Protection Act with the same ocean-front sea level of 0.85m.

2.6 Discussion

Results presented in this research demonstrate the complexity of geographic issues related to the seemingly straightforward and reasonable Georgia State legislation limiting development of Jekyll Island State Park to below 35% of the total island area. Considering only the calculation of the size of the Island, this research found four different sea levels defined and used by state and federal agencies (0.79-m, 0.85-m, 1.00-m, and 1.49-m).

Table 2.2. Area of Jekyll Island State Park at different sea levels (All sea levels are referenced to NAVD 88).

	Proposed Sea Levels (m)		Total Island Size (km²)	Total Area and Percent of Developed Upland		Developable Areas (km²)
				(km²)	(%)	
Single Shoreline Approach	Georgia State	1.00 (JIA)	16.42	5.55*	33.8%	0.25
				5.66**	34.5%	0.09
		1.49 (Coastal Marshland Protect Act)	14.63	5.55	37.9%	Not developable
				5.66	38.7%	Not developable
	Federal organization	0.85 (NOAA interpolated)	17.44	5.55	31.8%	0.60
				5.66	32.4%	0.44
		0.79 (NOAA verified)	17.94	5.55	30.9%	0.78
				5.66	31.5%	0.62
Different Back-barrier and Ocean-front Sea Levels Approach	F 0.85 B 0.94 (0.85+0.09)		16.90	5.55	32.8%	0.36
				5.66	33.5%	0.25
	F 0.85 B 1.49		15.36	5.55	36.1 %	Not developable
				5.66	36.8%	Not developable

* 5.5 km² of developed land per 1996 JIA Maser Plan, JIA (1996).
* 5.66 km² of developed land per JIA (2008).

The use of different sea levels to establish barrier island shorelines results in variable calculations of the total area of island upland. When considering a single shoreline for the entire Jekyll Island State Park, the total island size is the largest for the NOAA verified sea level of 0.79-m (17.94-km²) and the smallest for the CMPA sea level of 1.49-m (14.63-km²). Thus there is a difference of up to 3.31-km² or 7.2 % of the Island area, dependent upon the accepted sea level adopted by a particular state or federal agency and whether a single shoreline or variable back-barrier and ocean-front shoreline approach is used.

Considering different back-barrier and ocean-front shorelines, the total island size is 16.90-km² for the case of 0.94-m back-barrier sea level and 15.36-km² for the case of 1.49-m.

Compared to the Island size of 17.44-km² at 0.85-m sea level for the entire island, the total island size decreased by 0.54-km² considering a back-barrier sea level of 0.94-m. There is a further decrease of 2.08-km² of upland when the CMPA back-barrier 1.49-m sea level is considered.

The total developable lands on Jekyll Island State Park are consequently impacted by these changes in island upland areas. As stated above, the Georgia JIA is mandated to limit development of the Island to 35%. Holding the total developed land area constant at 5.55-km², as published in the 1996 Jekyll Island State Park Management Plan, the percentages of developed land calculated using the various shorelines and sizes of Jekyll Island State Park changes accordingly and in four cases there are no remaining developable lands (See Table 2.2). Additionally, as noted previously, the recently recalculated developed area by JIA is 5.66-km² (JIA, 2008).

When considering the total area of developed lands to be 5.55-km² as published in the 1996 JIA Master Plan and the different total island sizes based on the NOAA and JIA shorelines, the percent of developed lands is close to, but does not exceed, the state limit of 35%. Table 2.2 lists percent of developed land ranging from 30.9% for the 0.79-m NOAA verified shoreline to 33.8% for the JIA 1.00-m shoreline. The percent of developed land however, exceeds the state limit (37.9%) when using the CMPA shoreline of 1.49 m. These percentages of developed lands all increase slightly when using the 2008 JIA Master Plan (currently published as a draft plan) total developed land of 5.66-km². The percent of developed lands in this case range from 31.5% to 34.5% using NOAA/JIA shorelines, and increases to 38.7% under the CMPA scenario. These results hold true when considering different back-barrier and ocean-front shorelines. Under the NOAA 0.85-m front and 0.94-m back-barrier shorelines, the percent of developed lands is 32.8% using the 1996 JIA developed land statistic and 33.5% using the draft 2008 JIA developed land

area. Only when considering the CMPA back-barrier shoreline does the percent of developed land exceed the State limit (i.e., 36.1% and 36.8%) for 1996 and 2008 JIA developed land totals, respectively.

2.7 Conclusion

2.7.1 Summary

This research investigated methods to assess the impact of variable legal criteria in defining tidal datums for shoreline delineation and separately demarcated back-barrier and ocean-front side shorelines of coastal barrier islands. A number of different standards were found to be used by state and federal agencies to demarcate the shoreline of Jekyll Island, GA. Even small differences in sea levels were shown to result in substantial differences in total barrier island size. Although it is not within the scope of this research to identify the optimal sea level standards for demarcating barrier islands, best methods using the most current remote sensing imagery and finest resolution elevation data (e.g., LiDAR) were demonstrated to be critical for accurately and regularly monitoring the total size of dynamic coastal barrier islands. In addition, island managers must account for differences between back-barrier and ocean-front sea levels.

The application of various state and federal delineations of shorelines to a very detailed and accurate digital terrain model created from LiDAR bare earth data provided island boundaries that were generally similar on the ocean/beach (east shoreline) side but differed significantly on the western inland/marsh side. These differences affect jurisdictional marshes for protection under the CMPA as well as available developable lands allowed under the State limit of 35% developed to 65% undeveloped lands. In addition, this research demonstrated a single shoreline does not accurately reflect the real-world conditions of back-barrier island sea levels

being slightly higher (0.09-m in the case of Jekyll Island State Park) compared to the ocean-front side.

2.7.2 Future Research

Future work should verify back-barrier and ocean-front sea levels on Jekyll Island to confirm or revise the 0.09-m difference that was estimated from St. Simons Island tide stations. Indeed field managements of tide levels of several different coastal barrier islands should be undertaken to explore variation and similarities in back-barrier sea levels in order to insure defensible and reliable methods to estimate back-barrier sea levels.

While this research focused on the total size of barrier islands, future work also should address critical issues involving the definition of developed and undeveloped lands to improve methods and policy for documenting the current status of island development. It is suggested that the legal definition of developable lands should include language that acknowledges the dynamic nature of coastal barrier islands and implements a regular monitoring provision to measure both island size and developed lands. Acceptance and agreement on the definitions of developed lands are critical for resolving conflicts arising from differences in development and conservation perspectives towards the ultimate goal of sustainability. For example, in the 1996 Master plan, custom definitions provided by JIA for developed and undeveloped areas (JIA, 1996), caused some public confusion. Thus, a consensus on land use class definitions is needed to create a comprehensive decision making system. In future research, we will continue this research direction to provide geospatial tools to manage and plan island services, infrastructures and facilities such that coastal resources are preserved. Overall, we anticipate our results demonstrating methods for demarcating U.S. barrier islands will assist both conservation

advocates and promoters of island development towards a lasting balance between sustainable development and environmental protection.

Acknowledgements

The research project was supported by the Center for Remote Sensing and Mapping Science (CRMS) of the Department of Geography at the University of Georgia and the Initiative to Protect Jekyll Island State Park (IPJI).

References

Bagwell, T. E., 2001. *Images of America: Jekyll Island State Park A State Park*, Charleston, SC: Arcadia Publishing, 128p.

Braud, D.H., and Feng, W., 1998. Semi-automated Construction of the Louisiana Coastline Digital Land/water Boundary using Landsat Thematic Mapper Satellite Imagery. Technical Report 97-002, *Department of Geography & Anthropology Louisiana State University Louisiana Applied Oil Spill Research and Development Program*, OSRAPD.

Cabin Bluff Management, 2007. *Jekyll Island State Park Conservation Plan*.

Chen, L.C., and Rau, J.Y., 1988. Detection of shoreline changes for tideland areas using multitemporal satellite images. *International Journal of Remote Sensing* 19(17), 3383-3397.

Church, J.A., and White, N.J., 2006. A 20th century acceleration in global sea-level rise. *Geophysical Research Letters* 33, 1-4.

Frazier, P.S., and Page, K.J., 2000. Water body detection and delineation with Landsat TM data. *Photogrammetric Engineering and Remote Sensing* 66(12), 1467-1467.

GADNR, 2011. *Links to Websites of the Georgia Coastal Barrier Islands*. Coastal Resources Division in Georgia, http://crd.dnr.state.ga.us/content/displaycontent.asp?txtDocument=422 (Accessed 28.03.2010).

Gibeaut, J.C., White, W.A., Hepner, Tiffany, Gutiérrez, Roberto, Tremblay, T.A., Smyth, R.C., and Andrews, J.R., 2000. *Texas Shoreline Change Project: Gulf of Mexico Shoreline change from the Brazos River to Pass Cavallo*: The University of Texas at Austin, Bureau of Economic Geology, report prepared for the Texas Coastal Coordination Council pursuant to National Oceanic and Atmospheric Administration Award No. NA870Z0251, 32.

Gibeaut, J.C., Waldinger, R., Hepner, T., Tremblay, T.A., and White, W.A., 2003. *Changes in Bay Shoreline Position*, West Bay system, Texas. The University of Texas at Austin, Bureau of Economic Geology, report of the Texas Coastal Coordination Council pursuant to National Oceanic and Atmospheric Administration Award No. NA07OZ0134, 27. http://www.beg.utexas.edu/coastal/presentations_reports/WestBayfinalreport.pdf (Accessed 20.10. 2010).

Gill, S.K., and Schultz, J.R., 2001. *Tidal Datums and Their Applications*. NOAA Special Publication NOS CO-OPS 1, 111p.

Harvey, F., 2006. Reconfiguring Administrative Geographies in the United States. *ACME: An International E-Journal for Critical Geographies 4(1), 57-79*, http://www.acme-journal.org/vol4/FH.pdf (Accessed 09.27.2010).

Hayes, M., 2005. *Barrier Islands*. Encyclopedia of Coastal Science. M. Swartz (ed.), Elsevier, pp. 117-119.

Hoyt, J.H., 1967. Barrier island formation. *Geological Society of America Bulletin* 78(9), 1125-1136.

Hunter, J., 2008. Jekyll Island State Park. *The New Georgia Encyclopedia* last updated in Sep 15, 2008, http://www.georgiaencyclopedia.org/nge/Article.jsp?id=h-928 (Accessed 03.26. 2011).

IPJI, 2009. *The Initiative to Protect Jekyll Island State Park (IPJI): Who We Are and What We Stand For*. http://www.savejekyllIsland.org/who.html (Accessed 26.04. 2009).

Jackson, C.W., 2007. Back-barrier shoreline change history: Cumberland Island, Georgia, 1857-2002. *Southern Geology* 45(1), 25-37.

Jackson, C.W.J., 2010. Spatio-temporal Analysis of Barrier Island Shoreline Change [electronic resource] : The Georgia Coast, USA Retrieved from University of Georgia Catalog database, (Accessed, 05.12.2011).

JIA, 1996. *The Jekyll Island State Park State Park Authority (JIA): Final Master Plan for The Management Preservation, Protection, and Development of Jekyll Island State Park.* http://www.jekyllislandauthority.org (Accessed 08.02. 2008).

JIA, 2004. *Jekyll Island State Park Island-wide Master Plan Update.* http://www.jekyllislandauthority.org (Accessed 04.05.2011).

JIA, 2008. *LiDAR Island Mapping*, projected by Thomas & Hutton Engineering Co. http://www.jekyllislandauthority.org (Accessed 12.25.2010).

Lenz, R.J., 1999. *Longstreet Highroad Guide to the Georgia Coast and Okefenokee*. Athens, GA: Longstreet Press, 336p.

Maune, David F., 2007. *Digital Elevation Model Technologies and Applications: The DEM User's Manual* (2nd ed.), Bethesda, Maryland: American Society for Photogrammertry and Remote Sensing, 655p.

McDonald, B., 2010. *Remember Jekyll Island State Park*, Minneapolis, MN: Langdon Street Press, 290p.

McCash, J.H., 2005. *Jekyll Island's Early Years* : *From Prehistory through Reconstruction*, Athens, GA: University of Georgia Press, 280p.

Mulcare, D.M., 2004. NGS Toolkit, Part 9: The National Geodetic Survey VERTCON Tool. http://www.ngs.noaa.gov/TOOLS/Professional_Surveyor_Articles/VERTCON.pdf (Accessed 11.11. 2010).

NOAA, 2010. Vertical Datum Transformation: Integrating America's Elevation Data. http://vdatum.noaa.gov/ (Accessed 10.05.2010).

NOAA, 2011a. Shoreline Website: a Guide to National Shoreline Data and Terms (Boundary Determination). http://www.ngs.noaa.gov/RSD/coastal/importance.html (Accessed 09.27.2011).

NOAA, 2011b. Turning Operational Oceanographic Data into Meaningful Information for the Nation. Center for Operational Oceanographic Products and Services: last revised March 08, 2011 http://tidesandcurrents.noaa.gov/ (Accessed 12.05.2010).

NOAA, 2011c. TIDAL DATUMS, NOAA Tide & Currents. http://tidesandcurrents.noaa.gov/datum_options.html (Accessed 04.05, 2011).

NOAA, 2011d. Mean sea level Trend: Fort Pulaski, Georgia, http://tidesandcurrents.noaa.gov/sltrends/sltrends_station.shtml?stnid=8670870 (Accessed 04.05. 2011).

Parker, B., Milbert, D., Hess, K.., and Gill, S., 2003. National VDatum – The Implementation of a National Vertical Datum Transformation Database: Proceedings of the U.S. Hydrographic 2003 Conference. *The Hydrographic Society of America*, March 23-27.

Pfeffer, W.T., Harper, J.T., and O'Neel, S., 2008. Kinematic constraints on glacier contributions to 21st-century sea-level rise. *Science* 321(5894), 1340-1343.

Ryu, J.H., Won, J.S., and Min, K.D., 2002. Waterline extraction from Landsat TM data in a tidal flat - A case study in Gomso Bay, Korea. *Remote Sensing of Environ*ment 83(3), 442-456.

Schoettle, H.E.T., 1996. *A Guide to a Georgia Barrier Island : featuring Jekyll Island State Park with St. Simons and Sapelo Islands and a Field Guide to Jekyll Island State Park,* Simons Island, GA: Watermarks Publishing, 160p.

Smith, L.C., 1997. Satellite remote sensing of river inundation area, stage, and discharge: A review. *Hydrol Process* 11(10), 1427-1439.

Szabados, M., 2008. Understanding Sea Level Change. American Congress on Surveying and Mapping (ACSM) Bulletin http://masgcorg/climate/cop/Documents/SeaLevelChangepdf (Accessed 12.05. 2010).

Yang, B. Y., Madden, M., Kim, J. W., and Jordan, T. R., Geospatial analysis of barrier island beach availability to tourists, *Tourism Management*, in press.

Zhang, K. and Leatherman, S., 2011. Barrier island population along the U.S. Atlantic and Gulf coasts. *Journal of Coastal Research* 27(2), 356-63.

Zilkoski, D.B., Balazs, E.I., and Bengston, J.M., 1991. *Datum Definition Study for The North American Vertical Datum of 1988*. NGS Internal Report, http://www.ngs.noaa.gov/web/about_ngs/history/Datum_Definition_Study_for_88.pdf (Accessed 10.09.2010).

Zilkoski, D.B., Richards, J.H., and Young, G.M., 1992. Results of the general adjustment of the North American Vertical Datum of 1988. *Surveying and Land Information Systems* 52(3), 133-49.

CHAPTER 3

GEOSPATIAL ANALYSIS OF BARRIER ISLAND BEACH AVAILABILITY TO TOURISTS[2]

[2] Yang, B. Y., Madden, M., Kim, J. W., and Jordan, T. R., Accepted by *Tourism Management*. Reprinted here with permission of ELSEVIER, 08/26/2011.

Abstract

This study geospatially analyzes beach availability for global recreational tourism management with focus on a case study of Jekyll Island off the coast of Georgia, USA. Aerial digital imagery in combination with Light Detection and Ranging (LiDAR) data and geographic information system (GIS) mapping and analysis are employed to delineate accurate shorelines with regard to accessible and available beach area. This analysis demonstrates geospatial techniques for the identification, delineation, qualification and geovisualization of dry beaches, a popular tourist destination worldwide that is subjected to diurnal flooding by tides. The accurate depiction of shorelines using remotely sensed differences in Mean Higher High Water (MHHW) and Mean Lower Low Water (MLLW) levels is required to identify dry beach areas available for coastal tourism and management. Such information allows tourists to choose beach areas suitable for recreational or ecological activities. Dry beach availability also assists coastal restoration managers to plan and implement beach conservation measures. Results predict shoreline changes and dry beach access while promoting minimal impacts by tourists on fragile coastal dune ecosystems.

Key words: LiDAR, GIS, Coastal tourism, Beach availability, and Shoreline change.

3.1 Introduction

The coastal zone offers ecosystem services that are of great environmental and economic significance (Page and Connell, 2006). It provides not only diverse wildlife habitats and unique natural resources, but also multiple economic values to people as spaces for residences, outdoor recreation, and nurseries of commercial fisheries. It also provides pollution filtration, inland protection from tides and storms, barrier to salt intrusion and access to off-shore waters (Klein, Osleeb and Viola, 2004)

Coastal barrier islands have long been recognized as attractive tourist destinations with a variety of coastal landforms such as dunes, beaches and inlets (Godschalk, 1987; Davis and Fitzgerald, 2004). In particular, "the beach area of barrier islands is so attractive to tourism development with abundant recreational and ecotourism opportunities that their existence is the economic mainstay of many barrier island communities (Beatley, Brower and Schwab, 2002)." According to Hall (2001), coastal-based tourism and recreation have become one of the significant growing areas of contemporary tourism. Oh *et al*., (2009) indicated "coastal tourism and recreation in the United States represented about half of the ocean economy's $117 billion in gross domestic product in 2000."

Barrier islands are naturally dynamic high energy areas that are easily changed over time (Hoyt, 1967; Davis and Fitzgerald, 2004). They are constantly vulnerable to the forces of wind, waves, sediment transport, the effects of hurricanes and sea level rise (Beatley *et al*., 2002). Moreover, the shorelines fluctuate diurnally between a Mean Higher High Water (MHHW) level through a Mean Lower Low Water (MLLW) level (Moore, Ruggiero, & List, 2010). Tidal ranges along the United States coast, for example, vary from the 0.91-1.8 m (3-6 ft) (NOAA, 2010a) to over 16.3 m (53 ft) in the Bay of Fundy in Nova Scotia, Canada (Canadian Hydrographic

Service, 2006). With sea levels fluctuating over space and time, the size and shape of beaches are constantly changing. In Georgia, seaward beaches of the barrier islands typically experience a tidal range of 2 m (6 ½ ft), but exceed 3 m (10 ft) during the highest spring tides (GDNR, 2010).

These tidal differences create an extremely narrow and fluent section of dry beach interface between the inland fragile dunes and the ocean side saturated wet beach. The dry beach is critical habitat to endangered sea turtles, shore birds and numerous invertebrates (Beatley *et al*., 2002). It is also prime real estate for coastal residents, businesses and tourists. While long time residents are accustomed to diurnal tidal ranges, tourists from the mainland may not realize beach availability is limited by the tides to certain times of the day. In other words, the diurnal tidal ranges greatly affect beach availability and often catch tourists off guard if they are not familiar with tide charts and coastal maps. So, tourists also may not be able to easily determine how many hours of the day they will be able to enjoy the beach between the low and high tides. Such unpredictability decreases tourists' attraction to the beach areas of barrier islands and may negatively affect the economic benefits of coastal visitors on local economies. In addition, coastal managers tasked with beach preservation require information on changes in beach area due to natural processes of erosion and accretion.

In response to the importance of beach availability, effective analysis of dry beach first requires accurately mapping shorelines and associated beach areas over time. However, most studies of beach availability have been focused on economic and political issues, and very little has been done in analyzing beach availability with consideration of geographical features of coastal areas. Therefore, the purpose of this paper is to spatially analyze beach availability on Jekyll Island State Park, one of the primary barrier islands in Georgia (Figure 3.1). Specifically, the objectives of this research are: 1) analyze beach movement by beach accretion and erosion

based on the rate of shoreline change; 2) calculate available beach areas at different tide levels for different seasons using geospatial technologies; 3) identify the best candidate beach sites for recreational purposes; and 4) construct a Web-based GIS application for mobile devices that helps the public plan coastal activities. Ultimately, this research attempts to create a new model for tourists to make effective decisions for timing recreation of activities in coastal beach areas. In addition, these results can offer potential solutions for planners and managers to predict dynamic and complex shoreline changes in light of development plan and environmental protection of critical beach habitats for demands of beach access.

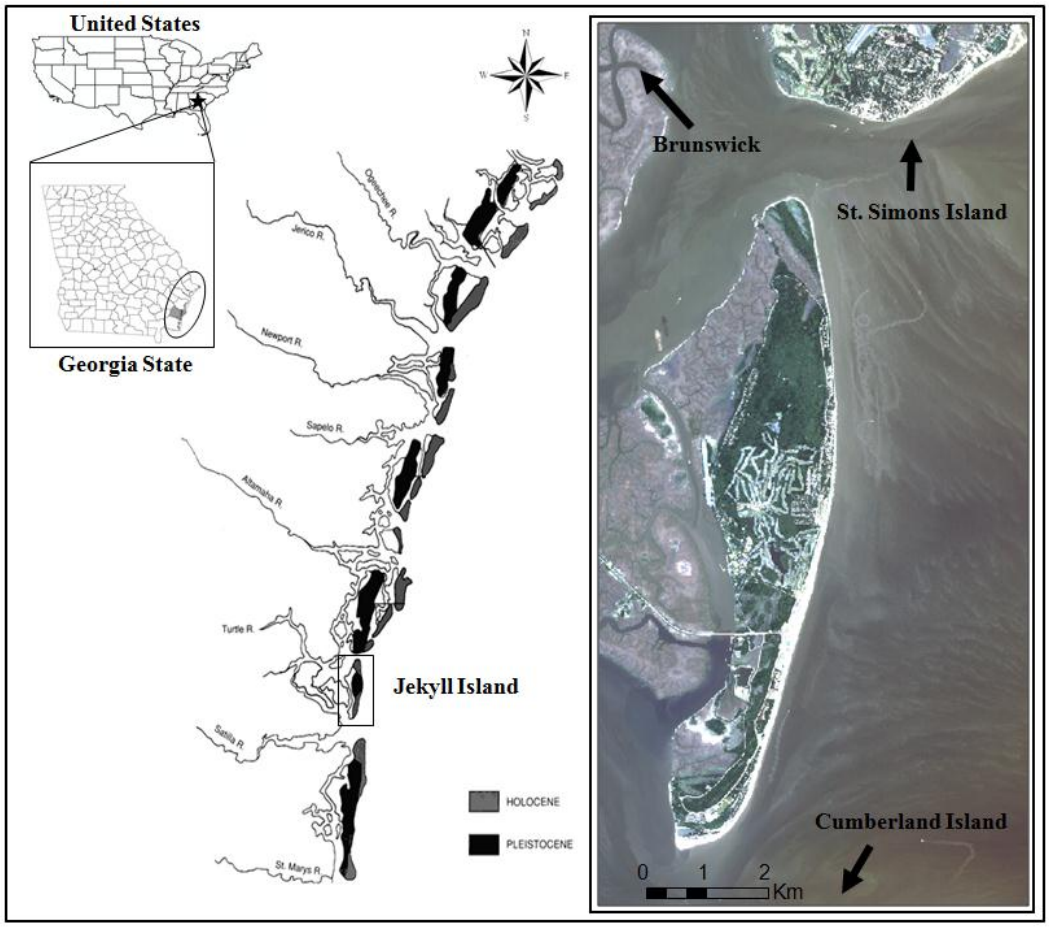

Figure 3.1. Jekyll Island study area in Glynn County, Georgia, United States.

This research paper is structured as follows. In Section 2, background in terms of barrier island beach availability and shoreline change, literature review and limitation related to shoreline delineation, and study area are introduced. In Section 3, methods used in this study are investigated, and results are addressed in Section 4. Finally, major implications and research summary are described with conclusions in Section 5 and 6, respectively.

3.2 Background

3.2.1 Barrier Island Beach Availability and Shoreline Change

In geomorphology, beach is defined as the accumulation of loose material such as mud, sand, shingle, and pebbles on the shore of a lake or the ocean (Kaufman and Pilkey, 1979). In particular, the beaches of barrier islands can play a pivotal role as the first line of defense against the forces of wind, waves, currents, and coastal storms (Dolan and Harry, 1987) Furthermore, the size, shape and shoreline of beach areas are changed dramatically by: 1) the dune systems, a complex of sand and coastal vegetation which transfers sediment back and forth between the beach; and 2) a variety of natural events such as along shore currents, hurricanes and coastal storms that erode beach sand and transport sediment to new areas for deposit, i.e., beach accretion (Beatley *et al*., 2002). As a result, the width of barrier island beaches is ever changing from year to year and even season to season.

According to a recent National Sea Grant report, 122 million people visit American beaches each year (Springuel and Schmitt, 2007) and beach areas are highly valuable tourist resources (Miller and Auyong, 1991); Goodhead & Johnson, 1996; Hall, 2001; (Agarwal, 2002); Bramwell, 2003; Jennings, 2004; (Page and Connell, 2006). Page and Connell (2006) suggest beaches offer natural, historical, psychological, and economic benefits that attract tourists. In

terms of natural significance, beaches provide diverse environments as well as attractive ecosystems which may form the basis for ecotourism (Goodhead and Johnson, 1996; Jennings, 2004). Historically, coastal areas are extremely valuable as sites of prehistoric occupation through European settlement and establishment of the first town and cites. Psychologically, visitors to a beach area can be attracted by sense of place that is created by a unique coastal townscape, both historic and modern architecture and tourist-related features such as piers, promenades, and gardens (Page and Connell, 2006). In addition, beaches provide spaces for outdoor recreation, wildlife habitat, nurseries of commercial fisheries and ecosystem services for multiple economic values. Houston (1995, pp. 1-4, 2002 and 2008) indicated that the coast encompassing beach and near-shore waters provides an environment conductive to recreation and leisure supporting the biggest tourism trade of any environmental type in the world. For example, Miami beach alone brings in more revenue than the combined totals for Yellowstone, the Grand Canyon and Yosemite National Park added together. The beach area of barrier islands is so attractive to tourism development with abundant recreational opportunities that their existence is the economic mainstay of many barrier island communities (Beatley *et al*., 2002).

In terms of accessibility or public beach access, since 1972 when the first U.S. Coastal Zone Management Act (CZMA) was passed (NOAA, 1972), great attention has been paid to beach accessibility, especially public access for recreational purposes (Carmichae, 1995; Mongeau, 2003). This accessibility is directly related to beach availability. In other words, once visitors have physically reached (i.e., accessed) the dry beach area, their next concern is the width and length of dry beach that is available to them for recreational and ecotourism activities at any particular time and date. There are studies regarding public access to the coasts for recreational purposes. Brower and Dreyfoos (1979) identified private ownership as one of the

inhibitors to tourists and even local residents' right to access the coast. They indicated the dry sand area is often privately owned and there are spatial differences of accessibility to the coast between wet and dry sand areas, restricting beach use for tourism and recreation. Kline and Swallow (1998) pointed out a lack of consideration for the value of public beach access through their review of the majority of previous coastal research. There are studies regarding specific methods and tools for improving the public access to shorelines (Pogue and Lee, 1998 and 1999; Oh, Dixon, Mjelde and Draper, 2008; Oh, Draper and Dixon, 2009 and 2010; Thomson and Dalton, 2010). Porgue and Lee (1999), for example, introduced various tools and processes such as acquisition, planning, regulations, technical assistance and public outreach in order to encourage the provision of public beach access. Thomson and Dalton (2010) pointed out a lack of reliable data on how people utilize a specific shoreline in the process of planning for access and suggested the integration of field surveys and geospatial technologies such as geographic information system (GIS) and Global Positioning System (GPS) offer reasonable solutions to develop a geodatabase for more effective shoreline management.

Despite a number of studies of access to shoreline and it remains difficult to identify beach availability on barrier islands because of fluctuating tidal ranges each day. As noted above, beaches of barrier islands are rapidly reshaped by dramatic natural events such as hurricanes, typhoons, tsunamis, earthquakes and severe storms, in addition to constant impacts from wind current and more gradual processes of beach accretion and erosion (Esnard, Brower and Bortz, 2001). Moreover, sea level rise and fall by tidal effects make shorelines of barrier islands fluctuate several times between a Mean Higher High Water (MHHW) level through a Mean Lower Low Water (MLLW) level during the course of a day (Davis and Fitzgerald, 2004; Moore, Ruggiero and List, 2010). These complexities of barrier island shorelines make it difficult for

tourists to know the optimum times and places for accessing beaches for recreational purposes. As a result, tourists are unable to access some beach areas at certain times of the day or determine how long beach areas will be available.

Therefore, it is essential for enhanced tourism management that geographical considerations of dynamic coastal systems should be implemented for identifying beach availability on barrier islands. Specifically, reasonable methods and tools are needed to delineate accurate shorelines and associated beach areas as they change over time. However, so far, very little has been done to analyze beach availability with consideration of geographical features of barrier islands and tourism.

3.2.2 Previous Methods for Detecting Shorelines

Various approaches in geography have been used to delineate shorelines with three major categories for detecting shoreline changes: ground surveying, photogrammetric measurement of remotely sensed images and modern Light Detection and Ranging (LiDAR) technology (Chen & Rau, 1998). Grounding surveying using traditional total station surveying equipment and GPS survey techniques are the most accurate method, but also the most time consuming and labor intensive. Remote sensing and photogrammetry are useful means of making accurate shoreline measurements over large areas from above ground images such as airborne aerial photographs and spaceborne satellite images. However, users of the spaceborne imagery have little control over the timing of satellite data acquisitions. Air photo acquisition, on the other hand, is more flexible and can be custom planned to coincide with a particular tidal stage. The manual interpretation of aerial photographs as a technique for detecting shoreline change began in the late 1960's (Moffitt, 1969). From an image, the wet and dry parts of shorelines are manually

interpreted and this line has traditionally been used to represent the shoreline and calculate shoreline change rate (Overton and Fisher, 2003). Figure 3.2 shows ground photos of wet/dry beaches at different locations on Jekyll Island. Figure 2d shows the wet/dry shoreline drawn on an aerial photograph and Mean High Water (MHW) level in 1999. The highest water level (HWL) is also often interpreted from aerial photography.

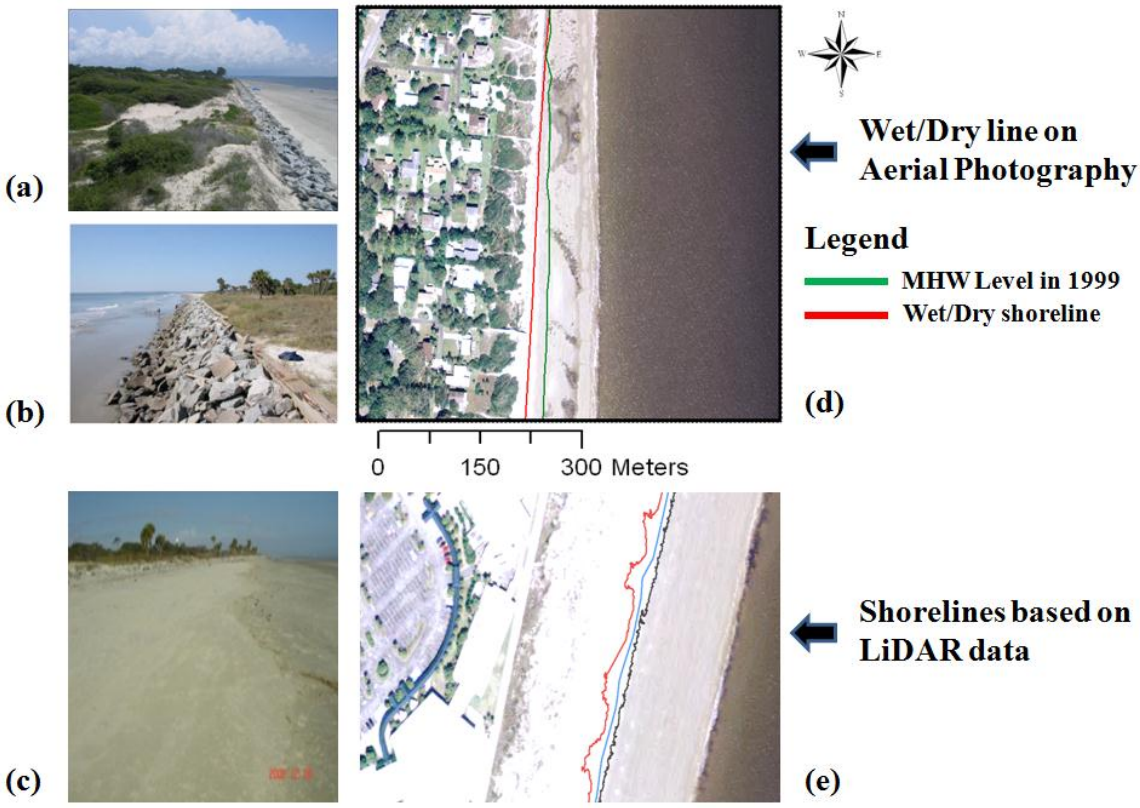

Figure 3.2. Wet/Dry shorelines based on ground photos (a, b, and c) and an aerial photograph (d), as well as shorelines of MHW level derived from LiDAR data (e).

The wet/dry line position, however, is a function of real-time wave action and is tide dependent (Martin, 1997). In some instances, the wet/dry line can be considered equivalent to, or an approximation of, the often-used high water line, which has received thorough scientific attention (Moore, Ruggiero and List, 2010). Although the wet/dry line position can define a real

shoreline at a specific time, the exact MHW level cannot be recognized on imagery captured at an instant in time during the tidal stage. The MHW level, however, has been used officially by the Georgia State Legislation as the shoreline that defines the boundary between land and sea. Therefore, a geospatial method of mapping this tidal stage is important to barrier island managers.

In recent years, a new altimetry technology has been used to extract MHW shorelines from topographic LiDAR data (Figure 3.2e). LiDAR is an active remote sensing technology that like radar transmits pulses of light energy and reaches reflected energy to find information about distant targets. Specifically, LiDAR transmits visible and near infrared wavelengths of the electromagnetic spectrum and calculates the range to an object by measuring the time delay between transmission of a pulse and detection of the reflected signal (Cracknell and Hayes, 2007). Unlike radar, LiDAR transmits up to 200,000 pulses per second and is capable of detecting up to five levels of returns for each pulse for canopy penetration and detection of subtle variations of the ground surface (ASPRS, 2010). Although expensive to acquire, airborne topographic LiDAR technology can generate high-resolution elevation data over large areas relatively quickly, and it is particularly useful for coastal applications because vertical measurements are accurate to approximately 15 cm root mean square error (RMSE) for bare earth points (Maune & American Society for Photogrammetry and Remote Sensing, 2007). LiDAR surveys have been used to investigate, for instance, large-scale beach morphology (Stockdon, Sallenger, List and Holman, 2002), human impacts in the coastal zone and hurricane-induced beach change (Robertson W., Zhang and Leatherman, 2005).

3.2.3 Limitations in Shoreline Delineation

In spite of more accurate and advanced methods to represent shorelines, challenges remain. First is the alternating rise and fall of the sea level, as influenced by the gravitational attraction of the moon and sun (Davis *et al.,* 2004). Horizontal movement of water often accompanies the rising and falling of the tide and this is called the tidal current. Twice per day there is a low tide and a high tide, which has differences in height between them and the differences called the tidal range (NOAA, 2010). This range can be measured with reference to a tidal datum, which is a standard elevation defined at a certain phase of the tide (Hicks, 2006). There is a range of tidal datums that are used as references to measure local water levels relative to fixed points known as bench marks. Table 1 lists a range of tidal datums maintained by the Center for Operational Oceanographic Products and Services (COOPS), which is part of an integrated National Ocean Service (NOS) program in the National Oceanic and Atmospheric Administration (NOAA).

Table 3.1. Tidal Datum Ranges (*Source*: NOAA, 2010b).

Tidal datums	Definition (Tide and Current Glossary)
MHHW	Mean Higher High Water (MHHW) is the average of the higher high water height of each tidal day observed over the National Tidal Datum Epoch.
MHW	Mean High Water (MHW) is the average of all the high water heights observed over the National Tidal Datum Epoch.
MSL	Mean Sea Level (MSL) is the arithmetic mean of mean high water and mean low water.
MLW	Mean Low Water (MLW) is the average of all the low water heights observed over the National Tidal Datum Epoch.
MLLW	Mean Lower Low Water (MLLW) is the average of the lower low water height of each tidal day observed over the National Tidal Datum Epoch.

The second limitation in shoreline delineation is the effects of surge caused by low pressure weather systems and strong winds blowing on shore which increase water levels on the beach (Davis *et al*., 2004). The effects can rapidly and dramatically alter shorelines and cause beach erosion.

Third among the potential problems of shoreline delineation is the limitation of representing very dynamic tidal changes along narrow shorelines. Although LiDAR offers the most accurate topographic data for low relief areas, the airborne LiDAR sensor used to collect data of Jekyll Island State Park was focused on land surface detection and did not collect data below the water level along the shore. In other words, the airborne LiDAR could not topographically model the entire intertidal zone because the data acquisition was a snapshot of a single tidal level. Although specialized bathymetric LiDAR surveys can measure the depth of the water to some extent, water penetration by typical airborne LiDAR is limited due to high reflection of LiDAR pulses surfaces on water and poor penetration. Therefore, alternative methods to delineate shorelines at all possible tidal ranges were addressed in this study.

3.2.4 Study Area

Jekyll Island State Park (Figure 3.1) encompasses a barrier island approximately 11-km (6.84 mi) long and 2.4-km (1.5 mi) wide located in Glynn County along the Georgia coast (Lenz, 1999). In spite of being comparatively small, the Island offers a diversity of marine habitat, beach, dune, saltwater marsh, upland, and freshwater habitats that support an estimated 845 plant species, 219 invertebrates, 215 fish, 41 amphibians, 66 reptiles, 346 birds, and 50 mammal species, as well as over 16 km of unspoiled beaches (Cabin Bluff Management, 2007). In addition, Jekyll Island protects a wealth of marine wildlife, including sea turtles, shrimp, and

waterfowl. Owned by the State of Georgia since 1974, it is managed by the Jekyll Island State Park Authority (JIA). Temperatures are on the warm side of temperate with normal summer daytime highs in the 26 to 32° Celsius range and winter temperatures normally ranging from 4.5 to 16° Celsius with short colder periods. The tide changes about every 6 hours resulting in 2 low and 2 high tides daily.

Jekyll Island is located at 31° 03'46"N and 81°24'53"W,11-km south east of the city of Brunswick, Georgia with St. Simons Island to the north and Cumberland Island to the south. The Island has a wealth of both historic and natural attractions including many recreational activities such as fishing, boating, dolphin and whale tours, golf, and heritage tourism. According to a visitation analysis by JIA, Jekyll Island visitation peaked at approximately 2.1 million in 1989-1990, but is now down about 23% from this historical peak. What is more, they estimate Jekyll Island will need to attract 2.6 to 2.7 million visitors per year to raise sufficient income to fund operations and required capital improvements (Bleakly Advisory Group, 2008) . The current annual visitation is estimated at just below 1.5 million. Thus, the State of Georgia is interested in the revitalization of Jekyll Island while, simultaneously, preserving its natural areas and protecting its valuable resources. Assessing beach availability to tourists is consistent with State objectives to increase visitors and enhance recreational and ecotourism experiences.

3.3 Methodology

3.3.1. LiDAR Topography and Shorelines

LiDAR data provide the basis for detailed topography and accurate shoreline delineation of Jekyll Island. Originally acquired by Glynn County, Georgia from March 1 to April 1, 2007, The LiDAR data consisted of a classified multiple return point cloud and a bare earth surface of

points of X, Y, and Z coordinates in the standard LAS 1.3 format. The accuracy of these data meets National Standard for Spatial Accuracy (NSSDA) standards. Namely, LiDAR point cloud elevation data are accurate to 0.18 m (about 6/10 of a foot). The lowest elevation in the Jekyll Island LiDAR DEM is -0.64 m (-2.1 ft) and the highest height is 14 m (45.9 ft). The aerial digital imagery provided for this research by Glynn County, was acquired in 2007 by the Optimal Geomatics Incorporation for the National Agriculture Imagery Program (NAIP) of the U.S. Department of Agriculture (USDA) with 50 cm (1.6 ft) spatial resolution (or pixel size). In order to incorporate the LiDAR data in a GIS database for editing and these data were first converted to an ArcGIS shapefile of point features (Figure 3.3).

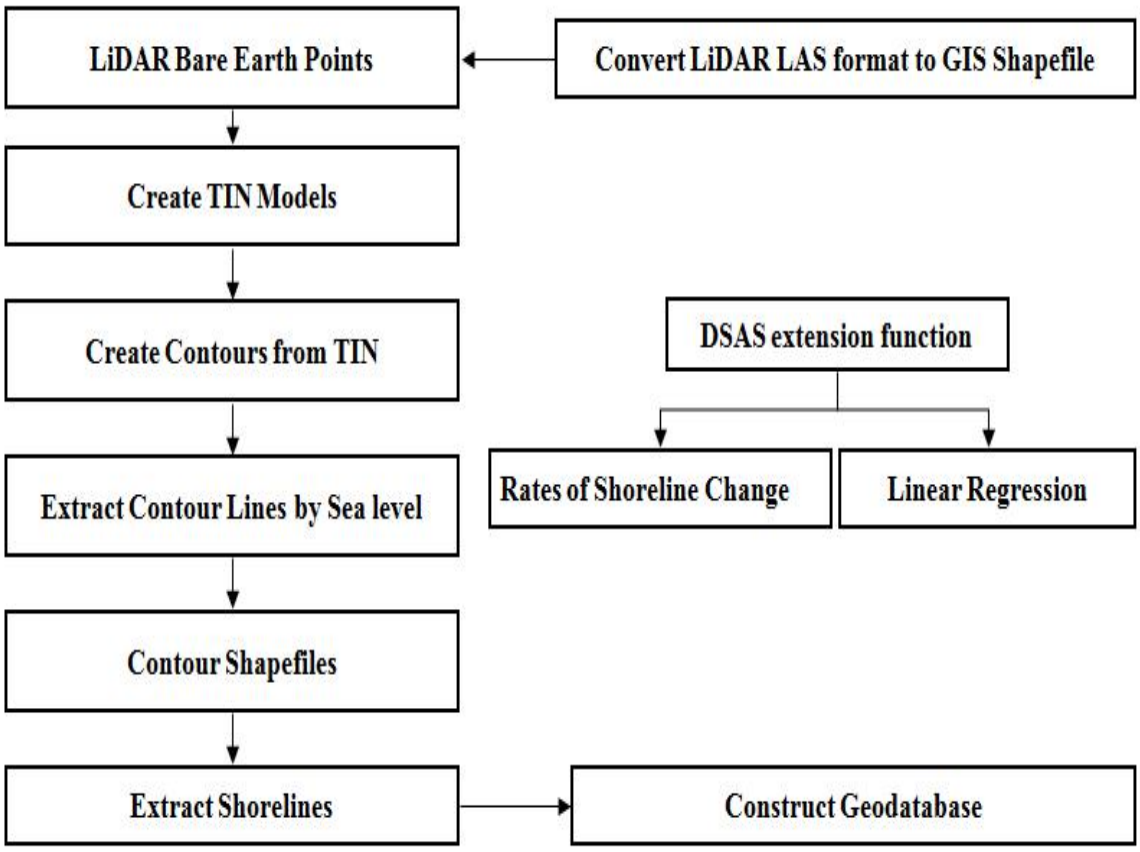

Figure 3.3. Workflow of extracting shorelines for beach area.

Subsequently, the bare earth point features are converted to a Triangular Irregular Network (TIN) model, which represents the terrain in more detail. In the next step, topographic contours with connecting points of the same elevation were created. The elevation interval used to extract the contours form the TIN is about 0.03 m (0.1 ft). Then, the shorelines in the range of possible tidal ranges were extracted, and converted to polylines. Finally, all extracted shorelines were saved in a single geodatabases, which efficiently manages geospatial data such as shapefiles, satellite imagery, and all GIS data of vector and raster types.

A ground coordinate system was used for the geodatabase based on the North American Datum of 1983 (NAD 83), the Geodetic Reference System of 1980 (GRS 80) ellipsoid, and the Universal Transverse Mercator (UTM) (zone 17) projection for X and Y coordinate system. For Z values, data were referenced to the North American Vertical Datum of 1988 (NAVD 88).

3.3.2 Monitoring Beach Accretion and Erosion

Jekyll Island was formed during the Pleistocene to Holocene eras and the existing shoreline is the result of the interaction of wind, waves, currents, sand supply and, slowly rising sea level, especially beach accretion and erosion (Henry, 2005). In this study, Jekyll Island beach accretion and erosion was calculated to examine the spatial and temporal availability of sandy beach for wildlife, human activities and ecosystem services. To do this, The Digital Shoreline Analysis System (DSAS) version 4.2, developed by the U.S. Geological Survey (USGS) (Thieler, 2009) was used to calculate shoreline rate of change statistics from multiple historic shoreline positions established in this study from historical records and current aerial photographs and LiDAR data of multiple return points.

To obtain rates of shoreline change, a linear regression model was used because it is the most commonly applied statistical technique and the most statistically robust quantitative method for expressing shoreline movement and estimating rates of change (Crowell and Leatherman, 1999). The historic shoreline data used in this research consisted of shorelines at MHW levels from maps published in 1857-1870 and 1920-1925, compiled by Georgia Southern University from historic records. In addition, the shoreline in1971-1973 was extracted from topographic maps created by NOAA and USGS. A shoreline in 1999 also was available from USGS that was based on LiDAR acquisition at mean high water level. Finally, we extracted a LiDAR-derived shoreline of average MHW for 1998 to 2008.

In general, historical shoreline data consist of positional errors reported as root mean square errors (RMSE) due to: 1) georeferencing error, 2) digitizing error, 3) T-sheet survey error, and 4) LiDAR position error. More specifically, the historical shorelines (excluding LiDAR-derived shorelines) were compiled as topographic maps known as "T-sheets," which were georeferenced and converted from the North American Datum of 1927 (NAD 27) to NAD 83. Total RMSE for the georeferencing process was maintained below 1 pixel, which is approximately ±4 m at a scale of 1:20,000 and approximately ±1.5 m at a scale of 1:10,000 (Morton and Miller, 2005). Overall, RMS errors of the historical shoreline for the southeast Atlantic coast used in this study can be summarized as follows: 1) georeferencing error is less than ±4 m; 2) digitizing error is less ±1 m; 3) maximum T-sheet survey error is ±10 m for maps provided before 1920s and ±3 m in 1970s; and 4) LiDAR position error is ±1.5 m (Morton and Miller, 2005).

3.4 Results

3.4. 1 Jekyll Island Shoreline Changes

As shown in Figure 3.4, rates of shoreline change based on the historical shoreline data from 1857/1870, 1924, 1971 and 1999, here has been a total of 39% erosion and 61% accretion on the ocean side of Jekyll Island. The highlighted sections of transect lines indicate eroded (Figure 3.4c) and accreted areas (Figure 3.4d). Based on136 transects, the mean rate of shoreline change between 1857 and 1999 was 0.8m/yr. Erosion during this 142 year period averaged -0.7m/yr. while the accretion rate were double and averaged 2.0 m/yr. Table 3.2 indicates additional statistical analysis on shoreline change, generated by DSAS 4.2.

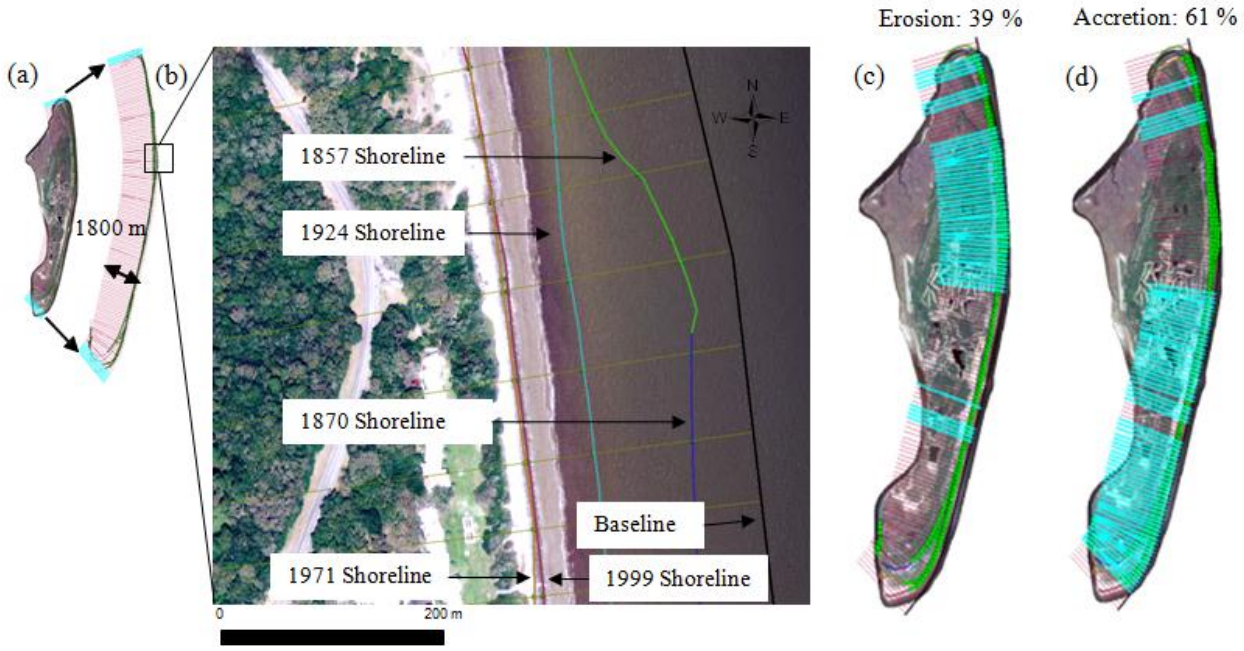

Figure 3.4. Transect lines and intersect points to calculate rates of shoreline movement.

Table 3.2. Historical shoreline-change trend derived from linear regression rates using four shorelines (1857 to 1999).

Jekyll Island (1857~1999)	Num. of Transects	Mean Shoreline Change Rate (m/yr)	(%) Erosion	Erosion Rates (m/yr)		(%) Accretion	Accretion Rates (m/yr)	
				Max	Mean		Max	Mean
	136	0.8	39	-1.6	-0.7	61	13.5	2.0

For further examination of shoreline change, the 2008 MHW shoreline by LiDAR was used to calculate beach erosion and accretion (Figure 3.5). To do this, the 0.79 m (2.6 ft) MHW level, which is verified data measured at a bench mark of St. Simons Island from 1999 to 2008, was used and all values were referenced to the NAVD 88 datum.

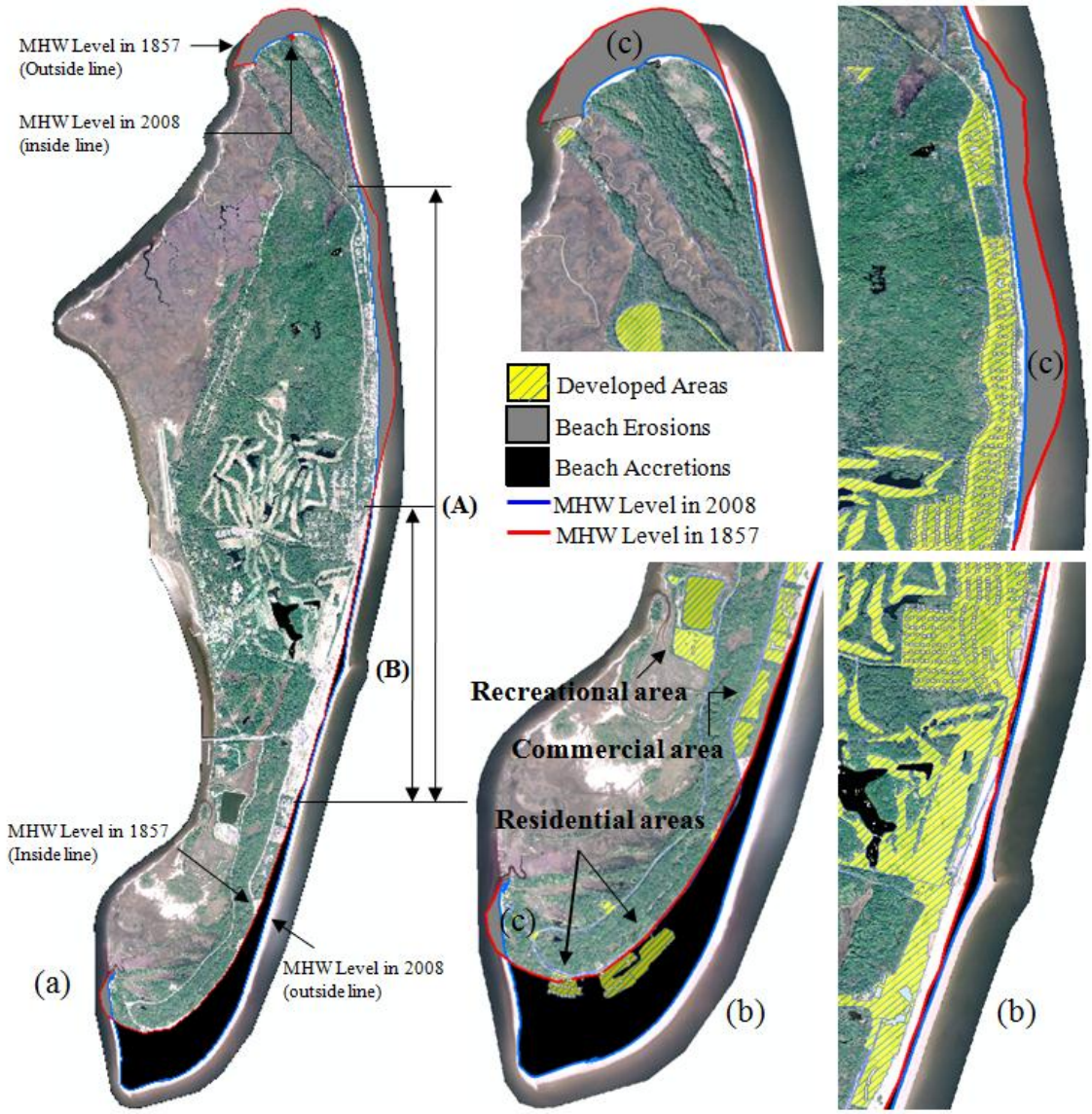

Figure 3.5. Beach accretion and erosion of sandy beach. Revetment rocks known as Johnson's rocks are shown in (a) at A. A portion of revetment rocks shown in B has been buried by sand.

As shown in Figure 3.5, the shoreline at MHW for 1857 is delineated and it differs considerably from the shoreline at 0.79 m (2.6 ft) MHW for 2008. During the last 150 years, the southern portion of the Island has been developed with residential and commercial land uses in

areas of accretion shown in black (Figure 3.5b). During this same period, the area in the northern portion and in the back of the southern portion shown in gray (Figure 3.5c) have been eroded. The cumulative area of erosion over the 150-year time period was 0.76 km² (75.52 ha) and cumulative accretion was 1.22 km² (121.51 ha). Notably, Figure 3.5 at A indicates the original location of revetment known as Johnson's rocks built in 1961. Over the years, approximately half of the revetment rocks have been buried by sand affected by beach accretion (Figure 3.5 at B). Consistent with U.S. east coast barrier islands, the greatest shoreline change occurs along the northern portion for erosion and southern portion for accretion of Jekyll Island.

3.4.2 Beach Availability

Dunes, consisting of accreted sands and specially adapted flora and fauna, are a particularly fragile component of the barrier island ecosystem. Despite their susceptibility to high winds and wave action, they play a critical role in maintaining the integrity of the Island and protecting development that occurs behind the dune line (Beatley, Brower and Schwab, 2002). Although dunes were used historically for recreation such as driving all terrain vehicles, current laws restrict such destructive activities today and they are interesting sites for ecotourism.

According to the Georgia Shore Protection Act (O.C.G.A. 2-5-230), construction in sand dunes is limited to temporary structures such as elevated walk ways, and then only by permit from the Shore Protection Committee. Structures such as boat basins, docks, marinas, and boat ramps are not allowed in the dunes. Thus, dunes were excluded in this study from the analysis of beach availability for recreational purposes. Only sands that are seaward from the dune line were included as beach areas for tourists.

3.4.2.1 Tidal Ranges

Historical tidal ranges were examined in order to determine seasonal variability in shorelines. Based on historical Tide Data, provided by TIDES and CURRENTS from the NOAA, average sea level heights for 10 years were applied in each tidal range. Generally, a seasonal tide value uses a 19-year arithmetic average so as not to bias the estimate of the tidal range or datum. However, currently available actual data, which are based on measured sea level at tide gauges rather than predicted levels projected using tidal ranges, are provided and verified by NOAA for 1999 through 2008 in the Historic Tide Data. The tide ranges are referenced to the NAVD 88 vertical datum and the tidal bench mark is located on St. Simons Island, Georgia, which is at Latitude: 31° 7.9' N and Longitude: 81° 23.8' W.

As noted in Table 3.3, all tide data are separated by season and averaged in each tidal range with spring tide data averaged from March to May, summer from June to August, fall from September to November, and winter from December to February. The highest water level (HWL) of 1.43 m (4.7 ft) was found in fall while the lowest water level (LWL) of -1.86 m (-6.1 ft) was in the winter. Thus Jekyll Island can have a total tide range over 3.05 m (10 ft).

Table 3.3. Tidal ranges for 10 years.

1999 -2008	HWL Average	MHW Average	MSL Average	Lowest Average
Spring	1.34 (4.4)	0.79 (2.6)	-0.23 (-0.7)	-1.80 (-5.9)
Summer	1.34 (4.4)	0.79 (2.6)	-0.18 (-0.6)	-1.68 (-5.5)
Fall	1.43 (4.7)	0.91 (3.0)	-0.03 (-0.1)	-1.52 (-5.0)
Winter	1.25 (4.1)	0.70 (2.3)	- 0.27 (-0.9)	-1.86 (-6.1)

3.4.2.2 Seasonal Analysis

As shown in Figure 3.6, red, blue and green colors represent available dry beach at HWL 1.34 m (4.4 ft) (A), MHW 0.79 m (2.6 ft) (B) and MSL -0.21 m (-0.7 ft) (C). These water levels represent the extremes of shorelines and, thus the amount of dry beach available to tourists during a particular season. The red area in Figure 6 shows limited dry beach available during high spring tides (i.e., at HWL), the red and blue areas depict dry beach at MHW levels and the red, blue and green areas combined represent dry beach available when intermediate tides (i.e., at MSL) occur. The inset images in Figure 3.6 show differences in dry beach availability for only part of the day (red HWL area) or all day long (blue and green, MHW and MSL area) for particular portions of Jekyll Island. For example, in the spring season, only a small portion of the north end (a) and back side of the barrier island (e) are selectively available at entire tidal range while portions (d) and southern parts of (e) are available for all day. However, portions of (b) and (c) are unavailable for most tidal ranges. These areas have the most restricted beach availability, which means it is difficult for visitors to have access to sandy beaches for recreational purposes for the entire day. Careful planning would be needed to select portions of Jekyll Island where tourists could spend all day on the beach. By and large, all seasons show similar patterns for beach vulnerability to tides and availability.

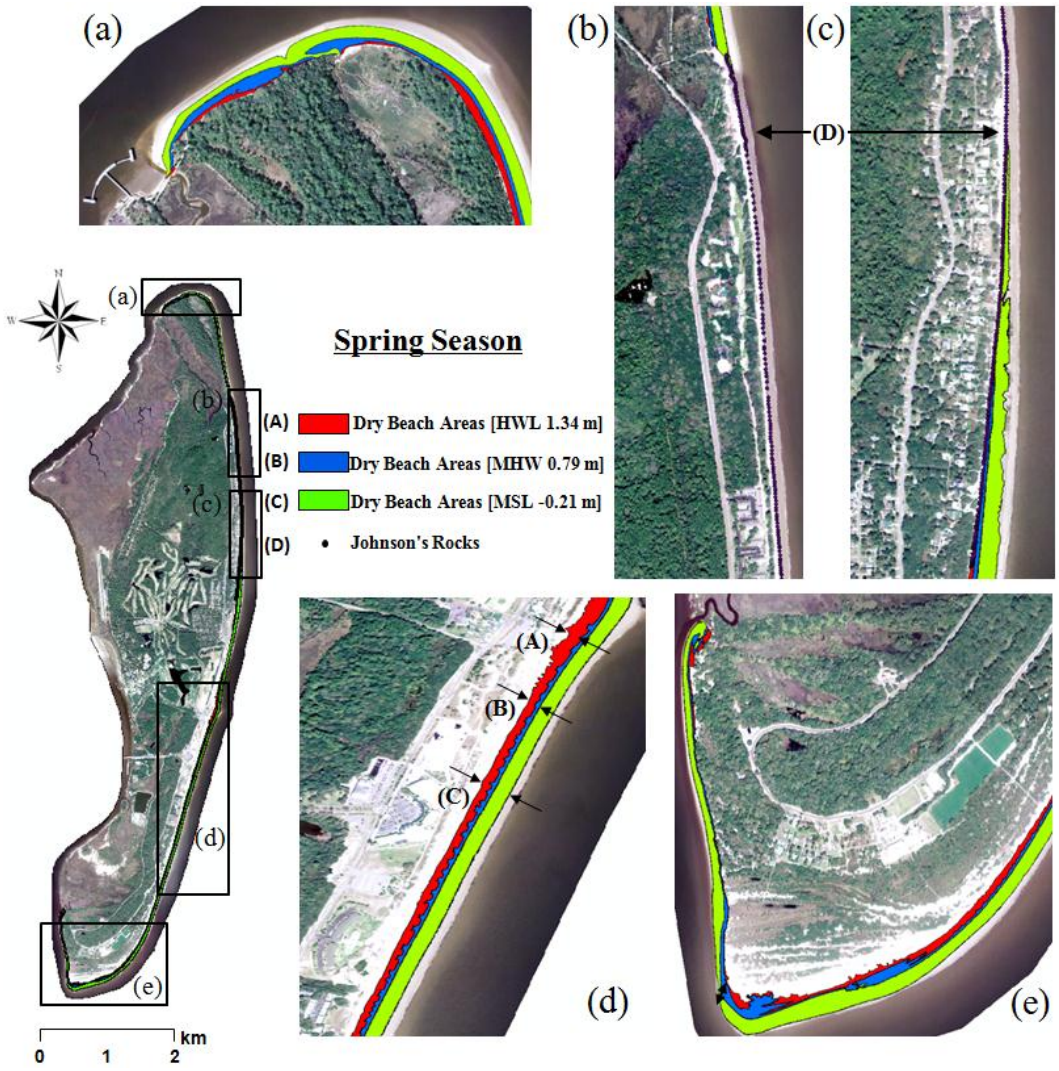

Figure 3.6. Areas of beach available to the tourists in spring.

As shown in Figure 3.7a, the revetment rocks known as Johnson's Rocks line the east coast of Jekyll Island north of the golf course (note the location of "B" on Figure 3.7b), these rocks were placed along the beach/land boundary in 1961 to protect developed areas from wave action and inundation. Although the revetment rocks have prevented erosion of the upland, they have increased erosion of the beach such that this area in all seasons does not have any available dry beach.

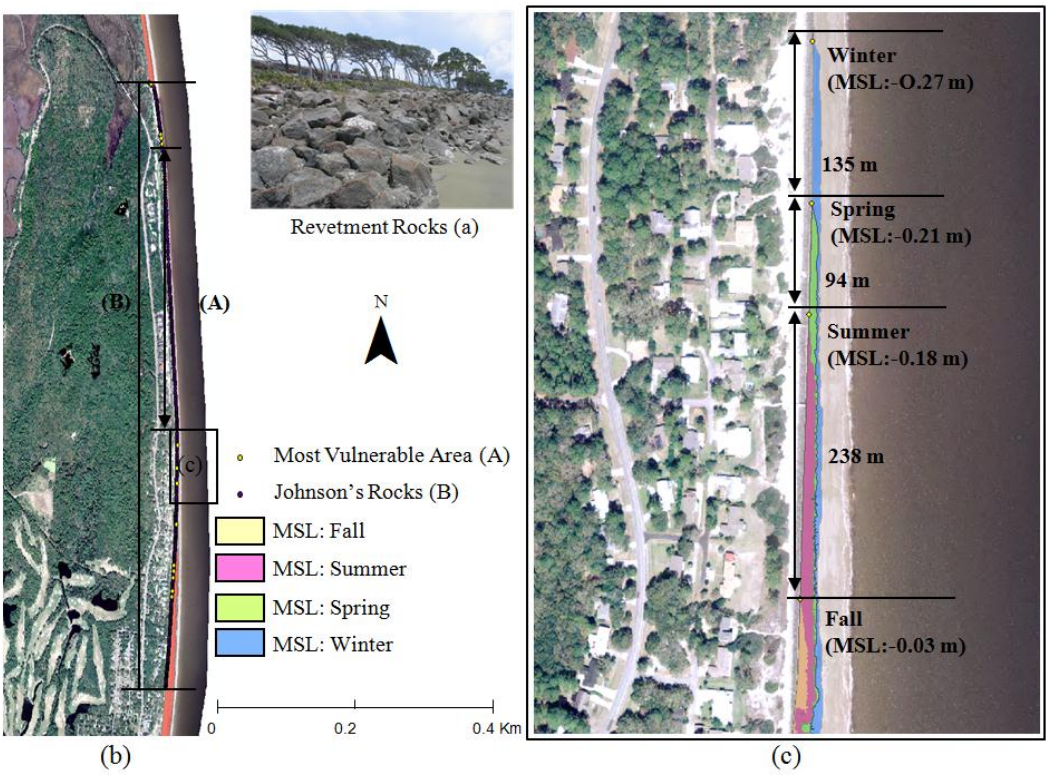

Figure 3.7. South of the Johnson's Rocks revetment, the amount of available dry beach at MSL varies seasonally ranging from 135 m of exposed beach in the northern portion during the winter to 934 m of beach in the fall.

Generally, the spring and fall seasons have the greatest tide amplitude, meaning the highest and lowest water levels are recorded at these times. In this research, NOAA tide data averaged over 10 years show the winter season has the lowest mean sea level and more available beach area. As shown in Figure 3.7c, the length of the available dry beach will vary seasonally. For example, there is a 238m (0.15 mile) difference in the length of beach that is available at MSL between the fall and summer seasons, 94m (0.06 mile) between the spring and summer seasons, and 135m (0.08 mile) between the winter and spring seasons. Overall, there is a 934 m (0.58mile) length of beach that exhibits seasonal differences in available dry beach at MSL.

3.4.2.3 Determining Tide Level of Aerial Photographs

As described above, the lowest height of the LiDAR data for Jekyll Island is -0.64 m (-2.1 ft) and the highest upland height is 14 m (45.9 ft). According to verified tide level records for last 10 years, the highest height was 1.65m (5.4 ft) on October, 2002 and the lowest height was -2.29 m (-7.5 ft) on April 2002. Although, airborne laser bathymetry (ALB) can measure the depths of moderately clear, near-shore coastal waters and lakes (Hickman and Hogg, 1969), the airborne LiDAR in this study was designed to collect data of the upland earth surface. Since the lowest height of the LiDAR is -0.64 m (-2.1 ft) and the tidal range is known to extend to -2.29 m (-7.5 ft), a different source of remote sensing data was required to delineate the dry beach available at a lower tide level, i.e., an expanded dry beach area. The March 11, 2007 aerial photographs show dry beach at a lower tide, but it was necessary to determine the tide level based on the time the air photos were taken. Tide level records compared to the date and time aerial photographs were flown can be used to determine. The water level of the dry and wet beach lines delineated from the air photos. Thus, this research estimated the height of the tide on the date the aerial photographs were flown.

As shown in Figure 3.8, information from the metadata of the aerial photographs was used to reconstruct, the 4 flight lines and flight times of photos taken along the shoreline. A total of 37 photos were acquired from 11:06 am to 12:15 pm, March 11, 2007. In addition, real tide levels were recorded by NOAA ranging from -0.62 m (-2.05 ft) to -0.94 m (-3.1 ft) at 5:24 am through 23:42 pm on March 11th (Figure 3.9). Based on this information, it estimated that the water level was between -0.82 m (-2.7 ft) and -0.85 m (-2.8 ft) during the exposures of the aerial photographs. Thus, this research determined -0.85 m (-2.8 ft) was the tide level of the boundary of the dry beach on the air photos and thus defined the beach availability.

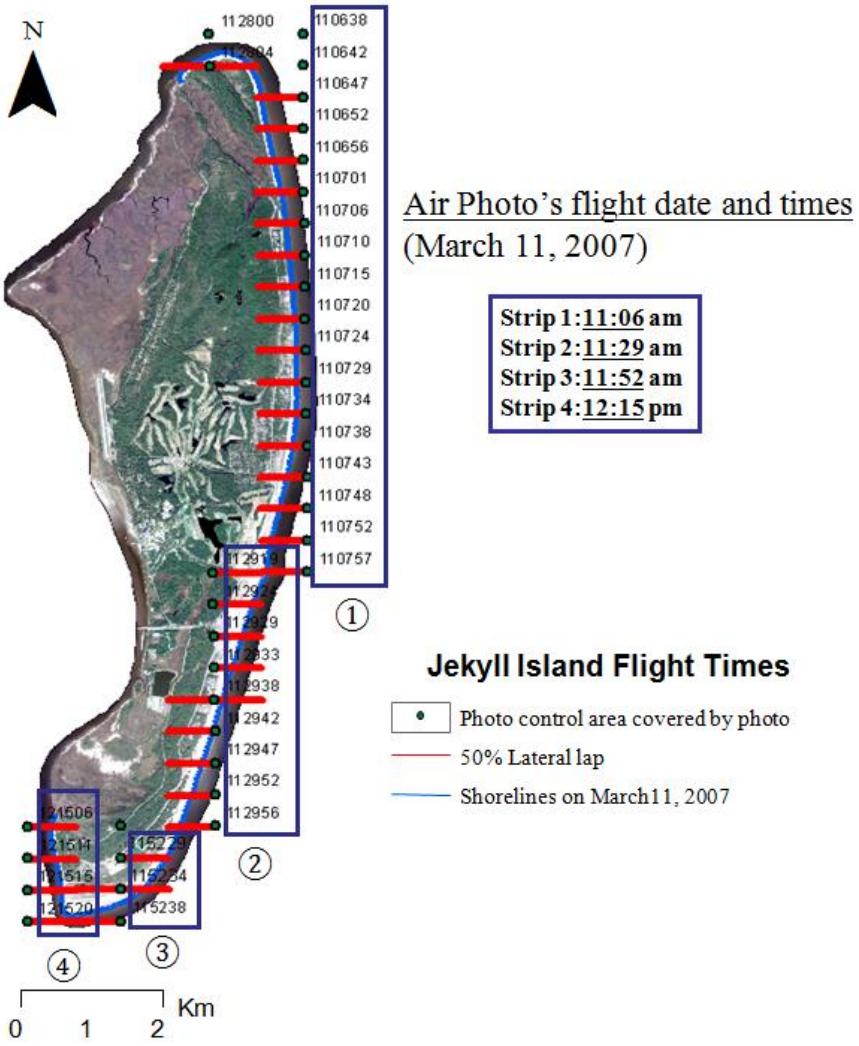

Figure 3.8. Coverage and time of aerial photographs acquired on March 11, 2007. Based on the time each aerial photograph was taken, tide charts may be used to determine the tidal stage of the wet/dry beach line visible on the photos.

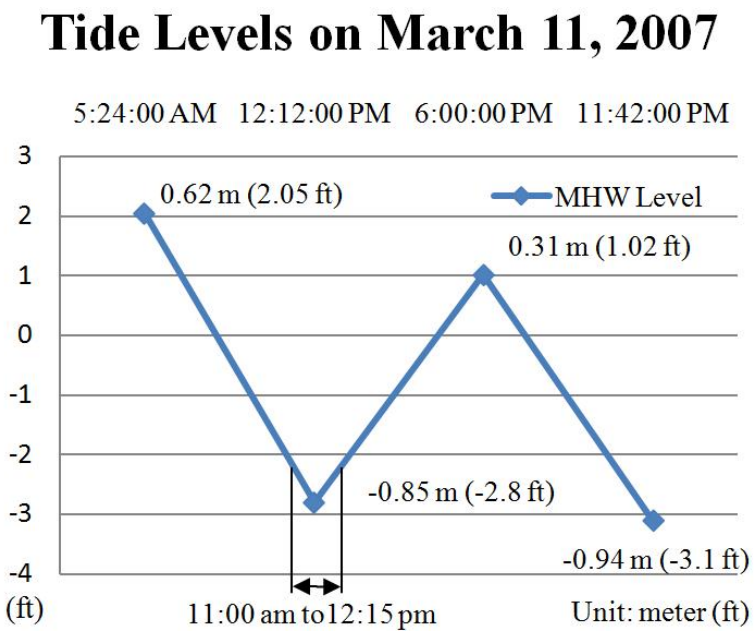

Figure 3.9. Estimated water level at the date and times of 4 flight lines of aerial photographs acquired March 11, 2007 between 11:00 am and 12:15 pm.

Once the water level of the shoreline depicted in the 2007 aerial photographs was established as -0.85 m (-2.8 ft), it was possible to project the expected shoreline at different seasons and tide levels, using trends in previously determined tidal ranges. For example, Figure 3.10 illustrates available beach for various tidal stages on Jekyll Island that are predicted during winter months. A combination of shoreline modeling and visualization of predicted shorelines superimposed on the Jekyll island aerial photograph would provide tourists with a tool for planning the time and duration of their activities on the beach in any particular part of the Island.

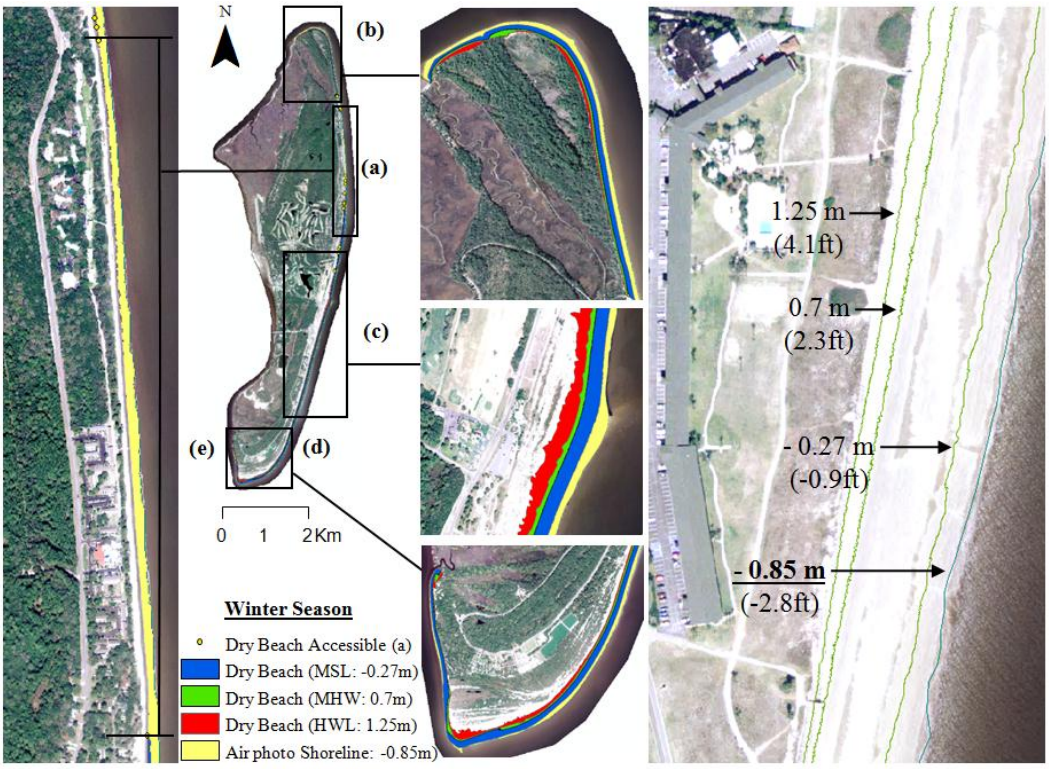

Figure 3.10. Available dry beach areas for different tide levels during the winter season were estimated relative to the water level of the beach line -0.85 m (-2.8 ft) imaged on the aerial photograph at the time of its exposure (approximately 11:00 am-12:15pm) on March 11, 2007.

The shoreline on the aerial photographs that was determined to be a water level of -0.85 m (-2.8 ft) shows all areas were accessible, even the most vulnerable areas around the revetment rocks. Specifically, Figure 3.10a shows beach area in yellow that is only available at times when the water level is below -0.85 m (-2.8 ft) and thus is not suitable for recreational activities on the beach for an entire day. The areas shown in Figure 3.10b and d are available at times when the tide is less than -0.27 m (-0.9 ft) (MSL). The beach area shown in red, blue, and yellow (Figure 3.10c) is available at all times of the day, which means it identifies the best recreational areas for tourists.

Due to seasonal and diurnal tidal changes, a summary of the amount of available beach changes, accordingly, can be complied. Table 3.4 lists the area and percent of beach available for each 3-month season along with the tidal ranges (highest to lowest water levels). It also indicates if beach is available part of the day or all day long. As shown in Table 4, the winter season is the best for beach availability on Jekyll Island. In the spring and summer when tourism on Jekyll Island is typically high, less than 25% of the dry beach is accessible for part of the day at MHW. It is therefore important to inform tourists of the optimal times to plan their visits because the percent of available beach can range from as low as less than 10% for part of the day in the fall.

Table 3.4. Beach availability by seasons.

Seasons (Months)	Tide Ranges	Water Level (m)	Available Beach Area		Percent Accessible Beach	Time Accessible
			km²	Acres		
Spring	(1) Highest Water Level (HWL)	1.34	0.14	34.8	12.8%	Part of the day
	(2) Mean Highest Water Level (MHW)	0.79	0.28	68.0	25.0%	
	(3) Mean Sea Level (MSL)	-0.23	0.75	186.1	68.4%	
	(4) Air photo shoreline	-0.85	1.10	272.2	100%	All day
	(5) Lowest Water Level	-1.80	>1.10	>272.2	100%	All day
Summer	(1) Highest Water Level (HWL)	1.34	0.14	34.8	12.8%	Part of the day
	(2) Mean Highest Water Level (MHW)	0.79	0.28	68.0	25.0%	
	(3) Mean Sea Level (MSL)	-0.18	0.74	182.5	67.03%	
	(4) Air photo shoreline	-0.85	1.10	272.2	100%	All day
	(5) Lowest Water Level	-1.68	> 1.10	> 272.2	100%	All day
Fall	(1) Highest Water Level (HWL)	1.43	0.10	24.8	9.1%	Part of the day
	(2) Mean Highest Water Level (MHW)	0.91	0.25	61.3	22.5%	
	(3) Mean Sea Level (MSL)	-0.03	0.65	161.1	59.2%	
	(4) Air photo shoreline	-0.85	1.10	272.2	100%	All day
	(5) Lowest Water Level	-1.5	> 1.10	> 272.2	100%	All day
Winter	(1) Highest Water Level (HWL)	1.25	0.17	43.0	15.8%	Part of the day
	(2) Mean Highest Water Level (MHW)	0.70	0.31	76.8	28.2%	
	(3) Mean Sea Level (MSL)	-0.27	0.78	193.7	71.1%	
	(4) Air photo shoreline	-0.85	1.10	272.2	100%	All day
	(5) Lowest Water Level	-1.86	> 1.10	> 272.2	100%	All day

3.4.3 Application of Web-based GIS

The historical shoreline changes and beach availability by seasons revealed in this research can be used by tourists to make plans and decide on the best beach area for their activities on any given day or season. Additionally, shoreline changes provide planners with information needed to monitor and manage beach availability and development of beach access points. As a result, this information should be well constructed to be efficiently managed, delivered, used, and even shared on the Web. To do so, in this research, an application of Web-based GIS was constructed by using ArcGIS Server 9.3. For an example for beach availability at the highest sea level in the winter season, a Keyhole Markup Language (KML) file was hyperlinked to text provided in the view. The application is served at URL address: http://www2.crms.uga.edu/beach_availability_analysis/ (Figure 3.11).

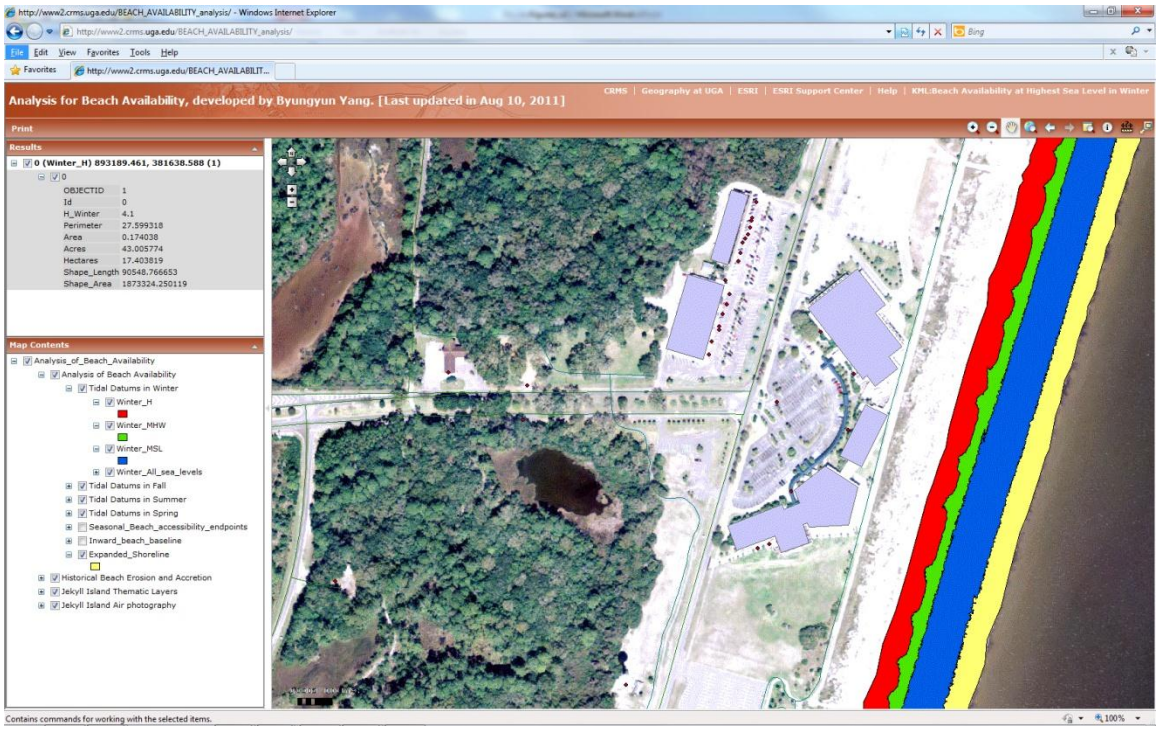

Figure 3.11. Application of Web-based GIS depicting a high resolution aerial photograph, building footprints, road access and estimated beach availability during HWL (red),

MHW (green), MSL (blue) and water level at the time the aerial photographs was acquired (yellow). Mobile devices such as smart phones can access these maps for tourist destination planning (Developed using ArcGIS Server).

Visitors or managers who want to find optimum beach areas or manage and monitor changes of beach availability can access these geospatial data by portable devices such as smart phones connected Internet providers. Data layers of images, roads, and building foot prints, for example, may be turned on and off to examine potential sites for beach walks, fishing, picnics, observing birds or wildlife. Although web-construction of geospatial data developed in this research does not serve real-time information, it does supply fundamental data for spatial decision support systems related to applications such as beach restoration, warnings to tourists concerning sensitive sea turtle nesting sites or beach cleanup operations.

3.5 Discussion and Summary

A number of federal, state and local regulations such as the Public Trust Doctrine, a Georgia state constitutional provision, or the Doctrine of Custom to protect the public right of access to some portion of the shoreline (Thompson, 2006; Thompson and Dalton, 2010) require planners, managers, and elected officials to understand how shorelines are accessed and how much dry beach is available during different times and seasons. This study identified beach availability for recreational use by tourists. To do this, changes in shorelines and dry beach were analyzed using historical shorelines and computing rates of shoreline change by linear regression modeling. In addition, a LiDAR-derived shoreline was used for recognizing serious beach accretion and erosion of sandy beach. In the next step, seasonal changes in sandy beach were

estimated from verified tidal values. Finally, shorelines visible in aerial photographs were delineated and the water level was estimated for identifying beach availability. The results indicated processes such as erosion, accretion, and possibly sea level rise since 1857 have caused changes in sandy beach, especially in the eroded northern portions of Jekyll Island and southern portions. These changes in island configuration also mean the time the beach can be used between high tides is greatly shortened. In addition, seasonal changes in tide levels affect times and percentage of available sandy beach on Jekyll Island that may be accessible for part of the day or all day depending on the tidal ranges. This information may be important to tourists due to restricted beach availability for recreational purposes. Also, examination of the delineated shoreline on aerial photographs revealed more available beach in the vulnerable rock revetment areas that can be used for tourist activities during low tide events. Finally, all finding are now being provided on-line via a Web-based GIS that can be used by the public and by resource managers.

On the basis of these results, some implications should be considered to ensure sustainable coastal tourism and recreation. First is the role of information in tourism. Specifically, these results can provide essential information for promoting seasonal tourism and planning tours or recreational activities. Access to information is prerequisite in order to create positive attention and attitudes that directly trigger enhanced action (Treby and Clark, 2004)**.** Therefore, maps and date regarding times and percentage of beach availability can allow travelers to make decisions about entering the beach for recreational purposes at a specific time and gives crucial notification to those who want to use the beach on the date of a potential visit. Second is the role of local government in communicating details about beach availability to the public. Appropriate systems or tools may be developed for easy access to map displays and

visualizations of projected tide levels with dry beach areas to promote coastal tourism. For example, specific information regarding beach availability may be presented through signs at access points or served by application of Web-based GIS such as that developed in this research. In particular, geospatial technologies via Internet and mobile devices such as smart phones can contribute to a spatial decision supporting system (SDSS) for efficient coastal tourism and management, and recreational planning.

Regarding coastal tourism and management, there are further considerations. With increasing interests in coastal areas, coastal tourism is one of the fastest growing segments having global economic impacts. Such interests and growth have made economic profits, along with the loss of environmental resources by human impacts (Hall, 2001). Although this research tried to investigate beach availability based on historical tide records and shoreline data sets, real-time information on actual beach availability is required for integration into applications of Web-based GIS. To do this, two considerations include real-time views of beach occupancy, local weather and storm conditions. Traditionally, beach occupancy is analyzed by direct observation which means the number of visitors to a beach can be estimated by delimited plots distributed at regular intervals along the entire extension of the beach (Roca, 2008). Although these estimations may be accurate, they reflect past conditions. An alternative is the use of a live web camera system. Many beaches around world use this live web camera with real time streaming to monitor beach occupancy and animal habitats. Although Jekyll Island does not have the web-cam monitoring system to date, the live web-camera would allow tourists and mangers to make better decisions for visitation, preservation and management of sandy beaches. Second, other factors such as wave height, wind speed and direction, storm surges, patterns of sediment migration, and even water temperature may be monitored and posted online for researchers and managers to

assess current conditions of beaches and coastal marshes (Phillips, 2008 and 2010; Thomas *et al*., 2011a and 2011b). Those factors are useful to make more realistic evaluations of shoreline changes and coastal processes. For example, according to the Coastal Data Information Program (CDIP), wave heights in Fernandina beach, Florida had a range of 0.37 m to 0.68 m on August 15, 2011. Located relatively close to Jekyll Island, this information can be critical as an additional factor to accurately estimate real-time shoreline changes or coastal processes by adding the previous past 10 years' average MHW sea level of 1.65 m (5.4 ft) to maximum possible wave heights of 0.68 m. Such information can be integrated into coastal monitoring systems for considering development plans, preservation policies and improved facilities for coastal tourism. As shown in Figure 3.12, the live web-camera system is proposed for further considerations in integrated Web GIS applications using geospatial data.

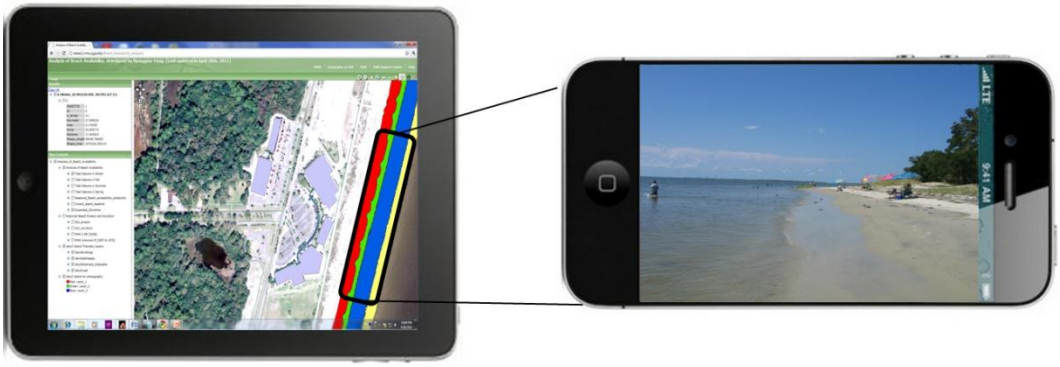

Figure 3.12. Real-time information into current a Web-based GIS application developed in this research.

3.6 Conclusion and Future Research

This research has attempted to identify beach availability for tourists by means of geospatial techniques, as well as provide information to tourists for visitor planning. Accordingly, the findings allow tourists to better understand when and where dry beaches will be

available for their recreational purposes and enable tourism managers to efficiently manage and monitor beaches for tourism.

This research also noted some limitations in the use of geospatial data and techniques. The use of 10-year averages of tidal ranges for seasonal analyses of dry beaches and tidal ranges may have restricted predictions because they were based on historical trends. Thus, very current or even real time data are needed to better identify available beach areas in light of recent coastal changes due to human activities and cumulative sea level rise. In addition, coastal islands are subject to beach accretion and erosion, as well as unexpected events, such as hurricanes and flooding. Predicted effects of these events on shorelines are required to improve information regarding available beach locations for residents and tourists.

In projected research, we plan to use climate satellites to analyze other factors such as wave heights and wind speed. The climate satellites such as Advanced Earth Observing Satellite 2 (ADEOS II), operated by the National Space Development Agency of Japan (NASDA), *National Aeronautics and Space Administration* (NASA), and Centre National d'Études Spatiales (CNES), or quick scatter meter (QuikSCAT) operated by NASA can measure wind data such as directions and speed and the Jason-1 satellite operated by both NASA and CNES is able to estimate sea-level acceleration or rise. These satellites are useful for better understanding coastal processes of making more realistic predictions of more realistic beach availability. Finally, we are confident these findings will help managers, residents, and tourists to obtain important information for beach management and help improve the quality of tourism in coastal areas, worldwide.

References

Agarwal, S., 2002. Restructuring seaside tourism - The resort lifecyle. *Annals of Tourism Research* 29(1), 25-55.

ASPRS., 2010. *Las Specification v 1.3-R11*. Maryland, Bethesda: American Society of Photogrammetry and Remote Sensing *Press*.

Beatley, T., Brower, D. J., & Schwab, A. K., 2002. *An Introduction to CoastalZzoneManagement* (2nd ed.), Washington, DC: Island Press, 329p.

Bleakly Advisory Group., 2008. *Analysis of Long Term Impacts of Development on Jekyll Island: Preliminary Revitalization & Fiscal Forecasts*. Jekyll Island State Park Authority, http://www.savejekyllisland.org/Visitation_Analysis_Business_Plan_09_15_Board_Presentation.pdf (Accessed 01.27.2011).

Bramwell, B., 2003. *Coastal Mass Tourism : Diversification and Sustainable Development in Southern Europe*. Clevedon; Buffalo: Channel View Publications, 357p.

Brower, D. J., and Dreyfoos, W., 1979. Public-access to ocean beaches - If You Find a Parking Space, How Do You Get to the Beach. *Coastal Zone Management Journal 5*, 61-81.

Cabin Bluff Management. 2007. *Jekyll Island Conservation Plan*.

Canadian Hydrographic Service., 2006. *Canadian Tide and Current Tables, 1:Atlantic Coast and Bay of Fundy*, Fisheries and Oceans Canada, Ottawa, Ontario.

Carmichae, A. G., 1995. Sunbathers Versus Property Owners: Public Access to. North Carolina's Beaches. *North Carolina Law Review 64(1985)*, 159-201.

Chen, L. C., and Rau, J. Y., 1998. Detection of shoreline changes for tideland areas using multi-temporal satellite images. *International Journal of Remote Sensing* 19(17), 3383-3397.

Cracknell, A. P., and Hayes, L., 2007. *Introduction to Remote Sensing* (2nd ed.), Boca Raton, FL: CRC Press, 335p.

Crowell, M., and Leatherman, S. P., 1999. Coastal Erosion Mapping and Management. *Journal of Coastal Research,* Coastal and Environmental Research Foundation, Royal Palm Beach Florida,Special Issue *28*, 196.

Davis, R.A., jr and Fitzgerald, D. M., 2004. *Beaches and Coasts*. Oxford, UK: Blackwell Publishing, 419p.

Dolan, R., and Harry, L., 1987. Beaches and Barrier Islands. *Scientific American* 257, 68-77.

Esnard, A. M., Brower, D., & Bortz, B., 2001. Coastal hazards and the built environment on barrier islands: A retrospective view of Nags Head in the late 1990s. *Coastal Management* 29(1), 53-72.

GDNR., 2010. *Coastal Resources Division: Georgia's Salt Marshes.* http://crd.dnr.state.ga.us/content/displaycontent.asp?txtDocument=22 (Accessed 12.14.10).

Godschalk, D. R., 1987. *The 1982 Coastal Barrier Resources Act: A New Federal Policy Tact*: University of Chicago Press.

Goodhead, T., and Johnson, D., 1996. *CoastalRrecreation Management : The sustainable development of maritime leisure*. London, UK.: E & FN Spon, 332p.

Hall, C. M., 2001. Trends in ocean and coastal tourism: the end of the last frontier? *Ocean & Coastal Management* 44(9-10), 601-618.

Henry, V. J., 2005. Jekyll Island Erosion. *The New Georgia Encyclopedia*, http://www.georgiaencyclopedia.org/nge/Article.jsp?id=h-2777 (Accessed 10.09.2009).

Hickman, G.D. and Hogg, J.E., 1969. Application of an airborne pulsed laser for near-shore bathymetric measurements, *Remote Sensing of Environment* 1(1), 47-58.

Hicks, S. D., 2006. Understanding Tides. *U.S. Department of Commerce National Oceanic and Atmospheric Administration National Ocean Service*, http://tidesandcurrents.noaa.gov/publications/Understanding_Tides_by_Steacy_finalFINAL11_30.pdf (Accessed 10.09.2010).

Houston, J. R., 1995. *The Economic Value of Beaches*, The CERCular, Coastal Engineering Research Center, Waterways Experiment Station, Vol. CERC-95-4, Dec 1995, 1-4.

Houston, J. R., 2002. The Economic Value of Beaches –2002 Update. *Shore & Beach* 70(1), 9-12.

Houston, J. R., 2008. The Economic Value of Beaches - 2008 Update. *Shore and Beach* 76(3), 22-26

Hoyt, J. H., 1967. Barrier Island Formation. *Geological Society of America Bulletin 78*, 1125-1136p.

Jennings, S., 2004. Coastal tourism and shoreline management. *Annals of Tourism Research* 31(4), 899-922.

Kaufman, W., and Pilkey, O. H., 1979. *The Beaches are Moving : the drowning of America's shoreline* (1st ed.), Garden City, N.Y.: Anchor Press, 336p.

Klein, Y. L., Osleeb, J. P., and Viola, M. R., 2004. Tourism-generated earnings in the coastal zone: A regional analysis. *Journal of Coastal Research* 20(4), 1080-1088.

Kline, J. D., and Swallow, S. K., 1998. The demand for local access to coastal recreation in southern New England. *Coastal Management* 26(3), 177-190.

Lenz, R. J., 1999. *Longstreet Highroad Guide to the Georgia Coast and Okefenokee*. Longstreet Press, GA., 255-272.

Martin, J., 1997. Analysis of the wet/dry line as an indicator of shoreline position on a sand beach. *Masters Thesis, North Carolina State University* 71.

Maune, D. F., 2007. *Digital Elevation Model Technologies and Applications : the DEM Users Manual* (2nd ed.), Bethesda, Md.: American Society for Photogrammetry and Remote Sensing, 655p.

Miller, M. L., and Auyong, J., 1991. Coastal zone tourism - a Potent Force Affecting Environment and Society. *Marine Policy* 15(2), 75-99.

Moffitt, F. H., 1969. History of shore growth from aerial photographs. *Shore and Beach* 4, 23-27.

Mongeau, D., 2003. Public beach access: An Annotated Bibliography. *Law Library Journal* 95(4), 515-556.

Moore, L. J., Ruggiero, P., and List, J. H., 2010. Comparing mean high water and high, water line shorelines: Should proxy-datum offsets be incorporated into shoreline change analysis. *Journal of Coastal Research* 22(4), 894-905.

Morton, R. A., Miller, T. L., 2005. National assessment of shoreline change. Part 2, Historical shoreline changes and associated coastal land loss along the U.S. southeast Atlantic Coast. In *USGS open file report 2005-1401*. [Reston, Va.]: U.S. Dept. of the Interior, U.S. Geological Survey.

NOAA., 1972. Coastal Zone Management Act in1972. http://www.nps.gov/history/local-law/FHPL_CstlZoneMngmt.pdf (Downloaded 10.10.2008).

NOAA., 2010a. TIDES&CURRENT. *: Frequently Asked Questions*, http://co-ops.nos.noaa.gov/faq2.html (Accessed 12.14.10).

NOAA., 2010b. TIDES&CURRENT: *TIDAL DATUMS* http://tidesandcurrents.noaa.gov/datum_options.html (Assessed 12.14.10).

Oh, C. O., Dixon, A. W., Mjelde, J. W., and Draper, J., 2008. Valuing visitors' economic benefits of public beach access points. *Ocean & Coastal Management* 51(12), 847-853.

Oh, C. O., Draper, J., and Dixon, A. W., 2009. Assessing Tourists' Multi-Attribute Preferences for Public Beach Access. *Coastal Management* 37(2), 119-135.

Oh, C. O., Draper, J., and Dixon, A. W., 2010. Comparing resident and tourist preferences for public beach access and related amenities. *Ocean & Coastal Management* 53(5-6), 245-251.

Overton, M. F., and Fisher, J. S., 2003. The 1998 Long-term erosion rate update for the North Carolina shoreline. *NC Department of Environment and Natural Resources, Division of Coastal Management, Raleigh, NC*, 17.

Page, S., and Connell, J., 2006. *Tourism: A Modern Synthesis Cengage Learning. (Third edition).* London,UK: Thomson Learning, 546p.

Phillips, M.R., 2008. Consequences of short term changes in coastal processes: a case study. *Earth Surface Processes and Landforms* 33(13), 2094 - 2107.

Phillips, M.R. and Crisp, S., 2010. Sea level trends and NAO influences: the Bristol Channel/Severn Estuary. *Global and Planetary Change* 73(3-4), 211 - 218.

Pogue, P., and Lee, V., 1998. *Effectiveness of State Coastal Management Programs in Providing Public Access to the Shore: A National Overview*. Washington, DC.: University of Rhode Island, Rhode Island Sea Grant, Coastal Resources Center, 55p.

Pogue, P., and Lee, V., 1999. Providing public access to the shore: The role of coastal zone management programs. *Coastal Management 27*, 219-237.

Roca, E., Riera, C., Villares, M., Fragell, R., and Junyent, R., 2008. A combined assessment of beach occupancy and public perceptions of beach quality: A case study in the Costa Brava, Spain. *Ocean & Coastal Management* 51(12), 839-846.

Robertson W., K., Zhang, D. W., and Leatherman, S. P., 2005. Shoreline and Beach Volume Change Before and After the 2004 Hurricane Season, Palm Beach County, Florida. *Shore and Beach* 73, 79-84.

Springuel, N., and Schmitt, C., 2007. Access to the waterfront: Issues and Solutions across the Nation. Portland, ME: Maine Sea Grant, 40p.

Stockdon, H. F., Sallenger, A. H., List, J. H., and Holman, R. A., 2002. Estimation of shoreline position and change using airborne topographic lidar data. *Journal of Coastal Research,* 18(3), 502-513.

Thieler, E. R., 2009. *The Digital Shoreline Analysis System (DSAS) version 4.0, an ArcGIS© extension for calculating historic shoreline change*. In *U S Geological Survey open-file report 2008-1278* (4.0 ed.). Reston, Va.: U.S. Geological Survey.

Thomas, T., Phillips, M.R., Williams, A.T., and Jenkins, R.E., 2011a. A multi-century record of linked nearshore and coastal change. *Earth Surface Processes and Landforms* 36(8), 995-1006.

Thomas, T., Phillips, M.R., Williams, A.T., and Jenkins, R.E., 2011b. Short-term beach rotation, wave climate and the North Atlantic Oscillation (NAO). Progress in *Physical Geography* 35(3), 333-352.

Thompson, R., 2006. Affordable twenty-four hour coastal access: Can we save a working stiff's paradise? . *Ocean and Coastal Law Journal* 12(1), 91-132.

Thompson, R., and Dalton, T., 2010. Measuring Public Access to the Shoreline: The Boat-Based Offset Survey Method. *Coastal Management* 38(4), 378-398.

Treby, E. J., and Clark, M. J., 2004. Refining a practical approach to participatory decision making: An example from coastal zone management. *Coastal Management* 32(4), 353-372.

CHAPTER 4

ASSESSING OPTIMAL IMAGE FUSION METHODS FOR VERY HIGH SPATIAL RESOLUTION SATELLITE IMAGES TO SUPPORT COASTAL MONITORING[3]

[3] Yang, B.Y., Kim, M.H. and Madden, M., Submitted to *ISPRS Journal of Photogrammetry and Remote Sensing.*

Abstract

In this study, we examined best image fusion approaches for generating pansharpened very high resolution (VHR) multispectral images to be utilized for monitoring coastal barrier island development. Selected fusion techniques assessed in this research come from three categories of spectral substitution (e.g., Brovey transform and Multiplicative merging), arithmetic merging (e.g., modified intensity-hue-saturation and principal component analysis), and spatial domain (e.g., high pass filter, and subtractive resolution merge). The image fusion methods selected for this study were capable of producing pansharpened VHR images with more than three bands. Comparisons of fusion techniques were applied to images from three satellite sensors: United States commercial satellites IKONOS and QuickBird, and the Korean KOMPSAT II. Pansharpened VHR multispectral images were assessed by spectral and spatial quality measurements. Results satisfying both spectral and spatial quality revealed optimum pansharpened techniques necessary for regular coastal mapping of barrier islands. These techniques may also be used to assess the quality of recently available VHR imagery acquired by numerous international, government and commercial VHR satellite programs.

Key words: Coastal monitoring, Barrier islands, Image fusion, KOMPSAT II, IKONOS, QuickBird satellite image, Quality assessment, and International satellite programs.

4.1 Introduction

A coastal region is a buffer zone that interfaces between a continent and an ocean, and it includes valuable natural resources such as wetlands, floodplains, estuaries, beaches, dunes, barrier islands, and coral reefs (Turner, 2000; EPA, 2011a). The development of coastal areas could devastate such natural resources that animals and vegetation rely on, and it can cause negative health impacts on people. The widespread concentration of pathogenic bacteria and viruses in surface waters of coastal zones was found to be associated with human development activities in Florida Keys (Paul *et al*., 1997; Griffin et *al*., 1999). In addition, the abundance and spatial distribution of pathogenic microbes, including enteric bacteria, fecal coliform bacteria and *Escherichia coli*, had an association with the growth of human development (Mallin *et al*, 2000). In particular, Mallin *et al*. (2000) discovered that the percentage of developed areas with man-made features, such as rooftops, roads, driveways, sidewalks, and parking lots, to a total land area was associated with fecal coliform abundance in surface water of coastal areas.

Taking nonpoint source pollution into account, the United States Congress issued the Coastal Zone Management Act in 1972 to protect coastal waters (NOAA, 2011). The amendment of this act was made in 1990, called Coastal Zone Act Reauthorization Amendments Section 6217, which requires 29 states and territories to develop coastal nonpoint pollution control programs (EPA, 2011b). Therefore, studying and monitoring of coastal environments can be an important tool for public health officials. Remote sensing has been widely utilized to monitor land use and land cover (LULC) changes to the level of detail of individual buildings, road networks and small freshwater marshes and water bodies. For this reason, it is crucial that coastal managers diligently monitor and map changes in natural physical features, as well as human

influences in coastal zones. Such action requires remote sensing imagery of very high spatial, spectral and temporal resolution.

Automated mapping techniques using remotely-sensed images from numerous international government and commercial satellite programs operational today and planned for the future offer a suitable solution for coastal mapping. Especially useful are images with pixel sizes ranging from approximately 0.5 to <5 m, (i.e., very high resolution (VHR) imagery) with at least four multispectral bands for classifying LULC. There is, however, a trade-off between the following: 1) satellite sensors that acquire VHR images of high spatial resolution (on the order of 0.5-1.0 m pixel), but only a single panchromatic band and; 2) sensors that acquire multispectral images with lower spatial resolution (typically 2 to 4-m) and multiple bands (typically 4) of color information ranging from blue to near infrared portions of the electromagnetic spectrum.

This trade-off has resulted in global image data archives containing imagery of various spatial and spectral resolutions from numerous satellite sensors that have potential for mapping dynamic coastal areas. Image processing techniques for image fusion, also known as pansharpening, provide methods for combining high spatial resolution panchromatic images with lower spatial resolution multispectral images to produce fused images at the finest spatial resolution and containing color information from the multiple spectral bands (Cliché *et al*., 1985; Welch and Ehlers, 1987; Ehlers, 1991). Image fusion techniques that were developed in the mid-1980s were subsequently assessed to evaluate the quality of the resulting fused images (Cliché *et al*., 1985; Welch, 1987; Ehlers, 1991; Ling *et al*., 2007; Ling *et al*., 2008; Kim *et al*., 2011). The resulting pansharpened images were found to enhance the information content provided by remotely-sensed images for interpretation and analysis for many applications including mapping

urban surface features, vegetation and rural land use (Couloigner *et al*., 1998; Dai and Khorram, 1999; Kurz, 2000; Lau, 2000; Tu *et al*., 2001; Chen *et al*., 2003; Sun *et al*., 2003).

Following Pohl and Genderen (1998) and Gangkofner (2008), image pansharpening techniques can be categorized into the following three types: spectral (or component) substitution, arithmetic transform, and spatial-domain merge. Spectral (or component) substitution techniques such as modified intensity-hue-saturation (MIHS) or principal component analysis (PCA) involve converting a multispectral image (e.g., red, green, and blue or RGB) into its color components (e.g., intensity, hue, and saturation or IHS), and replace intensity values with a panchromatic image to create a multispectral fused image of high spatial resolution (Ehlers, 1991; Pohl, 1998; Tu, 2001; Ling, 2007). Arithmetic merging methods create fused images using pixel-level arithmetic operations with panchromatic and multispectral images. Multiplicative (MP) and Brovey transform (BT) are examples of the arithmetic pansharpening technique. Spatial-domain fusion techniques similarly derive spatial information from a panchromatic image, which is injected into a multispectral image in a fusion procedure (Ranchin *et al*., 1997; Aiazzi *et al*., 2002; Klonus and Ehlers, 2007). High pass filter (HPF), subtractive resolution merge (SRM), and wavelet-based transform are classified as spatial-domain methods. In fact, there have also been some hybrid techniques that use combined methods of more than one group (Nunez and Otazu, 1999). Ehlers fusion, for example, uses IHS transformation joined with a Fourier domain filtering to obtain fused images (Klonus and Ehlers, 2007)**.** Another method uses IHS transformation with wavelet-based sharpening in a subsequent step (González-Audícana *et al*., 2004).

Given the many options available now for image fusion, this study aims at discovering the best image fusion approach from the three pansharpening categories (spectral substitution,

arithmetic merging, and spatial-domain methods) to support LULC change monitoring in a dynamic coastal region undergoing rapid development and physical changes due to wind and wave action. These narrow strips of beach, dunes and maritime forest are characterized by small patches of changing size, shape and land use. Frequent monitoring of this unique region requires the fusion of remotely sensed high resolution imagery available from a variety of sensors and using efficient and effective fusion methods. In this study, IKONOS, QuickBird, and the Korea Multi-Purpose Satellite II (KOMPSAT II, also known as Arirang-2) satellite VHR image data were pansharpened using selected fusion methods. Criteria for the image fusion techniques, selected for this study, included representation of the three pansharpening categories, suitability for use with available VHR satellite image data and capability to create fused images with more than three bands to accommodate future directions in multiband VHR imagery.

This research paper is structured as follows. In Section 2, the study area and data construction are described; in Section 3, image fusion methods and statistical analyses used in this research are addressed; and in Section 4 resulting pansharpened images are evaluated by spatial and spectral quality assessments, as well as visual inspections. In Section 5, the significance of results revealed in this research in terms of optimal methods for coastal studies is discussed. Finally, concise summarization is provided and future studies are addressed in Section 6.

4.2 Materials and Methods

4.2.1 Study Area and Satellite Images

Jekyll Island in Glynn County, Georgia, along the southeastern coast of the United States (US) was selected for this study because up-to-date LULC information from VHR satellite

imagery is required by state-level policy for monitoring the percentage of developed to undeveloped land. Figure 4.1 shows the location of the Island with an approximate size of 237 km^2 (58,472 acres) (AECOM, 2011). Jekyll Island includes various LULC types such as coastal marsh, beach, forest, dry hammock, a golf course, parks, roads, bicycle trails and residential/commercial areas. The state-owned island is managed by the Jekyll Island Authority to preserve its natural environment, offer favorable places and activities to attract tourists, and provide services to the tourists and island residents. Indeed, many retired people have recently moved to Jekyll Island due to the quiet atmosphere, natural coastal environment and relatively low population density. Once privately owned by the Jekyll Island Club, a small group of wealthy northern entrepreneurs in the late 19^{th} to mid-20^{th} centuries, the Island was evacuated during World War II and purchased by the State of Georgia in 1947 (Bagwell, 2001; McDonald, 2010). Following state construction of a bridge from the mainland in 1954, the Island was operated for residential leases and promoted for tourism. Today Jekyll Island has an average daily population of over 6,000 including visitors, residents, and a total of employees and 1.5 million annual visitors during 2007 (Bleakly Advisory Group, 2008).

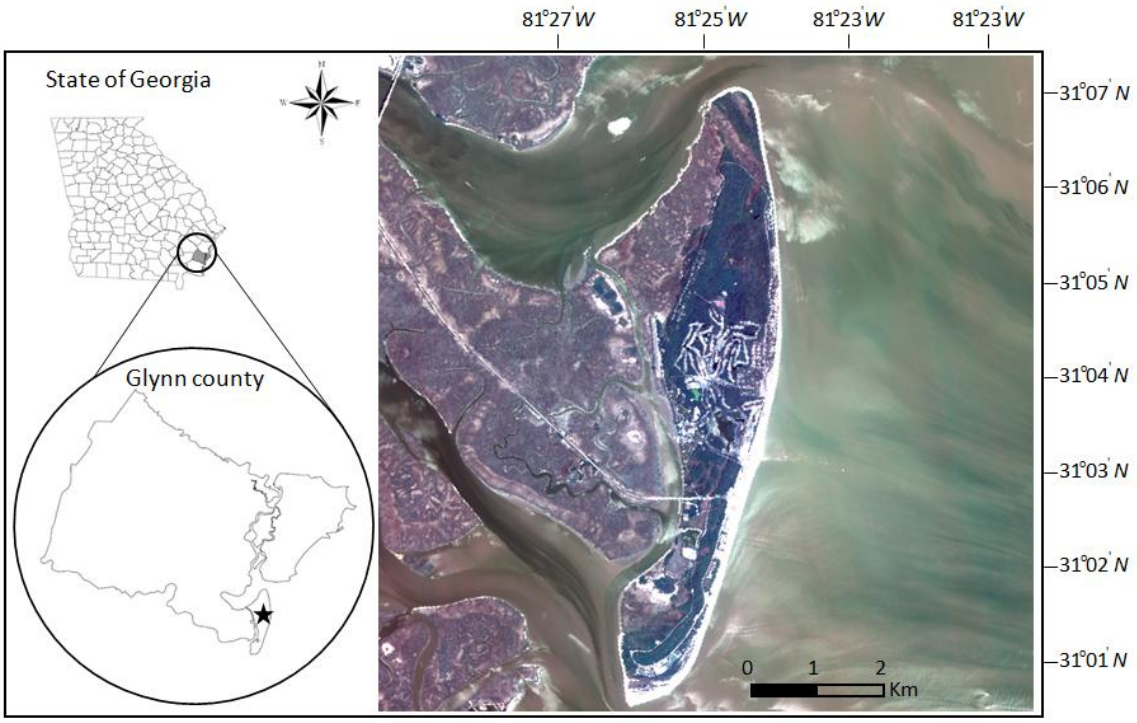

Figure 4.1. Jekyll Island indicator map. Glynn County is represented in grey color within the Georgia map located at upper left of the figure. A black star indicates the location of the Island. The image map of Jekyll Island on the right was produced from a United States Department of Agriculture (USDA) National Agriculture Imaging Program (NAIP) 2007 airborne digital camera image.

In recent years, the Island has faced a management issue of balancing development to increase the number of tourists with conservation of its natural area. Georgia State Act (No. 427) limits any new development if existing developed areas exceed 35% of the total area of the Island (JIA, 2004). The Jekyll Island Authority is preparing a master plan for future development within the conditions of Act 427 and therefore, urgently requires a current LULC map data to evaluate the percentage of developed areas. Current VHR satellite imagery is fundamental to the performance of LULC classification, and image fusion is essential to resolve very small ground

features [e.g., bicycle trails] not visible in typical 4-m VHR multispectral imagery of Jekyll Island.

This study utilized VHR imagery from IKONOS and QuickBird as well as KOMPSAT II satellite sensors. The IKONOS image was acquired on July 17, 2003, by GeoEye Inc. and the QuickBird image on January 3, 2004, by Digital Globe Inc. Both are US companies that provide commercial VHR satellite imagery to the public. The KOMPSAT II sensor was launched on July 28, 2006, by the Korean Aerospace Research Institute (KARI). All the satellite sensors provided VHR panchromatic images and multispectral images within blue, green, red, and near infrared (NIR) bands (Table 4.1). Figure 4.2 shows the multispectral images of each satellite image covering the Jekyll Island area, and Table 1 summarizes their spatial, spectral, and radiometric resolutions.

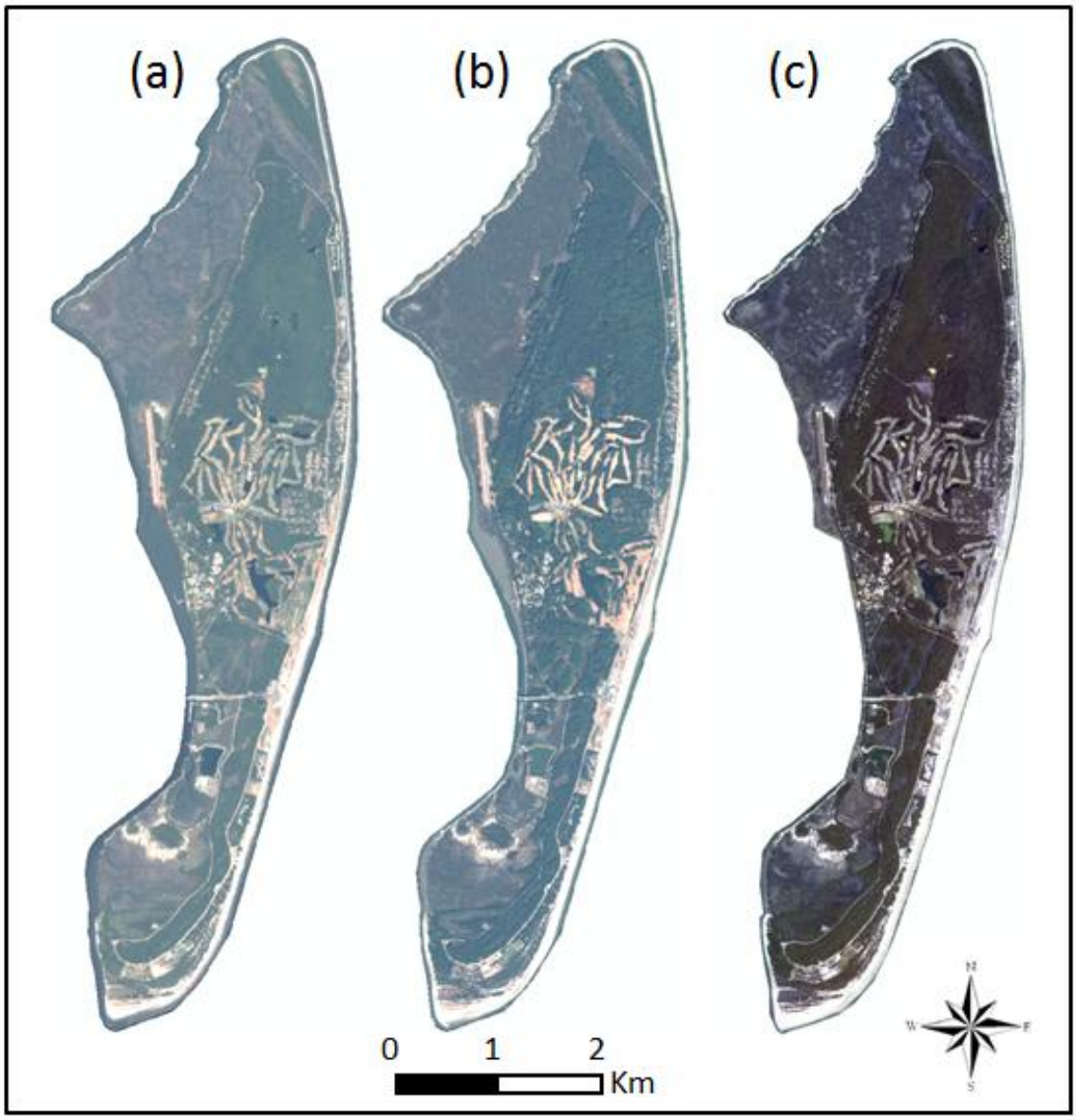

Figure 4.2. Multispectral satellite images shown in a true color composite using red, green and bluebands for RGB: (a) IKONOS, (b) QuickBird, and (c) KOMPSAT II.

Table 4.1. Basic technical characteristics of satellite images employed in this study.

Satellite and acuqisition date	Spectral band	Spectral resolution (μm)	Spatial resolution (meter)
IKONOS (July 17, 2003)	Panchromatic	0.45-0.90	1
	Blue	0.45–0.51	4
	Green	0.51–0.60	4
	Red	0.63–0.70	4
	NIR	0.76–0.85	4
QuickBird (January 3, 2004)	Panchromatic	0.45-0.90	0.61
	Blue	0.45 – 0.52	2.44
	Green	0.52 – 0.60	2.44
	Red	0.63 – 0.69	2.44
	NIR	0.76 – 0.90	2.44
KOMPSAT II (April 17, 2008)	Panchromatic	0.50 – 0.90	1
	Blue	0.45 – 0.52	4
	Green	0.52 – 0.60	4
	Red	0.63 – 0.69	4
	NIR	0.76 – 0.90	4

Note: IKONOS and QuickBird images have a radiometric resolution of 11 bit, and KOMPSAT II records images with that of 10 bit.

As shown in Table 4.1, the specification of KOMPSAT II is similar to IKONOS. First, KOMPSAT II and IKONOS both have spatial resolutions of 1m and 4m for panchromatic and multispectral bands, respectively. In addition, they have a similar range of 4-band spectral resolution (0.45 to 0.90 μm), and they are in sun-synchronous orbit at an altitude of 685 km for KOMPSAT II and 680 km for IKONOS. The two satellites provide across-track stereo images by multiple passes of the satellite using off-nadir pointing capability, and there are only small differences in swath width and radiometric resolution (11-bit IKONOS versus 10-bit KOMPSAT II). The QuickBird satellite sensor, on the other hand, has a spatial resolution of 61 cm for the

panchromatic band and 2.44 m for multispectral bands at nadir, as well as 11-bit radiometric resolution and a sun-synchronous orbit at an altitude of 482 km. In addition, the 4-band spectral range of the QuickBird sensor matches the range of IKONOS and KOMPSAT II (Table 4.1).

4.2.2 Methods

We created subset images of IKONOS, QuickBird and KOMPSAT II that included only the Jekyll Island area because our focus was on the Island. The subset images are very effective in terms of reducing processing time of image fusion techniques and optimizing results of fused images (Kim *et al*., 2011). So, all the subset scenes were rescaled to 8-bit radiometric resolution to maintain similar data format conditions for comparing pansharpening techniques. In this study, two different fusion techniques from each category were used to determine the optional fusion technique for monitoring LULC on Jekyll Island.

In the spectral substitution domain, the MIHS and PCA transform were utilized. Although traditional IHS has been frequently utilized for image fusion, it produces only a three-band pansharpened image (Vrabel, 1996; Zhou *et al*., 1998). The MIHS is an updated version of this technique that overcomes this limitation. In other words, MIHS produces the same number of multispectral bands in a pansharpened image as an original VHR input multispectral scene (ERDAS, 2010). The PCA method transforms a multivariate data set of inter-correlated variables into a new data set of un-correlated linear combinations of the original variables (Pohl and Van Genderen, 1998).

The BT and MP image fusion techniques were employed from the arithmetic merging domain. These methods normalize each of the multispectral bands in layered stacks by multiplying the pixel values by the intensity of the higher resolution panchromatic band (Pohl

and Van Genderen, 1998). The BT uses a ratio algorithm to combine the original panchromatic image with multispectral bands and was developed to visually increase the contrast of RGB images with a higher a degree of contrast in the low and high ends of the image histogram. The MP that uses a subtractive algorithm to fuse images and increase the intensity component is favored for highlighting urban features (ERDAS, 2010).

Lastly, the HPF and SRM merge techniques were chosen to represent the spatial-domain merging approach using high frequency inserting procedures known to deliver fusion results that are spectrally distorted to some degree (Aiazzi *et al*., 2002; Ehlers, 2005). The HPF technique implements the size of the high pass kernel which is used to filter the high resolution panchromatic image, then the multispectral image is resampled to the pixel size of the high resolution panchromatic image, and finally a fused image is created by linear stretch which is to have same data type as the panchromatic image. In other words, the HPF technique combines the panchromatic image with the multispectral image, resulting in a fused image (Aiazzi *et al*., 2002). The concept of SRM is similar to HPF, but it derives the high frequency component using a different method. The SRM is useful for satellite images with a ratio of multispectral to panchromatic image pixel sizes of approximately 4:1 (Lane, 2009).

The ultimate goal for creating resultant fused imagery is an increase in spatial resolution while avoiding color distortion as much as possible. Qualitative and quantitative approaches can be used to assess the spectral similarity of a pansharpened image with the original input multispectral bands. Although visual assessment is a qualitative approach that is commonly used to evaluate overall color similarity between fused and original multispectral images, this can be controversial because of human subjectivity (Li *et al*., 2000). On the contrary, quantitative

approaches calculate numeric indices that overcome the subjectivity of visual comparison (Zang, 2008).

This study evaluated the spectral quality of fused images using both qualitative and quantitative approaches. In addition to visual comparisons, we employed correlation coefficients (CC), relative difference to mean (RDM) and relative difference standard deviation (RDS) quantitative comparisons. The CC assesses band-by-band color similarity of fused imagery with a reference to the original multispectral image, and it has been widely utilized for assessing VHR satellite imagery (Wald *et al*., 1997; Karathanassi *et al*., 2007; Ling *et al*., 2008; Zhang, 2008; Yakhdani and Azizi, 2010; Kim *et al*., 2011). When the CC of two images is closer to +1, it indicates they are highly correlated, while the values approaching -1 indicate the two images are opposite of each other. RDM and RDS are spectral quality indices used to evaluate the differences between histograms of the frequency of spectral reflectance digital numbers (DNs) for pansharpened and individual bands of the multispectral images (Karathanassi *et al*., 2007; Kim *et al*., 2011). When the RDS or RDM values of two images is closer to 0 %, the difference between the fused original and multispectral images is not considered to be generally significant (Karathanassi *et al*., 2007).

Besides color information, fused imagery should also preserve the spatial detail of the original panchromatic image as much as possible. In order to quantify the spatial quality of pansharpened imagery, we applied a Sobel edge operator with a 3×3 moving window to both original panchromatic images and each band of fused imagery, as suggested by Gangkofner *et al*. (2008). Then, we computed root-mean-square-error (RMSE) of edge locations to examine the degree of spatial similarity between the two edge images (Pradhan *et al*., 2006; Gangkofner *et al*., 2008). In other words, RMSE can be used to quantify the average amount of spatial

distortion in each pixel. Figure 4.3 depicts a work flow for the entire procedure adopted in this study.

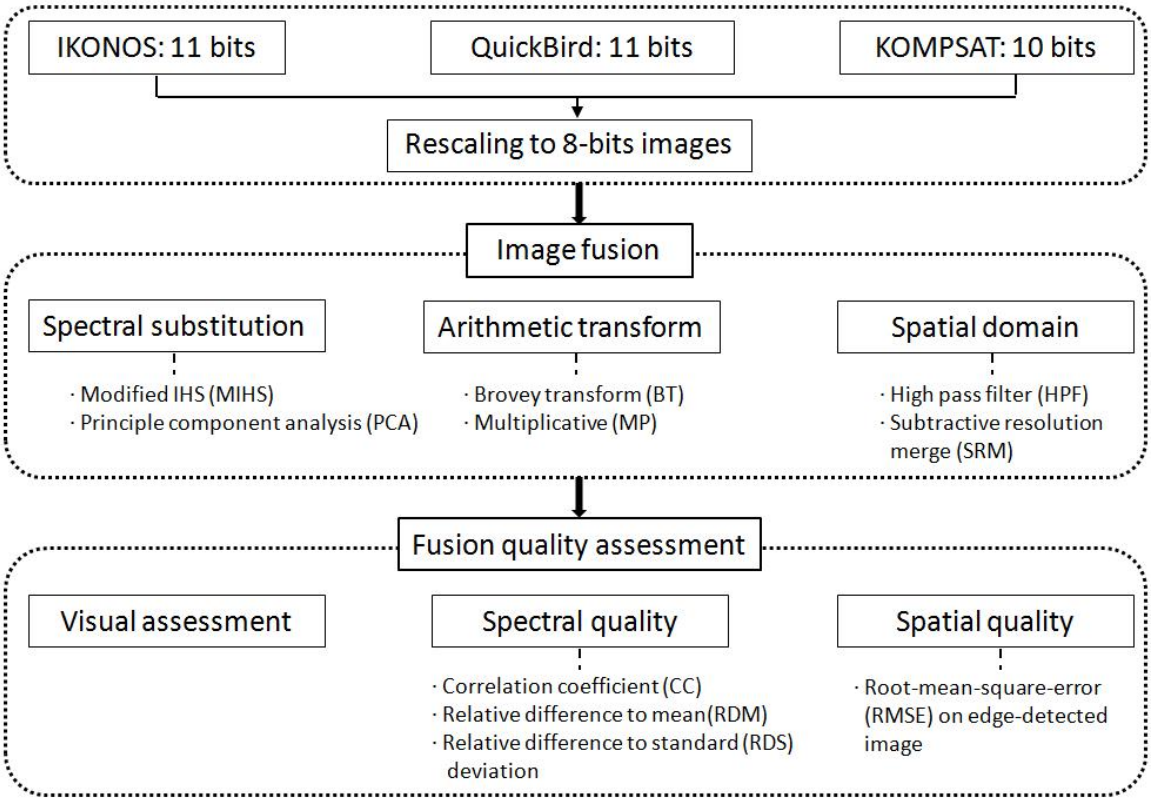

Figure 4.3. Flow chart of entire procedures for this study.

4.3 Results

4.3.1 Visual Assessment

Figure 4.4 displays a subset of the original panchromatic and multispectral images (a), as well as the resulting pansharpened images (b, c, and d) from the 6 tested fusion techniques. When visually compared to the original multispectral images, all of the pansharpened images were generally sharper and clearer. The results of specific pansharpening techniques produced images that differ visually in different degrees of deviations in color from the original true color images. For example, the subset in Figure 4.4 shows a section in the middle of Jekyll Island that

contains a golf course fairway, fields of mowed grass, small forest stands, individual trees, a parking lot, paved and unpaved roads, bike path, ponds, and buildings. Interestingly, white lines in a parking lot, the golf course fairway and cars in the parking lot are clearly visible on the fused images and the original panchromatic images, but not on the original multispectral images.

Although pansharpened images generally showed improvement to the human eye, it is difficult to say which technique produced the best fused images in terms of fidelity to the spectral information in the original multispectral images. As noted in Section 3, even though visual comparison is often the best way to assess fused results of panchromatic and multispectral image data, it remains subjective because of varying human perspectives (Wald, 2000). Thus, it was difficult to evaluate color distortion in the fused images. In the following sub-sections, the results of statistical approaches are presented to quantitatively evaluate the spectral and spatial quality of the fused images with the aim of providing more objective assessments of individual techniques.

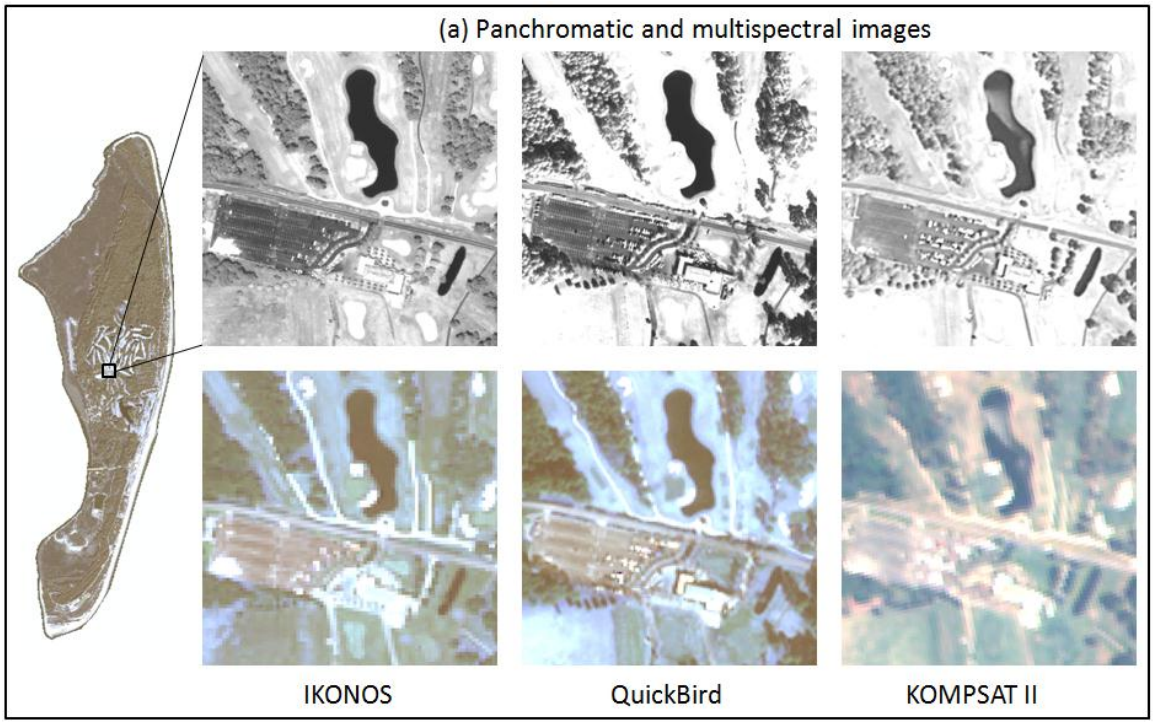

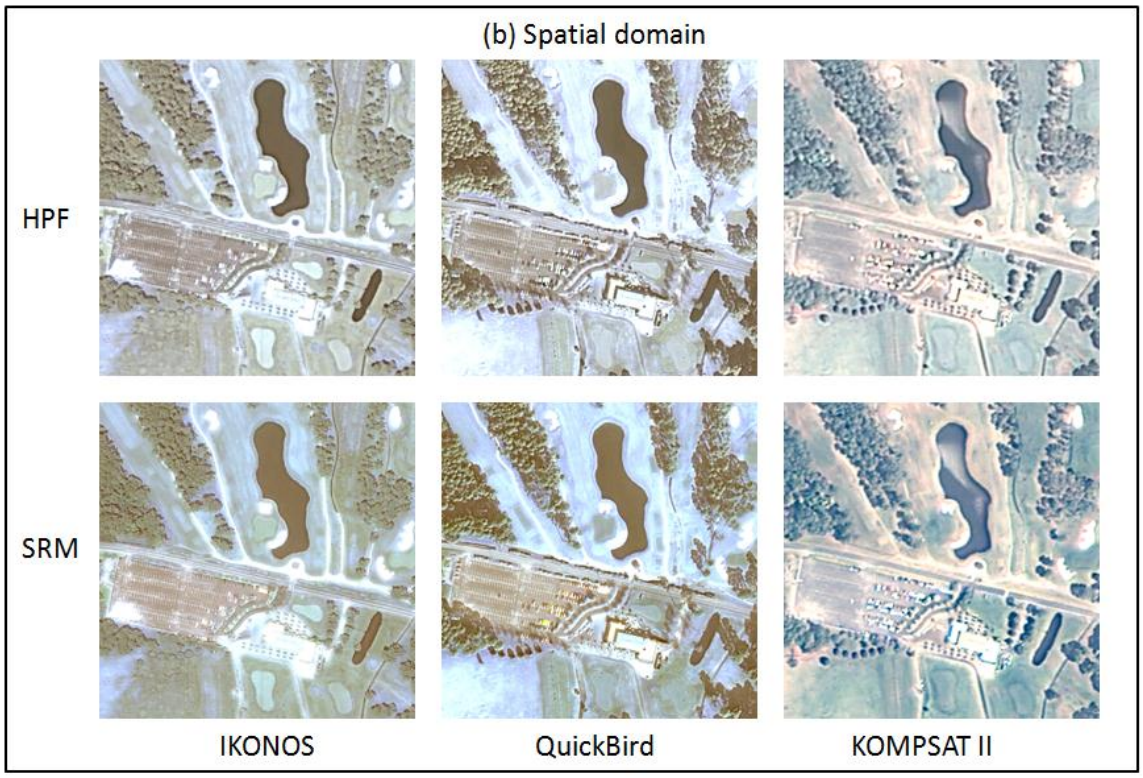
(b) Spatial domain
HPF
SRM
IKONOS
QuickBird
KOMPSAT II

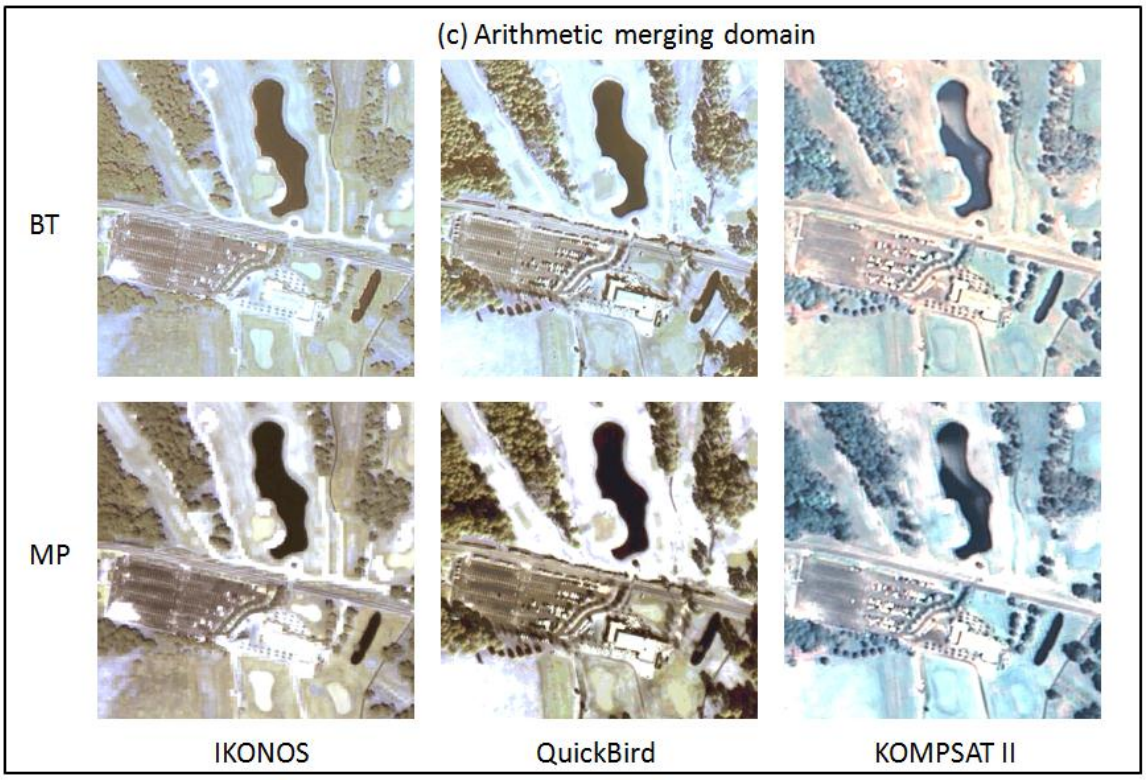
(c) Arithmetic merging domain
BT
MP
IKONOS
QuickBird
KOMPSAT II

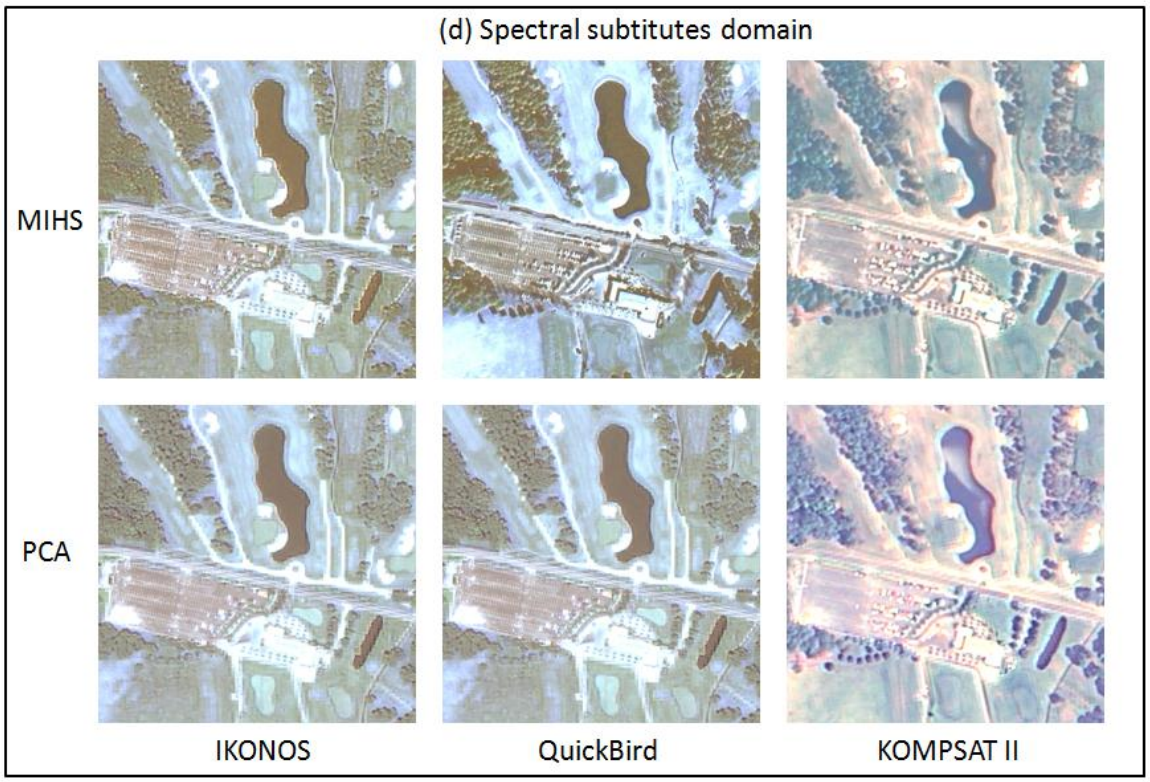

Figure 4.4. Fusion results for visual comparison (true color composite at a scale of 1:1,500).

4.3.2 Spectral Quality Assessment

Band-by-band CC values between original multispectral and pansharpened images for Jekyll Island area are presented in Table 4.2. Based on CC values, the results of all 6 fusion techniques were found to be very similar to the input multispectral images in terms of spectral information. Nonetheless, MIHS produced the highest CC values, (0.97 to 0.99) for pansharpened images across all four spectral bands for all three satellite images. The PCA fusion technique produced equivalent CC values to MIHS for IKONOS, and HPF produced CC values equal to MIHS for KOMPSAT II in all four bands. MP generated the poorest fusion results in terms of CC values, generally below 0.90.

Table 4.2. Correlation coefficients utilized to evaluate spectral quality of each pansharpened image.

Satellite image	Spectral bands	Fusion techniques					
		MIHS	PCA	BT	MP	HPF	SRM
IKONOS	Blue	0.99	0.99	0.98	0.87	0.98	0.99
	Green	0.99	0.99	0.98	0.88	0.98	0.99
	Red	0.99	0.99	0.98	0.90	0.97	0.97
	NIR	0.99	0.99	0.99	0.95	0.98	0.98
QuickBird	Blue	0.98	0.96	0.96	0.82	0.97	0.99
	Green	0.98	0.97	0.97	0.85	0.97	0.97
	Red	0.98	0.97	0.97	0.88	0.97	0.95
	NIR	0.97	0.97	0.97	0.89	0.97	0.95
KOMPSAT II	Blue	0.97	0.97	0.97	0.90	0.97	0.95
	Green	0.98	0.98	0.97	0.90	0.98	0.98
	Red	0.98	0.98	0.97	0.90	0.98	0.99
	NIR	0.98	0.95	0.97	0.94	0.98	0.96

Figure 4.5 depicts the histograms of the percentage of difference in digital number (DN) frequency between input multispectral and fused scenes in all four bands. Taking RDM values into account (Figure 4.5a, 5c, and 5e), pansharpened images with MIHS, HPF, and SRM generated the lowest mean values of relative differences. On the contrary, the fused results of MP produced the largest RDM values for all four bands in all three VHR satellite images, followed by BT and PCA. We obtained a range of RDM values with approximately 85% for all MP fusion results, 60% for BT and 10-to-40% for PCA. The PCA and BT techniques resulted in greater variations of RDM values across the three types of VHR satellite imagery. When applying the fusion techniques to QuickBird and KOMPSAT II, PCA and BT pansharpened results had a range of mean deviations with 24.0% to 67.0%. Regarding the IKONOS scene, PCA generated

smaller RDMs (Figure 4.5a) compared to the other two satellite images, as shown in Figure 4.5c and e, and BT also produced smaller RDMs for blue, green, and red bands of IKONOS imagery (<20%). However, the RDM values of NIR band for the IKONOS satellite imagery was 44.0% (see Fig. 5a) and was approximately 60% for all four bands of QuickBird and KOMPSAT II.

The patterns of RDS were similar to those of RDM across all VHR satellite images and fusion techniques, as shown in Figures 4.5b, d, and f. MIHS, HPF, and SRM resulted in RDS values less than 4.0% for all satellite scenes. When using PCA and BT methods, a range of 31.0% to 65.6% in RDS was observed for QuickBird and KOMPSAT II scenes. With the IKONOS imagery, PCA resulted in RDS values less than 8.0% for all spectral bands, and BT yielded RDS values less than 14.0% for blue, green, and red bands, and again a larger deviation in RDS (~40%) for the NIR band of the IKONOS scene. In addition, MP produced the largest RDS values across all bands in all satellite images, which ranged from 66.0% to 79.1%.

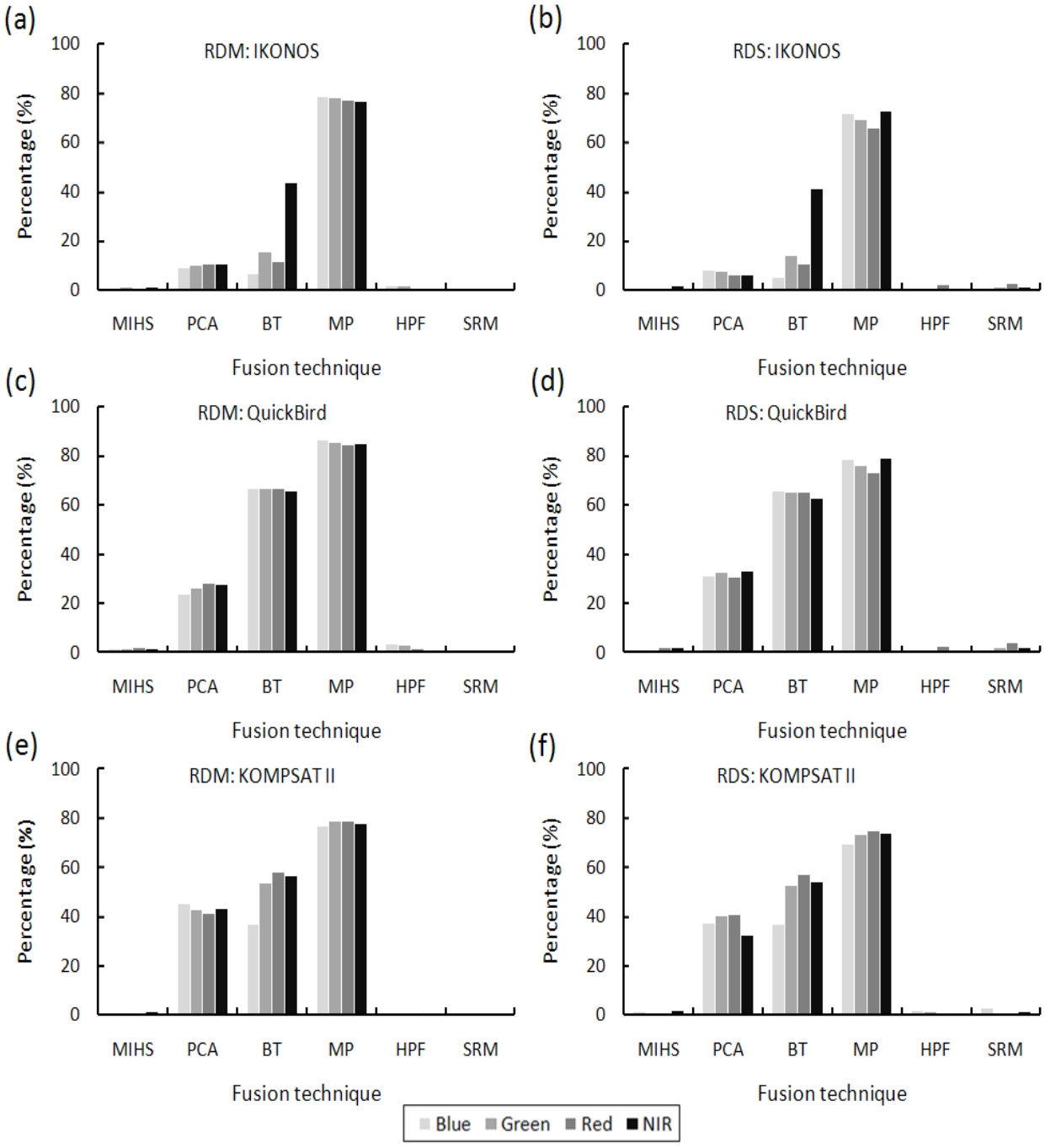

Figure 4.5. Summary of histogram changes between original multispectral and pansharpened images: (a) RDM of IKONOS, (b) RDS of IKONOS, (c) RDM of QuickBird, (d) RDS of QuickBird, (e) RDM of KOMPSAT II, and (f) RDS of KOMPSAT II.

4.3.3 Spatial Quality Assessment

The spatial information in a pansharpened image should be consistent with the spatial information of the original panchromatic scene, color information of an input multispectral image. In order to evaluate the spatial quality of the fused images, we computed RMSE values between the original panchromatic and the pansharpened scenes that were both filtered by a non-directional Sobel edge operator with a 3×3 moving window size, as used by Gangkofner *et al*. (2008). Since PCA, BT, and MP generated larger variations in relative mean and standard deviation of spectral histograms between input multispectral and fused images, we focused on MIHS, HPF, and SRM in assessing the spatial quality of pansharpened scenes in order to find best results satisfying both spectral and spatial quality assessment criteria.

Figure 4.6 shows RMSE values of the original panchromatic images with fused scenes after conducting Sobel edge detections. RMSE values by the Sobel filter reflect textural differences between original panchromatic images and fused scenes. In general, all three fusion techniques resulted in low RMSE values (less than 4) for IKONOS and QuickBird satellite images. The exception was the RMSE values of the NIR band for IKONOS that were larger than the other spectral bands, ranging from 4.5 to 8.6. We obtained larger RMSE values for KOMPSAT II imagery, compared to the other satellite scenes (largely above 4.0). The MIHS of KOMPSAT II showed the most consistency among the bands, which indicates better spatial fidelity than the other fusion techniques. The RMSE values of the NIR band for the KOMPSAT II scene were comparable in magnitude to IKONOS, ranging from 4.7 to 10.4. Overall the RMSE values for MIHS, HPF, and SRM were lowest (<4.0) for the QuickBird imagery.

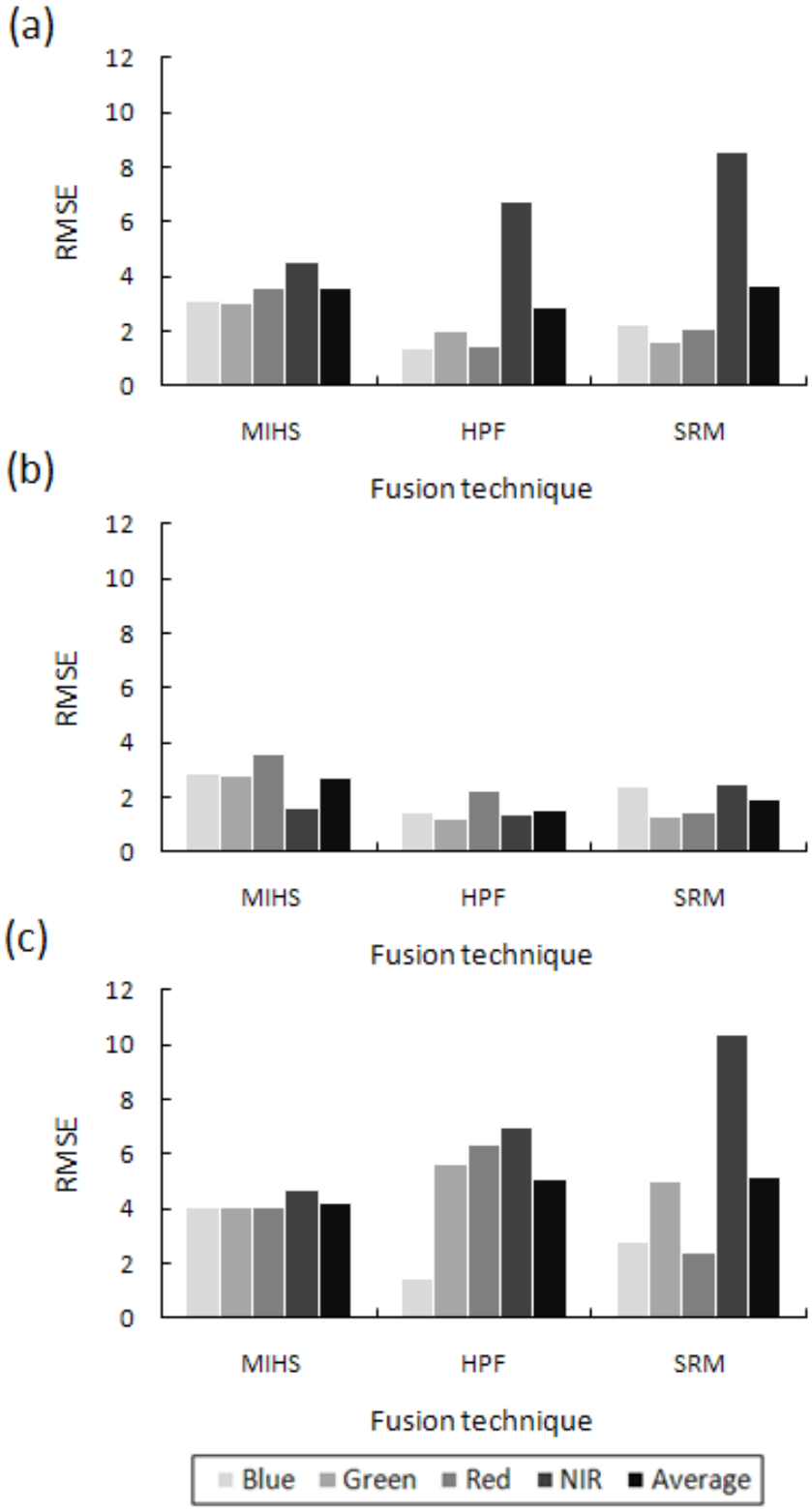

Figure 4.6. Results of RMSE computed with Sobel filtering: (a) IKONOS, (b) QuickBird, and (c) KOMPSAT II.

4.4 Discussion

Image fusion is a remote sensing technique that improves image interpretation by creating higher spatial resolution color imagery with VHR satellite panchromatic and multispectral images (Pradhan *et al*., 2006). The fused results, however, are known to have some degree of color distortion (Pohl and Genderen, 1998). For this reason, most studies have made efforts to develop new methods that potentially overcome the color distortion problem associated with conventional fusion methods. Although previous research has used various quantitative methods to evaluate the quality of fused images, a formalized approach to measure image quality is needed (Zhang, 2008). It is important to determine the best pansharpening techniques for classifying LULC using images of different numbers of spectral bands, and spatial resolutions. This is extremely valuable for improving such applications of satellite images as rural LULC classification, estimation of vegetation parameters, change analysis of LULC, and urban road mapping (Couloigner *et al*., 1998; Dai and Khorram, 1999; Kurz, 2000; Lau, 2000; Tu *et al*., 2001; Chen *et al*., 2003; Sun *et al*., 2003).

As noted earlier, coastal mapping for management of barrier islands should be updated regularly because barrier islands are easily and constantly being reformed by waves, wind, and tidal forces over time. This is especially true for Georgia's barrier islands because of the erosion process generated by tides ranges from 2 m (6 ft) to more than 3 m (10 ft) during the highest spring tides (GDNR, 2010). Additionally, unexpected events such as flooding by storm surges or direct hits by hurricanes can easily change the shape and total size of barrier islands worldwide. For these reasons, regular updates of coastal maps are made possible through the use of VHR remotely sensed imagery, which is increasingly available via numerous international satellite programs. For example, in this study current VHR imagery acquired by the Korean KOMPSAT

II satellite sensor in 2008 (Figure 4.7c) clearly depicts the current dry condition of two ponds on Jekyll Island that were open water in 2003 and 2004 (Figure 4.7a and Figure 4.7b, respectively) as depicted in IKONOS and QuickBird images.

(a) IKONOS (July 17, 2003); HPF (b) QuickBird (January 3, 2004); HPF (c) KOMPSAT II (April 17, 2008); MIHS

Figure 4.7. Results for the best fused images in each satellite image program (true color composite at a scale of 1:1,500) showing two pond areas in 2003 and 2004 (a and b) that are no longer filled with water in 2008 (c).

Although VHR imagery from different international satellite programs are readily available to resource managers, users must evaluate the quality of the data and derived products before basing management decisions and policy on analyses of these data. In this study, all fused multispectral images showed better spatial resolutions compared to the original multispectral images. Features that were especially detected in detail were very small objects such as centerlines in a parking lot, golf course fairways and individual cars.

Taking spectral quality assessment into account, satellite images from three different VHR sensors produced significantly high correction coefficients that demonstrated strong similarity between original multispectral bands and the fused images. Notably, MIHS had better results in all bands and all three image types (0.98 to 0.99) than the other pansharpening techniques. Comparisons of the differences in DN histograms using RDM and RDS, showed images pansharpened with MIHS, HPF, and SRM generated the lowest mean difference values

between original and fused images. In other words, the three pansharpening techniques do not greatly change the shape of the DN histogram of each band.

Regarding spatial quality assessment, we selected the methods with the best results (MIHS, HPF, and SRM) from the spectral quality assessment to quantify optimal fusion methods in terms of spatial quality for coastal mapping of barrier islands. As a result, QuickBird images showed improved results across all fusion methods with RMSE values of sobel filtered edges less than ± 4, while HPF, SRM, and MIHS had a range from ± 1.6 to ± 2.7. IKONOS and KOMPSAT II showed RMSE values are less than +6 in all fusion methods, ranging from ± 2.9 to ± 5.1. The MIHS fusion method with KOMPSAT II produced low RMSE values (average ± 4.2), which means the spatial quality of the MIHS merged image compared to that of the high-resolution panchromatic image was better than the other pansharpening techniques. The HPF fusion methods with QuickBird and IKONOS produced the lowest RMSE values, which are average ± 1.6 and ± 2.9, respectively.

Remotely-sensed imagery has been widely used to perform thematic LULC classification and extract specific ground features. Besides thematic classification and feature extraction, disease-vector habitats were identified and mapped in the past, particularly with coarse- and medium-resolution satellite images such as Advanced Very High Resolution Radiometer, Landsat Thematic Mapper, and Système Probatoire d'Observation de la Terre (Beck *et al*., 2000). In recent years, VHR satellite images, including QuickBird and GeoEye, were used to support surveillance of plague and West Nile Virus (Addink *et al*., 2010; Kim *et al*., 2011). Image fusion with VHR panchromatic and multispectral scenes facilitated the extraction of private outdoor swimming pools (Kim *et al*., 2011) and would be useful for detecting small natural and anthropogenic features, not appearing in VHR multispectral imagery. In summary, HPF in the

spatial domain was found to satisfy spectral and spatial quality assessments of pansharpened QuickBird and IKONOS satellite images. KOMPSAT II had the best results from the MIHS fusion method in the spectral substitution domain. Overall, MIHS in spectral and spatial quality assessments was found to be the best fusion technique for pansharpening images from all three satellite programs.

4.5 Conclusion

This research compared fusion techniques from different categories of image fusion methods commonly known as three domains (spectral substitution, arithmetic transform merge, and spatial-domain merge) proposed by Pohl and Van Genderen (1998). These comparisons were necessary to find the best method to produce optimal fused images which enable interpreters to make fine-scale LULC classifications of coastal barrier islands. This study focused on Jekyll Island, GA, because multispectral VHR images are needed to accurately identify small LULC features to detect developed and undeveloped areas related to state laws limiting future development.

In addition, with the growing demand for VHR satellite images around the World, practical use and interest in image data from international satellite sensors is increasing. In this research, a KOMPSAT II satellite image which is a part of the Korean National Space Program, showed comparable image fusion results to IKONOS and QuickBird satellites. These results may assist international users to evaluate image quality of increasingly available international satellite programs. Additionally, international satellite images may be competitively priced or even available free via the internet. Thus, many international satellite programs will be useful in terms of practical applications.

Future work for LULC classification of Jekyll Island will be conducted by the optimal image fusion operators revealed in this research. Pixel- and object-based image analysis of LULC for the Island will be considered under the same rule set of LULC classification. We expect increased benefits arising from the dual use of IKONOS and KOMPSAT II satellite imagery and future applications in the fields of geology, mapping, atmosphere, ocean, environment, disaster, epidemiology, coastal zones, land management, crop and vegetation monitoring by other VHR satellite images with multiple bands (over 4 bands) and future satellite sensors (e.g., KOMPSAT 3 and 5 of South Korea). We hope mutual benefits will be gained by access to fused image products from a growing pool of archived VHR imagery of the earth.

Acknowledgements

The authors thank the GeoEye Foundation and the Korean Aerospace Research Institute (KARI) for allowing the use of IKONOS and KOMPSAT II satellite images, respectively for this research. QuickBird satellite imagery from Digital Globe, Inc. was provided by the Center for Remote Sensing and Mapping Science (CRMS), Department of Geography, The University of Georgia. We acknowledge that the findings and conclusions in this report are those of the authors and do not necessarily represent the official position of US Centers for Disease Control and Prevention.

References

Addink, E.A., De Jong, S.M., Davis, S.A., Dubyanskiy, V., Burdelov, L.A., and Leirs, H., 2010. The use of high-resolution remote sensing for plague surveillance in Kazakhstan, *Remote Sensing of Environment* 114(3), 674-681.

AECOM, 2011. *Jekyll Island conservation plan* (Draft report 7 March, 2011). http://www.jekyllisland.com/files/conservation-plan-draft-march-2011.pdf (Accessed 05.18. 2011).

Aiazzi, B., Alparone, L., Baronti, S., Garzelli, A., 2002. Context-driven fusion of high spatial and spectral resolution images based on oversampled multiresolution analysis. *IEEE Transactions on Geoscience and Remote Sensing* 40(10), 2300-2312.

Bagwell, T. E., 2001. *Images of America: Jekyll Island State Park A State Park*, Charleston, SC: Arcadia Publishing, 272p.

Beck, L.R., Lobitz, B.M., and Wood, B.L., 2000. Remote sensing and human health: new sensors and new opportunities, *Emerging Infectious Disease* 6(3), 217-227.

Bleakly Advisory Group, 2008. *Analysis of Long Term Impacts of Development on Jekyll Island: Preliminary Revitalization & Fiscal Forecasts*. Jekyll Island State Park Authority, http://www.savejekyllisland.org/Visitation_Analysis_Business_Plan_09_15_Board_Presentation.pdf (Accessed 01.27. 2011).

Chen, C.M., Hepner, G.F., and Forster, R.R., 2003. Fusion of hyperspectral and radar data using the IHS transformation to enhance urban surface features. *ISPRS Journal of Photogrammetry and Remote Sensing* 58(1/2), 19-30.

Cliché, G., Bonn, F., and Teillet, P., 1985. Integration of the SPOT Pan channel into its multispectral mode for image sharpness enhancement. *Photogrammetric Engineering and Remote Sensing* 51(3), 311–316.

Couloigner, I., Ranchin, T., Valtonen, V.P., Wald, L., 1998. Benefit of the future SPOT-5 and of data fusion to urban roads mapping. *International Journal of Remote Sensing* 19(8), 1519-1532.

Dai, X., Khorram, S., 1999. Data fusion using artificial neural networks: a case study on multitemporal change analysis. *Computers Environment and Urban Systems* 23(1), 19-32.

Ehlers, M., 1991. Multisensor image fusion techniques in remote sensing. *ISPRS Journal of Photogrammetry and Remote Sensing* 46(1), 19–30.

Ehlers, M., 2005. Beyond pansharpening: Advances in data fusion for very high resolution remote sensing data, http://www.ipi.uni-hannover.de/fileadmin/institut/pdf/127-ehlers.pdf (Accessed 11.01.2010).

Environmental Protection Agency (EPA), 2011a. Agriculture: coastal zone management act, United States, http://www.epa.gov/agriculture/lzma.html#Summary%20of%20Coastal%20Zone%20Management%20Act%20and%20Amendments (Accessed 08.30.2011).

EPA, 2011b. Coastal zone act reauthorization amendments section 6217, United States, URL: http://water.epa.gov/polwaste/nps/czmact.cfm (Accessed 08.30.2011).

ERDAS, 2010. *ERDAS Imagine electronic Help document*. Atlanta, Georgia: The Earth to Business Company.

Gangkofner, U.G., Pradhan, P.S., and Holcomb, D.W., 2008. Optimizing the high-pass filter addition technique for image fusion. *Photogrammetric Engineering and Remote Sensing* 74(9), 1107-1118.

Gonzalez-Audicana, M., Saleta, J.L., Catalan, R.G., and Garcia, R., 2004. Fusion of multispectral and panchromatic images using improved IHS and PCA mergers based on wavelet decomposition. *IEEE Transaction on Geoscience and Remote Sensing* 42(6), 1291-1299.

Griffin, D.W., Gibson, C.J., Lipp, E.K., Riley, K., Paul, J.H., and Rose, J.B., 1999. Detection of viral pathogens by reserve transcriptase PCR and of microbial indicators by standard methods in the canals of the Florida Keys, *Applied and Environmental Microbiology* 65(9), 4118-4125.

JIA, 2004. *Jekyll Island State Park Island-wide Master Plan Update*. http://www.jekyllislandauthority.org/ (Accessed 05.18.2011).

Klonus, S., Ehlers, M., 2007. Image fusion using the Ehlers spectral characteristics preservation algorithm. *GIScience and Remote Sensing* 44(2), 93-116.

Karathanassi, V., Kolokousis, P., Ioannidou, S., 2007. A comparison study on fusion methods using evaluation indicators. *Internaional Journal of Remote Sensing* 28(10), 2309-2341.

Kim, M., Holt, J.B., Eisen, R.J., Padgett, K., Reisen, W.K., and Croft, J.B. Detection of swimming pools by geographic object-based image analysis to support West Nile Virus control efforts, *Photogrammetric Engineering and Remote Sensing* 77(11), 1169-1179.

Kim, M., Holt, J.B., and Madden, M., 2011. Comparison of Global-and Local-scale Pansharpening for Rapid Assessment of Humanitarian Emergencies. *Photogrammetric Engineering and Remote Sensing* 77(1), 51-63.

Kurz, F., 2000. Empirical Estimation of Vegetation Parameters Using Multisensor Data Fusion. *International Archives of Photogrammetry and Remote Sensing* 33, 733-737.

Lane, M.A., 2009, Multi-class Automated and semiautomated feature extraction Using ERDAS IMAGINE Objective. http://earth.eo.esa.int/rtd/Events/2009_ESA-EUSC-JRC/Papers/Pap_Lane.pdf, European Space Agency, Paris (Accessed 11.11.2010).

Lau, W., 2000. The Influences of image classification by fusion of spatially oriented images. *International Archives of Photogrammetry and Remote Sensing* 33, 752-759.

Ling, Y.R., Ehlers, M., Usery, E.L., and Madden, M., 2007. FFT-enhanced IHS transform method for fusing high-resolution satellite images. *ISPRS Journal of Photogrammetry and Remote Sensing* 61(6), 381-392.

Ling, Y.R., Ehlers, M., Usery, E.L., and Madden, M., 2008. Effects of spatial resolution ratio in image fusion. *International Journal of Remote Sensing* 29(7), 2157-2167.

Li, Y.Y., Venkatesh, Y.V., and Ko, C.C., 2000. Multisensor image fusion using influence factor modification and the ANOVA methods. *IEEE Transactions on Geoscience and Remote Sensing* 38(4), 1976-1988.

McDonald, B., 2010. *Remember Jekyll Island State Park*. Minneapolis, MN: Langdon Street Press, 290p.

Mallin, M.A., Williams, K.E., Esham, E.C., and Lowe, R.P., 2000. Effect of human development on bacteriological water quality in coastal watersheds, *Ecological Applications* 10 (4), 1047-1056.

National Oceanic and Atmospheric Administration (NOAA), 2011. Congressional action to help manage our nation's coasts, United States, http://coastalmanagement.noaa.gov/czm/czm_act.html (Accessed 08.30.2011).

Nunez, J., Otazu, X., Fors, O., Prades, A., Pala, V., and Arbiol, R., 1999. Multiresolution-based image fusion with additive wavelet decomposition, *IEEE Transactions on Geoscience and Remote Sensing* 37(3), 1204–1211.

Paul, J.H.,Rose, J.B., Jiang, S., Zhoug, X., Cochran, P., Kellogg, C., Kang J.B., Griffin, D., Frarah, S., and Lukasik, J., 1997. Evidence for groundwater and surface marine water contamination by waste disposal wells in Florida Keys, *Water Research* 31(6), 1448-1454.

Pohl, C., and Van Genderen, J.L., 1998. Multisensor image fusion in remote sensing: concepts, methods and applications. *International Journal of Remote Sensing* 19(5), 823-854.

Ranchin, T., Mangolini, M., Wald, L., 1997. Fusion of satellite images of different spatial resolutions: assessing the quality of resulting images. *Photogrammetric Engineering and Remote Sensing* 63(6), 691-699.

Pradhan, P., King, R., Younan, N.H., and Holcomb, D.W. 2006. The effect of decomposition levels in wavelet-based fusion for multiresolution and multi-sensor images, *IEEE Transactions on Geoscience and Remote Sensing* 44(12), 3674–3686.

Sun, W.X., Heidt, V., Gong, P., and Xu, G., 2003. Information fusion for rural land-use classification with high-resolution satellite imagery. *IEEE Transactions on Geoscience and Remote Sensing* 41(4), 883-890.

Tu, T.M., Su, S.C., Shyu, H.C., and Huang, P.S., 2001. A new look at IHS-like image fusion methods. *Information Fusion* 2(3), 177-186.

Turner, R.K., 2000. Integrating natural and socio-economic science in coastal management, *Journal of Marine Ssytems* 25(3-4), 447-460.

Vrabel, J., 1996. Multispectral imagery band sharpening study. *Photogrammetric Engineering and Remote Sensing* 62(9), 1075-1083.

Wald, L., Ranchin, T., and Mangolini, M., 1997. Fusion of satellite images of different spatial resolutions: Assessing the quality of resulting images. *Photogrammetric Engineering and Remote Sensing* 63(6), 691-699.

Wald, L., 2000. A conceptual approach to the fusion of Earth observation data. *Surveys in Geophysics* 21(2), 177-186.

Welch, R., and Ehlers, M., 1987. Merging Multiresolution Spot HRV and Landsat TM Data. *Photogrammetric Engineering and Remote Sensing* 53(3), 301-303.

Yakhdani, M.F., and Azizi, A., 2010. Quality assessment of image fusion techniques for multisensor high resolution satellite images (Case study: IRS-P5 and IRS-P6 Satellite Images). In: Wagner W., Székely, B. (eds.): ISPRS TC VII Symposium – 100 Years ISPRS, Vienna, Austria, July 5–7, 2010. IAPRS XXXVIII, http://www.isprs.org/proceedings/XXXVIII/part7/b/pdf/204_XXXVIII-part7B.pdf (Accessed 06.10.2010).

Zhang, Y., 2008. Methods for Image Fusion Quality Assessment a Review, Comparison and Analysis. *International Archives of Photogrammetry Remote Sensing and Spatial Information Sciences* 37(3), 1101-1110.

Zhou, J., Civco, D.L., and Silander, J.A., 1998. A wavelet transform method to merge landsat TM and SPOT panchromatic data. *International Journal of Remote Sensing* 19(4), 743-757.

CHAPTER 5

SUMMARY AND CONCLUSIONS

5.1 Summary

This dissertation considered various methods in GIScience for use in studies of sustainable development and preservation of coastal barrier islands using Jekyll Island, Georgia as a case study. In particular, all findings in the three manuscripts describing each study are intended to provide information to managers, scientists and policy makers with which to make better decisions to design sustainable development and preservation plans.

First, Chapter 2 presented geospatial methods to assess the impact of variable legal criteria in defining tidal datums for shoreline delineation and separately demarcating back-barrier and ocean-front side shorelines of coastal barrier islands. To do this, scientifically defensible standards to demarcate barrier islands and current geospatial techniques were used for accurately estimating the total area of coastal barrier islands with consideration of differences between back-barrier and ocean-front sea levels. Specifically, when it comes to the ocean-front side, NOAA 0.79-m (2.6 ft) and 0.85-m (2.8 ft) sea levels, based on NOAA verified and predicted values, respectively, along with a 1.0-m (3.3 ft) shoreline as documented in the 1996 JIA Master Plan, were used to delineate the shoreline of Jekyll Island State Park. Additionally, a marsh protection shoreline at 1.49-m (4.9 ft) was demarcated to reflect the Georgia State legislated Coastal Marshland Protection Act (CMPA).

Finally, integrated lines considering separate back-barrier and ocean-front side sea levels were delineated to more accurately model real-world conditions of 0.09-m (0.3 ft) higher sea levels on the back-barrier sides of coastal islands. The application of various state and federal delineations of shorelines to a very detailed and accurate digital terrain model created from LiDAR bare earth data provided island boundaries that were generally similar on the ocean/beach (east shoreline) side but differed significantly on the western inland/marsh side. These differences affect jurisdictional marshes for protection under the CMPA, as well as available developable lands allowed under the State limit of 35% developed to 65% undeveloped lands within Jekyll Island State Park. In addition, this research demonstrated a single shoreline does not accurately reflect the real-world conditions of slightly higher (by 0.09-m (0.3 ft) in the case of Jekyll Island State Park) back-barrier island sea levels compared to the ocean-front side. Future work should verify back-barrier and ocean-front sea levels on Jekyll Island to confirm the 0.09-m (0.3 ft) difference estimated from St. Simons Island tide stations. Indeed, field measurements of tide levels of several different coastal barrier islands are needed to explore variation and similarities in back-barrier sea levels toward defensible and reliable methods to estimate back-barrier sea levels.

In Chapter 3, this study identified beach availability for recreational use by tourists. To do this, changes in shorelines and dry beach were analyzed using historical shorelines and computing rates of shoreline change by linear regression modeling. In addition, a LiDAR-derived shoreline was used for recognizing serious beach accretion and erosion of sandy beach. In the next step, seasonal changes in sandy beach were estimated from verified tidal values. Shorelines visible in aerial photographs also were delineated and the water level was estimated for identifying beach availability. The results indicated processes such as erosion, accretion, and

possibly sea level rise since 1857 have caused changes in sandy beach, especially in the eroded northern portions and southern portions of Jekyll Island. These changes in island configuration also mean the time the beach can be used by tourists, residents and marine scientists between high tides is greatly shortened. In addition, seasonal changes in tide levels affect times and percentage of available sandy beach on Jekyll Island that may be accessible for part of the day or all day depending on the tidal ranges. This information may be important to tourists due to restricted beach availability for recreational purposes. Also, examination of the delineated shoreline on aerial photographs revealed more available beach in the vulnerable rock revetment areas from beach erosion that can be used for tourist activities during low tide events. Finally, all findings are now being provided on-line via a Web-based GIS that can be used by the public and by resource managers.

Chapter 4 attempted to compare different categories of image fusion methods, representing the three commonly known domains proposed by Pohl and Van Genderen (1998), namely, spectral substitution, arithmetic transform merge, and spatial-domain merge. These comparisons were necessary to find the optimal fused images to enable interpreters to better classify LULC of barrier islands. This study focused on Jekyll Island, Georgia because of the state managers' practical need for using VHR images and required accuracy in identifying the current status of developed and undeveloped lands. As a result, this study revealed the best image fusion operators for three VHR satellite images are provided by modified intensity-hue-saturation (MIHS), high pass filter (HPF) and subtractive resolution merge (SRM) in spectral substitutions and spatial domains. In particular, MIHS had better capabilities, producing stable results over all bands in both quality assessments. Therefore, HPF and SRM in the spatial

domain with MIHS in the spectral substitute domain are the best choices to produce improved interpretations of LULC and updating of regular coastal mapping of barrier islands.

5.2 Considerations for Subsequent Research

Based on the findings of this research, there are several considerations for future research that remain. First, in situations such as Jekyll Island State Park, the law on future development depends on the definitions of developed and undeveloped lands being clearly defined. There are, in fact, no standard definitions specified in this law so inconsistencies in what is considered *development* and *undeveloped areas* have actually caused public confusion in the understanding and implementation of the Islands Master Plans. Thus, a more reliable and confident decision making system is required for private and public consensus on developed vs. undeveloped features in this landscape, as is also the case in other coastal areas.

The second consideration involves analyzing differences in sea level rise on the back- and ocean-front side of the Island. Barrier islands along the Georgia coast are separated from the mainland by substantial areas of Spartina-dominated marsh land that may act to hold tide waters back when tides recede and effectively cause the back-side sea level in the marsh to be higher than the sea level of the ocean side. The difference of approximately 0.3-m may cause various effects such as back-side flooding during hurricane events or storm surges while the front side remains unflooded. Thus, site or segment-based risk analysis on the back- and ocean-front sides should be carried out to more specifically define the coastal landscape sensitivity to sea level rise.

With recent VHR satellite imagery having less than 1.0 to 5.0-m pixel sizes, the demand for automated image analysis of LULC classification is constantly growing. However, the higher spatial resolution results in more image complexity and the need for intelligent processes for segmentation and classification.

Automated classification procedures are sometimes desired because manual interpretation of LULC may lead to differences due to individuals perceiving image information in different ways based on their own knowledge and experience. While an observer can easily categorize an image into classes of interests, it is generally difficult to consistently reproduce the same results with multiple interpreters analyzing the same image.

Conventionally, automated LULC classification has used pixel-based spectral information from multiple bands as input to statistical methods that separate multidimensional clusters of digital numbers and assign LULC classes to each cluster. However, this approach has limitations in that imagery of high spatial resolution creates increase spectral variability within individual objects training sets for classification, which therefore, may not be spectrally unique or homogeneous.

Additionally, pixel-based classifications generally do not exploit the information contained in contextual relationships between each pixel and neighboring pixels. To overcome these limitations, Geographic Object-based Image Analysis (GEOBIA) has recently been proposed to classify developed and undeveloped areas (Blaschke *et al.,* 2008). This new semi-automated classification process that groups similar pixels into objects and then classifies these objects based on user-defined rules, GEOBIA also has limitations such as different results based on different human perceptions, over and under segmentation, and slow processing times. Another problem is that, even though individuals use one scene for LULC classification,

different classification systems such as the NOAA Coastal Change Analysis Program (C-CAP) that uses the Cowardin Wetland Classification System and the U.S. Geological Land Use/Land Cover Classification System, cause different classified results (Anderson *et al*., 1971; Cowardin *et al*., 1979). In future research, an ontology-driven image segmentation process in hierarchical steps should be addressed which includes constructing a semantic network for better image understanding. Therefore, it will be useful for arbitration in disputes related to the ambiguity between developed and undeveloped areas.

Overall, this dissertation demonstrated the successful use of geospatial data and analysis techniques to: 1) demarcate the boundaries of coastal barrier islands and demonstrate differences in island shape and area where various sea level elevations are used by different governing bodies; 2) develop geospatial tools to assist tourists, scientists and managers in planning beach access according to predicted tide levels; and 3) assess image fusion techniques to carefully examine best methods for integrating image data of different spatial and spectral resolutions for optimal mapping of LULC conditions on barrier islands. It is hoped that these results will further a balance between economic development opportunities and the preservation of valuable coastal resources.

APPENDIX I

EQUATIONS AND DIAGRAMS

Brovey transform

The Brovey transform technique of image fusion uses a mathematical combination of the color image and high resolution panchromatic data. Each band in the color image is multiplied by a ratio of the high resolution data divided by the sum of the color bands:

$$F1 = \frac{LR1}{LR1 + LR2 + LR3} HR$$

$$F2 = \frac{LR2}{LR1 + LR2 + LR3} HR$$

$$F3 = \frac{LR3}{LR1 + LR2 + LR3} HR$$

where F_i are the fused pansharpened bands, LR_i are the low spatial resolution original bands. HR is the high spatial resolution image band to be fused with the low spatial resolution bands.

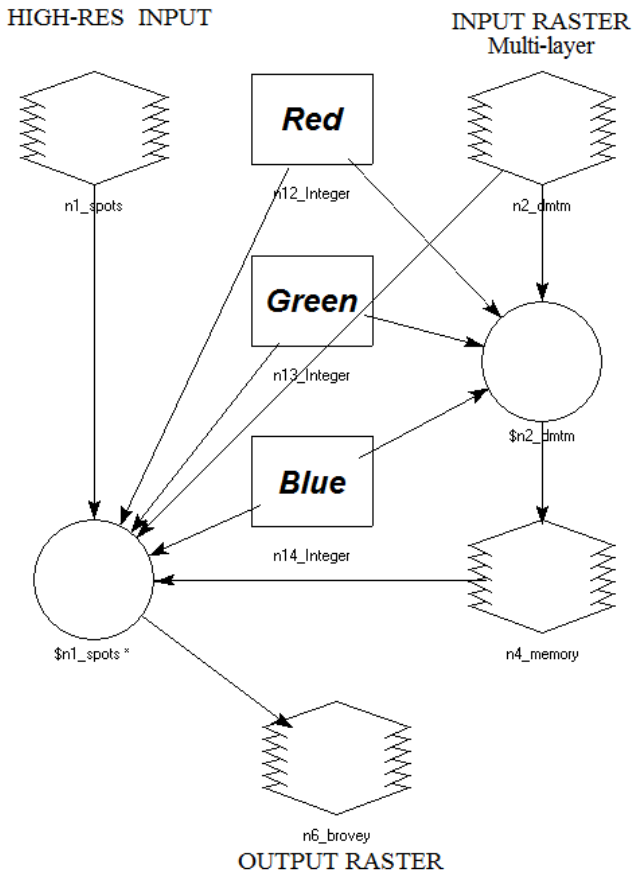

Figure A.1. Resolution Merge-Brovey Method (Source, ERDAS IMAGINE 2010).

The resulting the Brovey transform provides excellent contrast in the merged image domain, but affects the spectral characteristics a great deal. The Brovey sharpened image is not suitable for pixel-based classification as the pixel values are changes drastically (Veeraraghavan, 2004).

Correlation Coefficient (CC)

The Correlation Coefficient (CC) method of image fusion measures the correlation between the original and the fused images. The higher the correlation between the fused and the

original images, the better the estimation of fused image the spectral values to the original. The ideal value of CC is 1.

$$CC\ (A,B) = \frac{\sum\sum_{mn}(A_{mn} - \overline{A})(B_{mn} - \overline{B})}{\sqrt{\sum_{mn}(A_{mn} - \overline{A^2})\sum_{mn}(B_{mn} - \overline{B^2})}}$$

where $\overline{A}$ and $\overline{B}$ stand for the mean values of the corresponding data set, and CC is calculated globally for the entire image (Gangkofner e*t al*., 2008).

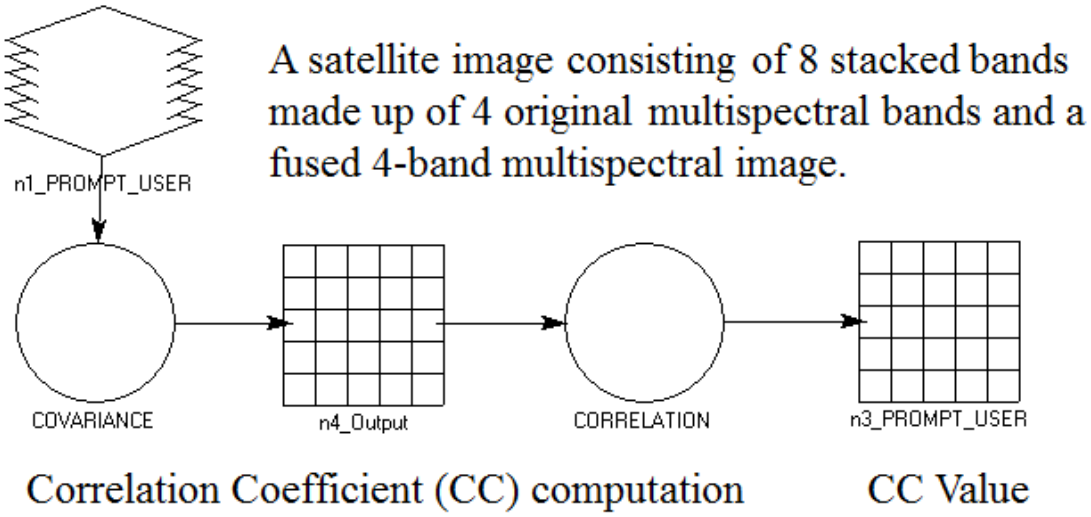

Figure A.2. Correlation Coefficient computation model developed in this research.

High-Pass Filter (HPF)

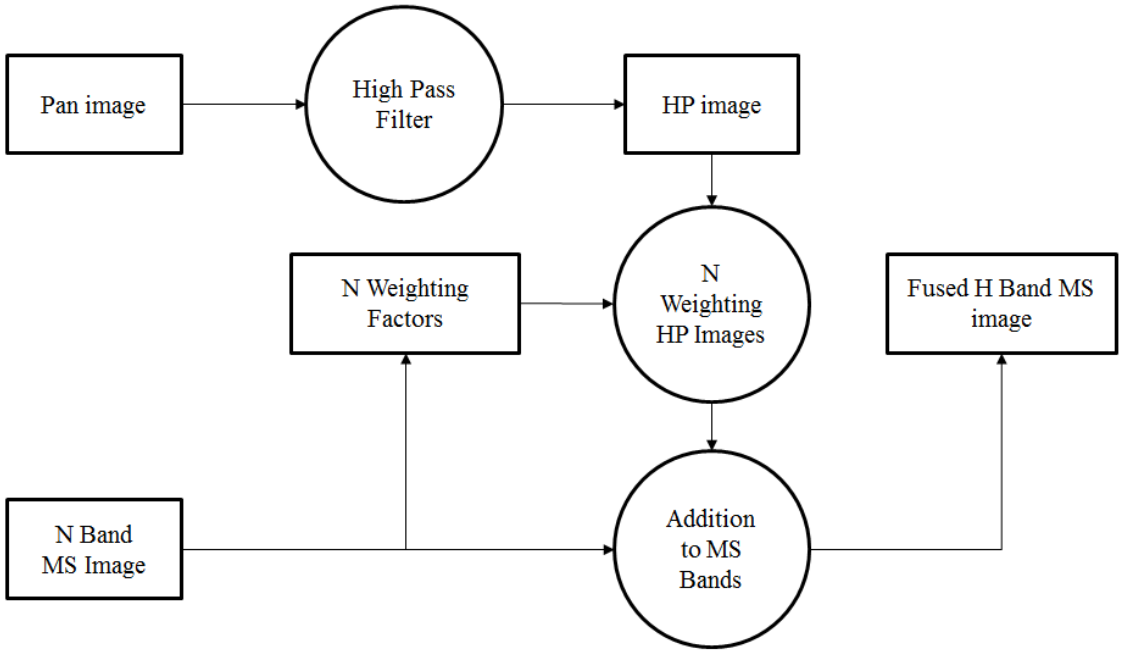

Figure A.3. HPF-based image fusion method (*Source*, ERDAS IMAGINE 2010).

Step 1: HP Filtering of the high-resolution image to extract the structural detail.

Step 2: Adding the HP filtered image to each band of the multispectral image using a standard deviation-based injection model.

Step 3: Linear Histogram Match to adapt SD and Mean of the Merged Image Bands to those of the original MS image bands.

Intensity-Hue-Saturation (IHS) or Modified Itensity-Hue-Saturation (MIHS)

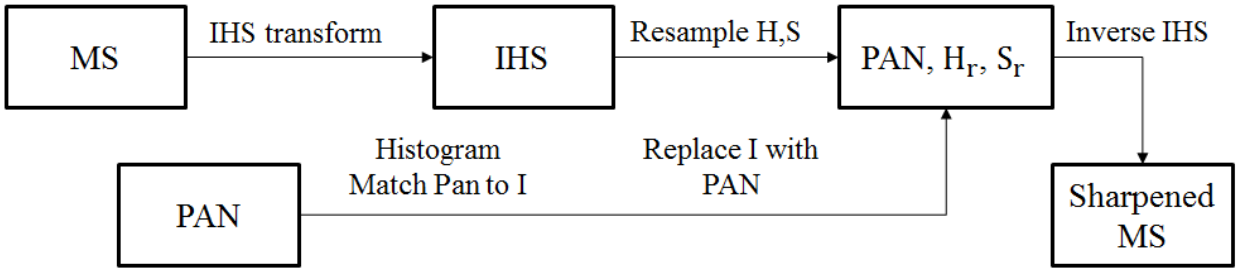

Figure A.4. Flow diagram of the IHS transformation based pansharpening (*Source*, ERDAS IMAGINE 2010).

Intensity-Hue-Saturation (HIS) and Modified IHS (MIHS) traosforms a multispectral image from the RGB color space into the IHS domain. The intensity component is replaced using the histogram matched panchromatic image. The hue and saturation components are resampled to the panchromatic resolution. The inverse IHS transformation is performed to get back into the RGB domain.

MIHS resolution merge function enables images with more than three bands to be merged by running multiple steps of the algorithm and merging the resulting layers (Siddiqui, 2003).

Principal Component Analysis (PCA)

This method calculates principal components, remaps the high resolution image into the data range of PC-1 and substitutes it for PC-1, then applies an inverse principal components transformation.

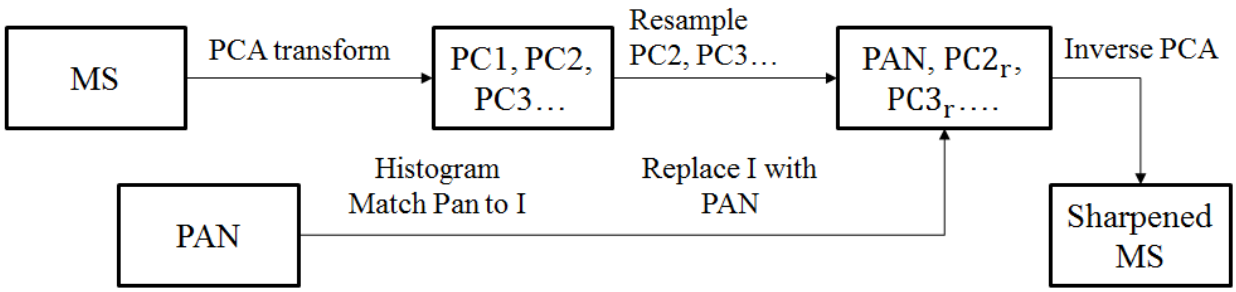

Figure A.5. Flow diagram of the PCA transform (*Source*, ERDAS IMAGINE 2010).

The first principal component is replaced by the panchromatic image. The inverse PCA transform is computed to go back to the image domain.

Step 1: Calculate PCA transform.

Step 2: Re-scale the high resolution image gray levels using an equation.

Step 3: Stack PCA image and rescaled high resolution image.

Step 4: Stacked image times inverse of PCA.

Linear Regression Rate-of-Change (LRR)

A linear regression rate-of-change (LRR) statistic can be determined by fitting a least squares regression line to all shoreline points for a particular transect. The regression line is placed so that the sum of the squared residuals (determined by squaring the offset distance of each data point from the regression line and adding the squared residuals together) is minimized. The rate is the slope of the line (Dolan, 1991).

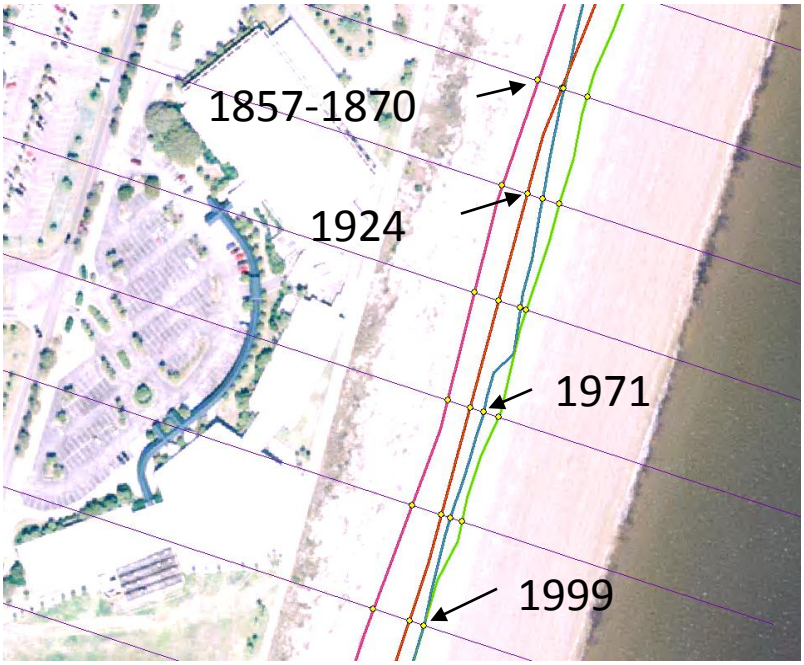

Figure A.6. In the example above, the linear regression rate was determined by plotting the shoreline positions with respect to time and calculating the linear regression equation of y = 1.34x – 2587.4. The slope of the equation describing the line is the rate (1.34 m/yr) (Source: USGS).

The advantages of linear regression include: 1) all the data are used, regardless of changes in trend or accuracy; 2) the method is purely computational; 3) it is based on accepted statistical concepts; and 4) it is east to employ (Dolan *et al*., 1991; Thieler *et al*., 2009).

Multiplicative (MP)

This method applies a simple multiplicative algorithm which integrates the two raster images. The Multiplicative Method is the simplest of the three methods. As it is computationally simple it is generally the fastest method and requires the least system resources. However, the resulting merged image does not retain the radiometry of the input multispectral image. Instead,

the intensity component is increased, making this technique good for highlighting urban features (which tend to be higher reflecting components in an image) (ERDAS, 2004).

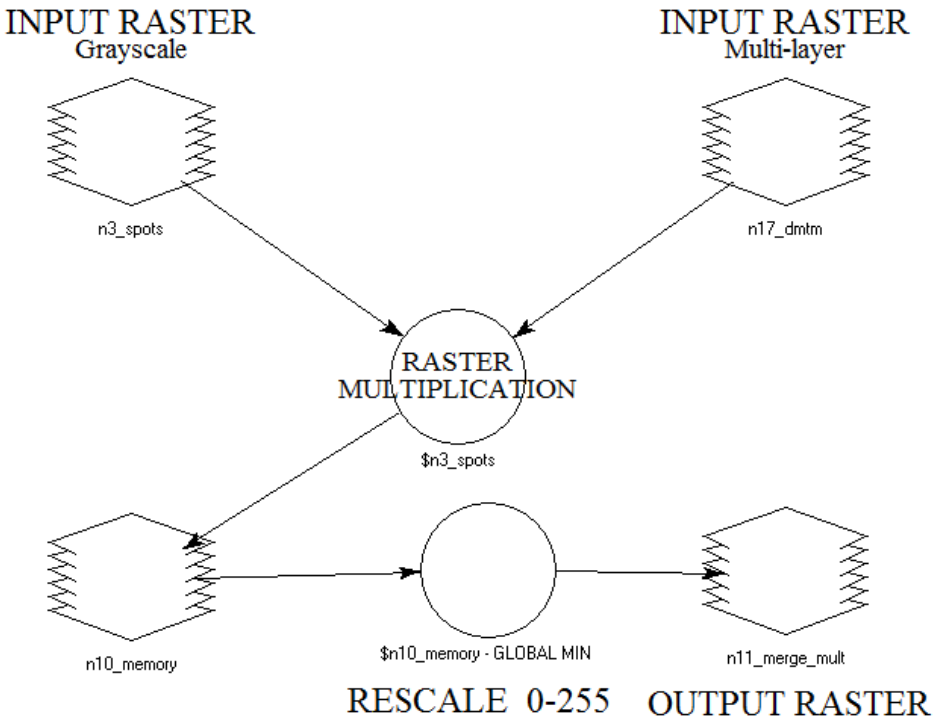

Figure A.7. Flow diagram of Multiplicative resolution merge (*Source*, ERDAS IMAGINE 2010).

Relative Difference of Means (RDM)

The relative difference of means (RDM) between the fused product and the original low spatial resolution multispectral image:

$$\text{RMD} = \frac{\overline{F} - \overline{LR}}{\overline{LR}}$$

where $\overline{F}$ is the mean value of the fused image and $\overline{LR}$ is the mean value of the original low spatial resolution image.

Relative Difference of Standard (RDS)

The relative difference of standard (RDS) (or variation) is the deviation between the fused product (σ_F^2) and the original low spatial resolution multispectral image (σ_{LR}^2):

$$\mathrm{RDS} = \frac{\sigma_F^2 - \sigma_{LR}^2}{\sigma_{LR}^2}$$

$$\text{Where: } \sigma_F^2 = \frac{1}{n-1}\sum_{n=1}^{N}(F_i - \overline{F})^2,\ \sigma_{LR}^2 = \frac{1}{n-1}\sum_{n=1}^{N}(LR_i - \overline{LR})^2.$$

The deviation index as referenced by Bethune *et al*. (1988), measuring the normalized global absolute difference of the fused image (F) with the low spatial resolution multispectral image (LR):

$$\text{Deviation index} = \frac{1}{(\text{rows} \times \text{columns})}\sum_{i=1}^{rows}\sum_{j=1}^{columns}\frac{\mathrm{F}_{i,j} - \mathrm{LR}_{i,j}}{\mathrm{LR}_{i,j}}$$

where $F_{i,j}$ is the fused image at pixel coordinated *i, j* and $LR_{i,j}$ *is the low spatial resolution image at pixel coordinates i, j.*

Root Mean Square Error (RMSE)

The Root Mean Square Error (RMSE) between each unsharpened multispectral band and the corresponding sharpened band is computed as a measure of spectral fidelity.

$$RMSE_K = \frac{\sum_{i=1}^{n}\sum_{j=1}^{n}\sqrt{(B_k(i,j) - F_k(i,j)^2}}{N^2}$$

where *B* and *F* refer to the MS images (resampled to the PAN image size) and the pan-sharpened images, respectively. The subscript *k* denotes the respective band number in the images

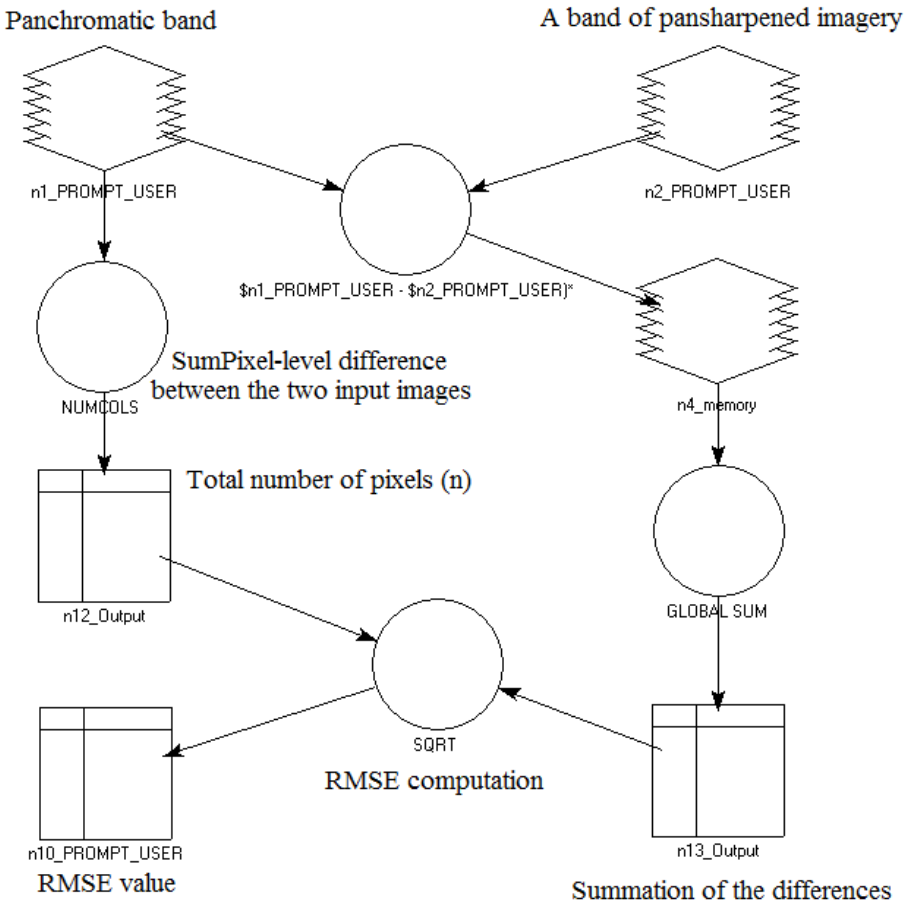

Figure A.8. RMSE Model of Sobel filtered fused and panchromatic bands developed in Model Maker of ERDAS IMAGINE 2010.

APPENDIX II

LIST OF DATUMS AND PROJECTIONS

Table B-1. List of Datums and Projections.

Horizontal datums
North American Datum of 1983 (NAD 83)
Vertical datums
National Geodetic Vertical Datum of 1929 (NGVD 29)
North American Vertical Datum of 1988 (NAVD 88)
Ellipsoid
Geodetic Reference System of 1980 (GRS 80)
Projection
Universal Transverse Mercator (UTM) zone 17
Tidal datums
Highest Water Level (HWL)
Mean Higher High Water (MHHW)
Mean High Water (MHW)
Mean Sea Level (MSL)
Mean Tide Level (MTL)
Mean Low Water (MLW)
Mean Lower Low Water (MLLW)
Lowest Water Level (LWL)

APPENDIX III

LIST OF ACRONYMS

Table B-2: List of Acronyms.

	Acronym	Full description
A	ALB	Airborne laser bathymetry
	ASPRS	American Society for Photogrammetry and Remote Sensing
	ADEOS II	Advanced Earth Observing Satellite 2
B	BAG	Bleakly Advisory Group
	BT	Brovey transform
C	CAP	Coastal Change Analysis Program
	CC	Correlation Coefficient
	CIR	Color Infrared
	CMPA	Coastal Marshlands Protection Act of 1970
	CNES	Centre National d'Études Spatiales
	COOPS	Center for Operational Oceanographic Products and Services
	CRMS	Center for Remote Sensing and Mapping Science
	CZMA	U.S. Coastal Zone Management Act
D	DN	Digital Number
	DSAS	Digital Shoreline Analysis System
	DSM	Digital Surface Model
E	ERDAS	Earth Resources Data Analysis System
	ESRI	Environmental Systems Research Institute
G	GA	Georgia State
	GEOBIA	Geographic Object-based Image Analysis
	GDNR	Georgia Department of Natural Resource
	GDOT	Georgia Department of Transportation
	GPS	Global Positioning System
	GRS 80	Geodetic Reference System of 1980
	GIS	Geographic Information System
	GIScience	Geographic information Science
H	HPF	High Pass Filter
	HWL	Highest Water Level
I	ICAD	The University of Georgia's Institute for Community and Area Development
	IPCC	Intergovernmental Panel on Climate Change
	IPJI	Initiative Protect Jekyll Island

J	JIA	Jekyll Island State Park Authority
K	KOMPSAT II	Korea Multi-Purpose Satellite II
L	LWL	Lowest Water Level
	LRR	Linear regression rate-of-change
	LULC	Land Use and Land Cover
	LiDAR	Light Detection and Ranging
M	MHHW	Mean Higher High Water
	MHW	Mean High Water
	MIHS	Modified Intensity-Hue-Saturation
	MLLW	Mean Lower Low Water
	MLW	Mean Low Water
	MP	Multiplicative
	MSL	Mean Sea Level
	MTL	Mean Tide Level
N	NAD 27	North American Datum of 1927
	NAD 83	North American Datum of 1983
	NAIP	National Agriculture Imagery Program
	NASA	National Aeronautics and Space Administration
	NASDA	National Space Development Agency of Japan
	NGS	National Geodetic Survey
	NGVD 29	National Geodetic Vertical Datum of 1929
	NAVD 88	North American Vertical Datum of 1988
	NOAA	National Oceanic and Atmospheric Administration
	NOS	National Ocean Service
	NSRS	National Spatial Reference System
	NSSDA	National Standard for Spatial Accuracy
	NTDE	The National Tidal Datum Epoch
O	OCS	NOAA's NGS, Office of Coast Survey
P	PCA	Principal Component Analysis
Q	QuikSCAT	Quick Scatterometer
R	RGB	Red, Green, and Blue
	RMSE	Root Mean Square Error
S	SDSS	Spatial Decision Supporting System
	SRM	Subtractive Resolution Merge
T	TIN	Triangulated Irregular Network
U	USDA	U.S. Department of Agriculture
	USGS	U.S. Geological Survey
	UTM	Universal Transverse Mercator
V	VHR	Very High Resolution
	VDatum	Vertical Datum Transformation Tool
	VERTCON	VERTical Datum CONversion
W	WCS	The World Conservation Strategy

References

Anderson, J.R., 1971, Land use classification schemes used in selected recent geographic applications of remote sensing. *Photogrammetric Engineering & Remote Sensing* 37(4), 379-387.

Blaschke, T., Lang, S., and Hay, G., 2008. *Object-based Image Analysis Spatial Concepts for Knowledge-driven Remote Sensing Applications*. In *Lecture notes in geoinformation and cartography*. Berlin: London: Springer, 817p.

Cowardin, L.M., Carter, V., Golet, F.C., and Laroe, E.T., 1979. *A Classification of Wetlands and Deep- water Habitats of the United States*. Washington, D.C.: U.S. Government Printing Office, Office of Biological Services, Fish and Wildlife Service, FWS/ OBS-79/31, stock number GPO 024-010-00524-6, 103p.

Dolan, R., Fenster, M.S., and Holme, S.J., 1991. Temporal analysis of shoreline recession and accretion. *Journal of Coastal Research* 7(3), 723–744.

Gangkofner, U.G., Pradhan, P.S., and Holcomb, D.W., 2008. Optimizing the high-pass filter addition technique for image fusion. *Photogrammetric Engineering and Remote Sensing* 74(9), 1107-1118.

Siddiqui, Y., 2003. The modified IHS method for fusing satellite Imagery. In: ASPRS 2003 Annual Conference Proceedings.

Thieler, E. R., 2009. *The Digital Shoreline Analysis System (DSAS) version 4.0, an ArcGIS© extension for calculating historic shoreline change*. In *U S Geological Survey open-file report 2008-1278* (4.0 ed.). Reston, Va.: U.S. Geological Survey.

Veeraraghavan V., Hara. C. G., and Younan N. H., 2004. Quantitative analysis of pansharpened images. *IEEE International Geoscience and Remote Sensing Symposium 2004 IGARSS 04 Proceedings* 2004 (2004), p 85-88.